Palaeontology
The Palaeontological Association
Registered Charity No 276369

A redescription of *Orovenator mayorum* (Sauropsida: Diapsida) using high-resolution µCT, and its consequences for early amniote phylogeny

Journal:	*Palaeontology*
Manuscript ID	PALA-02-18-4152-OA.R1
Manuscript Type:	Original Article
Date Submitted by the Author:	05-Jun-2018
Complete List of Authors:	Ford, David; University of Oxford Mathematical Physical and Life Sciences Division, Earth Sciences Benson, Roger; University of Oxford, Department of Earth Sciences
Key words:	Diapsida, Synapsida, phylogeny, amniote, varanopid, palaeoecology

A redescription of *Orovenator mayorum* (Sauropsida: Diapsida) using high-resolution µCT, and its consequences for early amniote phylogeny

DAVID P. FORD[1*] and ROGER B. J. BENSON[1]

[1]Department of Earth Sciences, University of Oxford, South Parks Road, Oxford OX1 3AN. E-mails: david.ford@earth.ox.ac.uk roger.benson@earth.ox.ac.uk

[*] Corresponding author

Abstract: The earliest known neodiapsid *Orovenator mayorum* from the early Permian of Oklahoma is redescribed using high-resolution µCT, revealing remarkable details of the skull anatomy. Our findings are relevant to both palaeoecology (suggesting burrowing and nocturnality) and phylogeny. *Orovenator* and other sauropsids share at least 16 character states with varanopids, many of which were not recognised by previous studies. These include a rounded subnarial shelf of the premaxilla, a posterodorsal extension of the external naris, the asymmetrical bifurcation of the anterior vomer, and a prominent dorsomedial shelf of the surangular. This exceptional degree of similarity between *Orovenator* and varanopids (a nominally synapsid clade) questions our current understanding of relationships among early amniotes. We test this by including *Orovenator* in a phylogenetic data matrix used in an earlier study to differentiate between early diapsids and synapsids, and find a monophyletic clade of *Orovenator* + varanopids within Diapsida. Recent phylogenetic research on early amniote evolution has focused on resolving intra-clade affiliations rather than the interrelationships of major taxonomic groups. Nevertheless, the relative incompleteness of existing phylogenetic character lists for early amniotes can only be remedied by detailed cross-clade

assessment. We therefore suggest that early amniote relationships require further scrutiny before we can confidently accept or reject our new phylogenetic hypothesis.

Key Words: Amniote, Diapsida, varanopid, Synapsida, phylogeny, palaeoecology,

AMNIOTES comprise all mammals and reptiles (including birds). Today they are a major component of global ecosystems, accounting for almost four fifths of land vertebrate diversity, yet much about their origin and early divergences remains obscure. Amniotes first appear in the fossil record in the late Carboniferous, with the earliest taxa known from the Pennsylvanian coal measures of Joggins, Nova Scotia (Carroll 1964). Fossils from this locality provide evidence that the mammal/reptile divergence had already occurred by the late Bashkirian (319-318 Ma) (Benton et al. 2015), as members of both the mammalian total-group (Synapsida) and reptilian total-group (Sauropsida) are already present (Müller and Reisz 2004, 2005a). The recent discoveries of the oldest caseid (Reisz and Fröbisch 2014) and parareptile (Modesto et al. 2015) in the late Upper Pennsylvanian (Gzhelian 304-299 Ma) confirm that the basal amniote dichotomy was well established by that time, and all major clades of early synapsids (caseasaurs, varanopids, edaphosaurids, ophiacodontids and sphenacodontians) and early sauropsids (parareptiles, captorhinids and diapsids) had emerged.

Early synapsids, characterised by a single, lateral, temporal fenestra, were both abundant and diverse in the early Permian (Reisz 2014, Angielczyk and Kammerer, in press). Sauropsids were somewhat less common, and principally represented by early-diverging clades: the parareptiles and captorhinids (MacDougall et al. 2017a, 2017b). By contrast diapsids, representing the sauropsid group that includes all extant reptiles and birds and typically possessing two temporal fenestrae, are rare in

early Permian deposits. Few diapsids of this age have been reported, other than the highly plesiomorphic araeoscelidians (Reisz 1981, de Braga and Reisz 1995, Vaughn 1955). In fact, apart from an isolated parietal (Carroll 1968), *Orovenator mayorum* from the Dolese Quarry, Richards Spur, Oklahoma, is the only non-araeoscelidian diapsid reported so far from the early Permian (Reisz et al. 2011). The Dolese Quarry has yielded a unique assemblage of early Permian terrestrial vertebrates from claystone fissures deposited in Lower Ordovician limestone (Reisz *et al.* 2015). Recent taphonomic analysis of the fossils and associated matrix has confirmed a karstic environment of cave systems preserved in an upland locality (MacDougall *et al.* 2017b). The radiometric (U-Pb) dating of speleothems from the cave systems has defined the absolute age of these deposits at 289 ± 0.68 Ma (Woodhead et al. 2010), equivalent to the early Artinskian (ICS v.2017/02).

Taxonomic classifications of early amniotes have been closely associated with patterns of temporal fenestration, and osteological differences were otherwise limited between the earliest synapsids and sauropsids (Reisz 1972). Patterns of temporal fenestration have largely prevailed as a key character in the systematic classification of amniotes since Osborn (1903) and are consistent with seminal studies on cladistic hypotheses (e.g. Gauthier *et al.* 1988, de Braga and Rieppel 1997, Laurin and Reisz 1995). Nevertheless, researchers have noted a high degree of variability of temporal fenestration amongst early amniotes, even within closely related groups (e.g. parareptiles; Cisneros *et al.* 2004, Tsuji *et al.* 2010). This apparent plasticity in temporal fenestration is further exemplified by the secondary loss of the lower temporal fenestra amongst araeoscelidian diapsids (Reisz *et al.* 1984) and the complete loss of temporal fenestration leading to the ‘anapsid’ condition of total-group turtles (Bever *et al.* 2015). Furthermore, recent studies have questioned the efficacy of characters based on temporal fenestration in performing broad-based phylogenetic analyses of early amniotes (MacDougall and Reisz 2014).

The presence of diapsid-like temporal fenestration in *Orovenator* was noted by Reisz *et al.* (2011). *Orovenator* was consequently recovered as the earliest known neodiapsid, the sister group to the araeoscelidian diapsids, based on analysis of a sauropsid-focused data matrix (Reisz *et al.* 2011). Subsequent phylogenetic analyses have therefore assumed diapsid affinities and examined the relationships of *Orovenator* relative to other sauropsids, with synapsids included only as a single, composite out-group (Chen *et al.* 2014, Bever *et al.* 2015) or omitted entirely (Pritchard and Nesbitt 2017).

Here, we use micro-computed tomography (μCT) to investigate the anatomy of *Orovenator*. This approach reveals remarkable detail of the cranial osteology of *Orovenator*, including the first complete three-dimensional visualisation of an early diapsid septomaxilla, the medial surface of the antorbital region and the structure of the nasolacrimal canal, a complete reconstruction of the palate and the pathways of major arteries in the basicranium and maxilla. Several anatomical features also provide evidence of the palaeoecology of *Orovenator*, indicating nocturnality and burrowing behaviour. We also use three dimensional modelling to present a reconstruction of the skull of *Orovenator* based on the scan data of the holotype and referred specimen.

Orovenator shares various character states with araeoscelidians such as *Petrolacosaurus kansensis* (Reisz 1981). However, we also report a series of morphological features shared with varanopids, a group that is typically assigned to Synapsida. Several such features, including the anterodorsal process of the surangular and posterolateral extension of the external naris, have been noted by earlier studies (Reisz *et al.* 2011). Although similarities have hitherto been documented between varanopids and early diapsids (Reisz and Modesto 2007,

Reisz et al. 2010), the present study demonstrates that the similarities are more numerous and detailed than previously recognised, calling into question the phylogenetic distinctness of varanopids from early diapsids. To explore these similarities further, we score *Orovenator* into an existing phylogenetic data matrix designed to recognise affinities between diapsids and varanopids . This analysis finds varanopids in a clade with *Orovenator*, among early diapsids, implying homoplasy between diapsid- and synapsid-like temporal fenestration. However, it is also clear that much relevant variation in anatomical character states has not been included together in existing phylogenetic data matrices for early amniotes. We therefore suggest that the paradigm of a Varanopidae as a clade within Synapsida, and not Sauropsida, should be subject to further scrutiny.

MATERIALS AND METHODS

Orovenator mayorum is represented by two specimens, OMNH 74606 (holotype) and OMNH 74607 (referred specimen), held in the collection of the Sam Noble Oklahoma Museum of Natural History, Norman, Oklahoma. The holotype is here considered as a juvenile, since is it approximately 33% smaller than and lacks the dermal sculpturing of the referred specimen.

Both specimens were scanned in a single field resulting in 1901 slices and a voxel size of 17.8 μm at the University of Texas High-Resolution CT Facility in Austin, Texas using the North Star Imaging ACTIS scanner, with 2048 x 2048 Perkin Elmer flat-panel detector and 0.72 mm aluminium filter. The beam was set to 160 kV, and 0.2 mA. The holotype of the varanopid *Mycterosaurus longiceps* (FMNH-UC 692) was scanned at the μCT facilities in the University of Chicago, Department of Organismal Biology and Anatomy, using the GE scanner with a 0.5 mm copper filter. The resolution achieved was 30.3 μm (135kV, 0.2 mA), with 3071 slices.

All specimens were digitally segmented using Mimics Materialise v. 18.0 x64 (http://biomedical.materialise.com/mimics). High-resolution models produced in Mimics were exported as .ply files, then imported into Blender (blender.org) and rendered as two-dimensional images for the figures used in the present study. All reconstructions of the skull of *Orovenator* were carried out in Blender using the available elements of both OMNH 74606 and 74607. Composite reconstructions of the skull were made with the downscaling of elements from OMNH 74607 by 33% of natural size. Mirror imaging or duplication from both specimens was used to replace some elements.

Institutional abbreviations. AM, Albany Museum, Grahamstown, South Africa; BP, Evolutionary Studies Institute, University of Witwatersrand, Johannesburg, South Africa; FMNH, Field Museum of Natural History, Chicago, USA; KUVP, University of Kansas Natural History Museum, Lawrence, USA; MCSNM Museo Civico di Storia Naturale, Milan, Italy; MCZ, Museum of Comparative Zoology, Harvard University, Cambridge, USA; OMNH, Sam Noble Oklahoma Museum of Natural History, Norman, USA; YPM, Yale Peabody Museum of Natural History, New Haven, USA.

SYSTEMATIC PALAEONTOLOGY

AMNIOTA Haeckel, 1866

SAUROPSIDA Huxley 1864

DIAPSIDA Osborn, 1903

NEODIAPSIDA Benton, 1985

Genus *OROVENATOR* Reisz *et al.,* 2011

Type species *Orovenator mayorum* Reisz *et al.* 2011

Material

OMNH 74606 (holotype), a partial skull including premaxillae, septomaxillae, maxillae, left lacrimal, left prefrontal, left nasal, right jugal, vomers, palatines, pterygoids, ectopterygoids, parabasisphenoid, right epipterygoid, left quadrate, partial stapes and scleral plates. OMNH 74707 (referred specimen), a partial skull including frontals, prefrontals, right parietal, lacrimal, pterygoid, palatine, partial supratemporal, partial atlas/axis and 3rd cervical and an isolated caudal. The referred specimen is assigned to the same species as the holotype based on the distinctive morphology of the lacrimal (Reisz *et al.* 2011).

Locality and horizon

Dolese Brothers Limestone Quarry, Richards Spur, Comanche County, Oklahoma, USA. Claystone fissure fills dated to 289 ± 0.68 Ma (Woodhead *et al.* 2010) in the Ordovician Arbuckle Limestone. Late Sakmarian/early Artinskian of the Cisuralian (early Permian).

Revised diagnosis

Small diapsid reptile (estimated adult skull length 45 mm) distinguished by a rounded transition of the dorsal and lateral surfaces of the subnarial bar of the premaxilla*, a moderate anterodorsal inclination of the anterior surface of the premaxillae (rostral process) *, an elongate external naris, a transversely curved lacrimal that forms an antorbital ridge on the snout (autapomorphy), a buttress and crest on the medial

surface of the maxilla dorsal to the 9th alveolus*, a parietal that extends anteriorly along the midline as far as the anterior-most point of the postfrontal, mediolaterally narrow suborbital fenestrae*, an elongate dentary that extends posteriorly to a point directly ventral to the inferred midpoint of the lateral temporal fenestra, and a surangular that forms a dorsal shelf above the adductor fossa and anteriorly forms a trough receiving the posterodorsal process of the coronoid (modified from Reisz *et al.* 2011, with additions annotated *).

DESCRIPTION

The Skull

Most bones of the skull and mandible are at least partially preserved in either OMNH 74606 (Fig. 1) or OMNH 74607 (Fig. 2). The occipital region, postorbital, squamosal, articular and most of the braincase are not preserved. Despite this, the approximate disposition of some of the missing bones can be deduced from the articular facets on the adjacent bones.

Snout. The dorsal surface of the snout is mediolaterally broad, and almost flat. This is accentuated by the dorsal exposure of the prefrontals and lacrimals (Fig. 3C). The snout of *Orovenator* is proportionately long; with the antorbital region approximately double the length of the postorbital region. The mediolateral width and dorsoventral height of the snout attenuate anteriorly resulting in a rather wedge-shaped appearance. The anterior end of the snout, constituted by the premaxilla and anterior part of the maxilla, is inflected anteroventrally from the level of the 5th maxillary alveolus (Fig. 3A). The external nares are elongate, ovoid openings that face anterolaterally and are enclosed principally by the premaxilla and maxilla. The

lacrimal and nasal only make a small contribution to the posterior margin of the external naris (Fig. 3B). The rostral process of the premaxilla is moderately procumbent.

Premaxilla. Both premaxillae are present in OMNH 74606. The premaxilla comprises a ventral subnarial ramus that bears a palatal flange medially, and a maxillary process posteriorly. Only the anteroventral portion of the base of the dorsal ramus is preserved in both the left and the right premaxilla. Nevertheless, aspects of its morphology can be reconstructed from a facet on the anterolateral process of the left nasal and from a preserved posterior section of the dorsal ramus of the right premaxilla, which remains articulated with part of the nasal (Fig. 1D). Both premaxillae have five alveoli, with one tooth missing from the right premaxilla (Fig. 4B). All premaxillary teeth are conical with pointed apices, and lack carinae. They are both isodont and homodont, but are smaller than the maxillary teeth. The teeth are set in shallow sockets, the labial wall is slightly pronounced and the lingual wall is absent.

The dorsal surface of the subnarial ramus, which forms the ventral floor of the external naris, grades smoothly into its mildly convex lateral surface (Fig. 4A). This is different from other early diapsids such as *Petrolacosaurus* (pers. obs. KUVP 9952) and *Araeoscelis* (pers. obs. MCZ 4380) or indeed most Paleozoic amniotes (Reisz and Berman 2001) in which there is an angular contact between the lateral and dorsal surfaces of the subnarial ramus. Instead, the condition in *Orovenator* is similar to the rounded subnarial bar seen in some early synapsids such as the varanopids *Archaeovenator* (Reisz and Dilkes 2003) and *Mesenosaurus* (Reisz and Berman 2001). Posteriorly the subnarial ramus narrows dorsoventrally to form a shelf that underlies the premaxillary process of the maxilla.

The maxillary process of the premaxilla comprises 48% of the total length of the premaxilla (Fig. 4A). It is mediolaterally narrow and sheet-like. Its lateral surface is overlapped by the maxilla and thus obscured in lateral view. The medial surface of the maxillary process forms the anterolateral margin of the internal naris. The process extends posteriorly from the subnarial ramus of the premaxilla and tapers to a point. The process articulates with a facet on the medial surface of the alveolar shelf of the maxilla (Fig. 5).

The alveolar surface of the premaxilla is approximately horizontal, sloping gently anteroventrally. The anterior surface of the truncated base of the dorsal ramus extends anterodorsally from the alveolar surface at and angle of approximately 35° from the perpendicular (Fig. 3A). This forms a moderately procumbent snout ('rostral process' sensu Reisz *et al.* 2009). The 'rostral process' is absent in other early diapsids, in which the base of the anterior symphysial margin is vertical, not inclined anterodorsally (*Petrolacosaurus;* Reisz 1981 and *Araeoscelis*; Reisz *et al.* 1984). It may therefore be autapomorphic for *Orovenator* amongst early diapsids. This feature is also present in caseasaurian synapsids (*Eothyris* and *Oedaleops*; Reisz *et al.* 2009*, Ennatosaurus*; Maddin *et al.* 2008*, Euromycter*; Sigogneau-Russell and Russell 1974, Reisz *et al.* 2011), and the diadectomorph *Limnoscelis* (Romer 1946). Maddin *et al.* (2008) considered that *Limnoscelis* and caseasaurians acquired this morphology independently, and its presence in *Orovenator* may indicate a third independent acquisition of this character state among early amniotes.

Two large foramina are located on the anterior surface of the dorsal process, and two smaller foramina are located lateral to these. The lateral surface of the premaxilla is otherwise smooth, with no sculpturing evident, unlike in *Petrolacosaurus* (Reisz 1981). The medial surface of the premaxilla bears a flat symphyseal surface for the

opposing premaxilla. This surface extends posteriorly to the level of the third premaxillary alveolus.

The palatal flange extends posteromedially from the medial surface of the premaxilla. The paired palatal flanges of the left and right premaxillae are recessed posteromedially such that they jointly form a midline notch that accommodates the anteromedial process of the vomer (Fig. 4B). The palatal flange continues posteriorly into a short, tapering spur of bone, the vomerine process, which inserts into a notch between the anteromedial and anterolateral processes of the vomer (Fig. 4C).

The dorsal rami of both premaxillae are not preserved.. Nevertheless, the position of the premaxillary contact with the nasal is indicated by a facet on the anterolateral process of nasal, and from the preserved posterior section of the dorsal ramus of the right premaxilla that remains in articulation with a fragment of the right nasal. The left nasal is incomplete anteromedially, but preserves a slender anterolateral process. This process has a slightly recessed lateral margin and bears a deep, anteroposteriorly elongate, groove-like facet with a prominent medial wall, which articulated with the ventral surface of the dorsal ramus of the premaxilla (Fig. 3A).

Although the right side of the skull roof is less well preserved than the left, a fragmentary piece of bone is preserved that we identify as the posterior portion of the dorsal ramus of the right premaxilla (Fig. 1D). This remains in contact with the right nasal, level with the posterior margin of the external naris. Our µCT data indicate that this fragment is separated from the anterior portion of the nasal by a well-defined suture. Several vascular foramina perforate the posterior part of the dorsal ramus. Similar foramina can also be found at the base of the dorsal ramus (anteroventrally). In contrast, foramina are absent from the nasal fragment. The dorsal ramus of the premaxilla therefore extends far posteriorly in *Orovenator*, forming much of the

medial margin of the external naris (Figs 3B, D), contrary to the anteroposteriorly short dorsal rami figured in Reisz et al. (2011). In other early diapsids, such as *Petrolacosaurus* (Reisz 1981) this process was restricted to the anterodorsal margin of the external naris. It is likely that anteriorly the rami were in contact anteromedially, separated posteriorly by medial processes of the nasals. The external naris of *Orovenator* was therefore anteroposteriorly elongate, as noted by Reisz *et al.* (2011).

Maxilla. The maxilla is the longest bone in the snout, and is best represented by the left maxilla of OMNH 74606 (Fig. 1B). The subnarial ramus of the right maxilla is damaged: the posteriormost portion and much of the dorsal process are missing. The left maxilla is missing only a small, posterior section of the dorsal process. The subnarial process tapers anteriorly to its contact with the premaxilla, where its dorsal surface forms the posteroventral margin of the external naris. The dorsal process is an anteroposteriorly elongate, mediolaterally thin sheet of bone with a dorsal margin that increases posteriorly in dorsoventral height from the posterior border of the external naris. It reaches its maximum height level with the 13th alveolus, after which it reduces in height posteriorly before merging with the suborbital ramus level with the 20th alveolus. The suborbital ramus is long, 37% of the total length of the maxilla, and terminates anterior to the posterior orbital margin (Fig. 3A). The dorsal process of the maxilla is subvertical for most of its length, but its anterior portion curves dorsomedially adjacent to the external naris. The dorsal process of the maxilla overlies the lateral surface of the lacrimal along its entire length (Fig. 3A), but does not contact the nasal due to the anterior extension of the lacrimal contributing to the posterior margin of the external naris. The left maxilla shows a complete count of 30 alveoli, compared to only 25 preserved in the right maxilla.

The alveolar surface of the maxilla is sinuous, with an anterior portion that arches dorsally, and so appears mildly concave in lateral view, and a posterior portion that is

bowed ventrally, and so appears mildly convex in lateral view. The lateral surface of the maxilla is smooth, but bears at least 23 small nutrient foramina, with one row of supralabial foramina, and others distributed on the surface of the dorsal process. A single, conspicuously large anterior maxillary foramen is positioned dorsal to the third maxillary alveolus, from which a shallow groove extends anteriorly (Fig. 3A). All foramina probably provide cutaneous egress for the maxillary branch of the trigeminal nerve (cranial nerve V) and accompanying blood vessels. Many amniotes possess a group of similar-sized supralabial foramina on the lateral surface of the maxilla (Laurin and Reisz 1995, Benoit et al. 2018). An anterior maxillary foramen noticeably larger than the other foramina, and often associated with an anteriorly orientated groove as seen in *Orovenator*, can be seen in many sauropsids. For example, the archosauromorphs *Prolacerta, Protorosuchus, Proterosuchus* and rhynchosaurs (e.g. *Mesosuchus*) (Modesto and Sues 2004) and the late Permian captorhinid *Saurorictus*, although absent in all earlier captorhinids (Modesto and Smith 2001). It is also present in most parareptiles (MacDougall *et al.* 2016). Despite its broad distribution amongst sauropsids it is absent in some diapsids including *Petrolacosaurus*, *Lanthanolania* and *Youngina* (Reisz 1981, Modesto and Reisz 2002, BP/1/70 pers. obs.). An enlarged anterior maxillary foramen is absent in those early synapsids in which the anterolateral surface of the maxilla is preserved (e.g. sphenacodontians; Spielmann *et al.* 2010, ophiacodontids; Berman *et al.*1995 and edaphosaurs; Modesto 1995), with the exception of the caseasaur *Oromycter* (Reisz 2005). However, it is present in the varanopids *Archaeovenator* (Reisz and Dilkes 2003), and *Heleosaurus* (Botha-Brink and Modesto 2009).

The suborbital ramus of the maxilla is dorsoventrally high anteriorly and tapers posteriorly, contributing partly to the anteroventral margin of the orbit when seen in lateral view (Fig. 3A). Posteriorly, the suborbital ramus narrows abruptly in a step-like fashion at the level of the 25th alveolus, exposing the lateral surface of the jugal (Fig.

1B). From here it continues to taper posteriorly, terminating anterior to the posterior margin of the orbit. The posterior suborbital ramus of the maxilla is dorsolaterally inclined 12° from the vertical, slightly overhanging the lateral alveolar margin, in a somewhat similar fashion to that described in *Archaeovenator* (Reisz and Dilkes 2003).

A transversely broad, anteroposteriorly oriented alveolar shelf projects from the medial surface of the maxilla ventrally. This shelf gradually thickens dorsoventrally from the 30th and posterior-most alveolus to a point level with the 9th alveolus. Here the alveolar shelf produces a robust 'supracanine' buttress, which is subtriangular in medial view (Fig. 5). A mediolaterally broad crest of bone extends posterodorsally from the apex of this buttress. This crest terminates close to the dorsal margin of the maxilla. The dorsal surface of the crest provides a broad articular surface for an elliptical ventral facet on the ventromedial ridge of the lacrimal. A deep posterior cavity is formed by the 'supracanine' buttress and crest, and enclosed ventrally by the alveolar shelf. *Orovenator* does not possess a caniniform tooth or region. The maxilla is preserved only in the juvenile specimen (OMNH 74606), and caniniforms can only be assumed to be absent at older ontogenetic stages. Nevertheless, some juvenile specimens of Permian amniotes are known to exhibit distinct caniniform teeth (e.g. *Heleosaurus* Botha-Brink and Modesto 2009). Therefore, the buttress and crest in *Orovenator* probably represents a different function (if any) than in various other taxa, in which it encloses the enlarged root of the caniniform teeth.

The medial 'supracanine' buttress and crest in *Orovenator* is an early example of this morphology amniotes. It is absent in many early sauropsids, including captorhinids (e.g. *Euconcordia*; Müller and Reisz 2005 and *Captorhinus laticeps;* Heaton 1979), the early parareptiles *Colobomycter vaughni* and *Delorhynchus* (MacDougall *et al.* 2016, Reisz *et al.* 2014), and in the early diapsid *Petrolacosaurus* (Reisz 1981).

Nevertheless, medial maxillary buttresses are present in some later diapsids. These include the *carina maxillaris* of lacertoid squamates (Augé and Smith 2009, Cernansky and Augé 2013), and in some early lepidosauromorphs, although they are less prominent (e.g. *Marmoretta*; Evans 1991 and *Diphydontosaurus;* Whiteside 1986). The morphology of the 'supracanine' buttress and crest in *Orovenator* is remarkably similar to that of non-archosauriform archosauromorph *Prolacerta* in which the buttress and crest are described as an "internal thickening behind the nasal capsule" (Gow 1975:100-101 BP/1/2671) (Fig. 18B).

The dorsoventral height of the alveolar shelf of *Orovenator* gently narrows anterior to the 'supracanine' buttress, and forms the medial premaxillary facet and premaxillary process anterior to the 5th maxillary alveolus. A shallow facet for the septomaxilla is present on the dorsal surface of the anterior-most region of the alveolar shelf.

The alveolar shelf bears two large openings for the alveolar canal, which are best seen in dorsomedial view (Fig. 5B). The posterior opening lies dorsal to the 22nd alveolus, immediately posterior to the position of the maxilla/palatine suture. The anterior and somewhat larger opening lies dorsal to the 10th alveolus. A sulcus extends posteriorly from the anterior opening, terminating immediately anterior to the maxilla/palatine suture. The anterior maxillary artery and alveolar nerve were therefore not canalised entirely along the length of the maxilla. The connecting ramus of the palatine is perforated, however, permitting the progress of the artery and nerve to the sulcus of the anterior alveolar canal. The facet for the palatine is not recessed, but is a smooth area of the alveolar shelf between the posterior opening of the alveolar canal and the entrance to the sulcus of the anterior opening. A small foramen on the dorsomedial margin of the palatine facet receives a branch of the alveolar nerve/blood vessel, which exits the lateral surface of the palatine ramus.

There is a shallow recess on the lateral margin of the posterior alveolar shelf, which receives the suborbital process of the jugal.

The maxillary tooth row occupies a shallow groove on the ventral surface of the alveolar shelf. Of the 30 alveoli that are present in the left maxilla, 22 contain partly or fully developed teeth. The scan reveals the apices of replacement teeth erupting from the labial surface of several alveoli. Dental implantation is broadly 'subthecodont' (*sensu* Fraser and Shelton 1988) with thin interdental plates. The labial wall of the alveolar row is slightly taller that the lingual wall, which is comprised of low, triangular paradental plates. Small ventral apices demarking the limit of each tooth position can be seen along the labial surface in lateral view. The dentition is homodont. The anterior six maxillary teeth are slightly larger that the premaxillary teeth and the seventh–14th maxillary teeth are the largest of the marginal dentition. Thereafter the teeth reduce in size with the two posterior-most teeth slightly smaller than those of the premaxilla. All maxillary teeth are sharply pointed, conical and slightly recurved with no carinae.

Septomaxilla. Both septomaxillae of OMNH 74606 are preserved disarticulated within the narial cavity and are visible in lateral view through the left external naris (Figs 1A, B). As preserved, the right septomaxilla is anterior to the left and its medial surface is visible externally. The left septomaxilla has been displaced so its ventral surface is exposed. The septomaxilla is preserved in many early sauropsids and synapsids (e.g. the captorhinid *Euconcordia*; Müller and Reisz 2005b, Reisz *et al.* 2016, the synapsid *Archaeovenator*; Reisz and Dilkes 2003, the diapsids *Petrolacosaurus*; Reisz 1981, and *Prolacerta*; Camp 1945 and the parareptile *Delorhynchus*; Reisz *et al.* 2014). However, because the septomaxilla is typically embedded in matrix within the narial cavity, 3D information is only available for a few taxa such as *Dimetrodon limbatus* (Romer and Price 1940) and the parareptile *Milleretta* (Gow 1972).

The septomaxilla of *Orovenator* is a complex bone. A sheet-like ventral plate extends medially as an anteroposteriorly broad medial shelf (Fig. 6A). The anterior portion of the ventral plate is inflected anterodorsally to form a sub-triangular anterior process (Fig. 6B). This process extends at an angle of 45° from the ventral plate, originating at the ventral margin of the anterior opening of the septomaxillary canal and probably resting on the premaxilla ventrally. An anteroposteriorly oriented septomaxillary canal is enclosed ventrally by the ventral plate and laterally and medially by laminae that met at the apex of the canal. From this apex a mediolaterally thin, sub-rectangular dorsal process inclines dorsomedially (Fig. 6C).

The ventrolateral ridge of the septomaxilla articulates into a shallow recess on the dorsal surface of the anterior-most region of the alveolar shelf of the maxilla. The septomaxilla is therefore positioned centrally in the narial cavity (Fig. 3A). The sheet-like dorsal process extends dorsomedially from the apex of the septomaxillary canal and terminates close to the dorsal margin of the external nares, virtually subdividing the narial opening into anterior and posterior orifices. This is somewhat similar to the position of the septomaxilla as described in the varanopid *Archaeovenator* (Reisz and Dilkes 2003). The ventral plate partially floors the narial chamber and encloses the anterodorsal surface of the vomer. The medial margin of the ventral plate probably extended to meet its partner at the midline of the snout.

Conflicting accounts exist of the morphology of the septomaxilla among early reptiles. The septomaxilla of *Captorhinus laticeps* (as *Eocaptorhinus laticeps*) is described as a “thin, rectangular sheet of bone that has been curved around a basic conical form” (Heaton, 1979:23 and fig.14). This funnel-like element had a lateral opening in the form of a C-shaped lamina visible within the narial cavity and a smaller medial

opening lying adjacent to the anterior vomer. Heaton further suggested that the septomaxillae of other early sauropsids were similar to this morphology where preserved. Indeed, *Captorhinus*, along with *Paleothyris, Petrolacosaurus* and *Youngina* are scored as possessing a septomaxilla shaped as a curled sheet in the character/taxon matrix of Reisz *et al.* 2010. This view was questioned by Modesto *et al.* (2007), describing the septomaxilla in the early Permian captorhinid *Labidosaurus* as “an irregular convoluted bone”, with a ventral lamina, a peaked medial process and dorsal process (Modesto *et al.* 2007: 239).

The main features of the septomaxilla in *Orovenator* are present in several taxa where the septomaxilla has been adequately described. A ventral or horizontal plate is found in in *Dimetrodon limbatus* (Romer and Price 1940), in the captorhinid *Labidosaurus* (Modesto et al. 2007) and in extant amphisbaenians and uropeltid snakes (Maisano et al. 2006, Olori and Bell 2012). The dorsal process, slightly medially inclined in *Orovenator* and *D. limbatus*, is also present in the Permian parareptiles *Colobomycter pholeter* (MacDougall *et al.* 2017) and *Milleretta rubidgei* (Gow 1972*)*, in the varanopid *Varanops*, where it is exposed facially (Campione and Reisz 2010), the ophiacodontid *Varanosaurus* (Berman et al. 1995) and *Labidosaurus* (Modesto et al. 2007). In some extant squamates the dorsal process curves dorsomedially to form the roof of a vaulted chamber that accommodates the vomeronasal organ (e.g. amphisbaenians; Maisano *et al.* 2006, gekkotans; Rieppel *et al.* 2008 and anilioid snakes; Rieppel 2007). The septomaxillary canal and anterior process of *Orovenator* are similar to those described in *D. limbatus* and other sphenacodontians (Brink *et al.* 2016).

The phylogenetically broad distribution of similar features of the septomaxilla is consistent with a shared function that may be plesiomorphic for amniotes. Watson (1914) and Hillenius (2000) suggested that the septomaxillary canal of early

synapsids housed the anterior progression of the nasolacrimal duct towards the vomeronasal organ (VNO), a paired chemosensory organ located in the anterior of the snout in some extant tetrapods (Bertmar 1981). In extant squamates the VNO is enclosed by the vomer ventrally and the septomaxilla dorsally (Rieppel et al. 2008), and it is connected to the vomeronasal duct either directly, as in snakes, or indirectly, as in most other squamates, via an opening at the anterior end of the choanal groove (Hillenius and Rehorek 2005). *Orovenator* provides the earliest known example of a 3-dimensionally preserved septomaxilla in diapsids, which together with the well-developed nasolacrimal duct of the lacrimal (Fig. 5B), suggests a similar function to that proposed for early synapsids (Hillenius 2000).

Lacrimal. The left lacrimal of OMNH 74606 is almost complete, lacking only a section of the anterodorsal lamina and a posterodorsal portion that contacted the prefrontal. Only fragments of the right lacrimal are preserved. The posterodorsal portion of the lacrimal, including the prefrontal contact, is best preserved in the right lacrimal of OMNH 74607. The lacrimal is comprised of a posteriorly located ventral process that overlaps the anterolateral surface of the prefrontal and forms the anteroventral margin of the orbit ventrally, and a dorsally located anterior process that overlaps the dorsolateral margin of the nasal and attenuates anteriorly to form the posterodorsal margin of the external naris (Fig. 3). The dorsal and dorsolateral surfaces are thin bone, and the sinuous ventral surface is thickened medially to accommodate the nasolacrimal canal and the epithelial tube housed within it, the nasolacrimal duct (*sensu* Witmer 1997). The contact between the lacrimal and the external naris is transversely narrow. It forms the posterior margin of a distinctive posterodorsal extension of the external naris, enclosed dorsally by the nasal and ventrally by the maxilla. A prominent posterodorsal extension is considered a synapomorphy of varanopids (Reisz and Dilkes 2003, Reisz *et al.* 2010).

The lacrimal has an anterodorsal surface that meets the lateral surface at a right angle, forming a rounded antorbital ridge (Reisz *et al.* 2011). This ridge extends anteriorly along the dorsolateral surface of the snout from the prefrontal posteriorly to the posterodorsal extension of the external naris. This morphology of the lacrimal is quite unique amongst early amniotes and is probably autapomorphic in *Orovenator.*

The dorsal surface of the lacrimal slopes anteroventrally towards the tip of the snout where it bears a transversely narrow anterior process that makes a small contribution to the posterodorsal margin of the external naris, preventing contact between the maxilla and the nasal. The sinuous ventral margin of the lacrimal is overlapped by the maxilla along most of its anteroposterior length. Posteroventrally it contacts the anteromedial surface of the suborbital process of the jugal.

The ventral process of the lacrimal bears a posteriorly directed orbital shelf, which extends from the mid-point of its contact with the prefrontal to the posteroventral tip of the lacrimal. This shelf contributes to the anteroventral margin of the orbit. In OMNH 74607, a deep conjunctival groove can be seen on the surface of this shelf. The ventral process of the prefrontal overlies the orbital shelf of the lacrimal medially (Fig.5). The lacrimal/prefrontal contact extends anteromedially along the dorsal surface of the skull up to the lateral margin of the nasal. In this region the lacrimal attains its greatest mediolateral width, and overlaps a lateral shelf on the dorsal surfaces of both the prefrontal and the nasal (Fig. 3C).

An anteroposteriorly elongate lacrimal that contributes to the orbit and bears a long anterior process that contacts the external naris is primitively present in amniotes (de Braga and Rieppel 1997). This morphology is retained in most early sauropsids, as seen in all non-diapsid eureptiles, including captorhinids (Carroll 1969, Fox and Bowman 1966, Heaton 1979) and in many early synapsids (Spindler *et al.* 2018,

Reisz and Dilkes 2003, Langston and Reisz 1981, Romer and Price 1940). The lacrimal of araeoscelidian diapsids makes an extensive contact with the external naris, and this is facilitated by the presence of a dorsoventrally low maxilla (Reisz 1981, Reisz *et al.* 1984). *Orovenator* exhibits an intermediate condition, in which the presence of a dorsal process of the maxilla constricts the lacrimal contact with the external naris. In later Permian neodiapsids (*Lanthanolania;* Modesto and Reisz 2003 and *Acerosodontosaurus*; Bickelmann et al. 2009), and some varanopids (*Mesenosaurus;* Reisz and Berman 2001 and *Mycterosaurus*; Berman and Reisz 1982), a tall dorsal process of the maxilla excludes the lacrimal from the external naris altogether.

The thickened ventromedial surface of the lacrimal bears a prominent ridge anteriorly (Fig. 5A). The ventral surface of this ridge is transversely concave (arcuate), and anterolaterally bears an elliptical facet that contacts and is supported ventrally by the medial crest of the maxilla. The ridge forms the ventral wall of the nasolacrimal canal. The pathway of the nasolacrimal canal can be traced posteriorly to three openings on the orbital shelf of the lacrimal. Two larger lacrimal puncti open into the conjunctival groove and a third smaller foramen into a medial groove close to the posterior tip of the lacrimal. The canaliculi leading from the three orbital openings conjoin anteriorly. Two more canaliculi branch off the main canal, one opens dorsally, another pierces the ventral wall of the canal (Fig. 5B).

Foramina entering the posterior surface of the lacrimal from the orbital margin have been documented in several other early eureptiles. Two such foramina are reported in the basal captorhinid *Euconcordia* (Müller and Reisz 2005b), the early Permian captorhinid *Reiszorhinus* (Sumida *et al.* 2010), and in the archosauromorph *Prolacerta* (Gow 1975). Three foramina have been described in *Petrolacosaurus* and *Captorhinus laticeps* (Reisz 1981, Heaton 1979), both with two large puncti within the

conjunctival groove and a third medial to them, a configuration very similar to that of *Orovenator*. The pathways of the internal canals are unknown in most of these taxa. However, the nasolacrimal canal of *Captorhinus laticeps* has been described, with two canaliculi forming a single lacrimal canal, joined at their junction by a third canaliculus, identified as housing the anterior orbital artery (Heaton 1979).

A deep cavity occupies the medial surface of the snout, bounded by the ventral surface of the nasolacrimal canal dorsally, the 'supracanine' buttress of the maxilla anteriorly, the alveolar shelf of the maxilla ventrally and the thin dorsal process of the maxilla laterally. This depression, and the elements that enclose it, is strikingly similar to morphology of the medial surface of the snout in *Prolacerta*, which lacks an antorbital fenestra (Gow 1975). The antorbital fenestra is a synapomorphy shared by crown-group archosaurs and by some members of their stem-lineage (Witmer 1997). The implications of this particular morphology are explored further below (see Discussion).

Prefrontal. The prefrontal in *Orovenator* is a triradiate element with an extensive and mildly concave dorsal surface. It provides the anterior and anterodorsal margin of the orbit. Both prefrontals are partially preserved in OMNH 74607. The most complete example is the left prefrontal of OMNH 74606, which is largely in articulation with the surrounding elements. The prefrontals are identical in both specimens, apart from several conspicuous foramina on the dorsal surface of the mature individual, OMNH 74607 (Fig. 7A).

The dorsal surface of the prefrontal is a thin sheet of bone with a triangular outline. It meets the ventral process at approximately 90° forming a distinct contrast between the dorsal and lateral surfaces of the antorbital region, which is continued anteriorly by the lacrimal (Fig. 7A). The anterolateral margin bears a broad shelf-like recess

that receives the lacrimal. Medially, the prefrontal overlies a similar recess on the nasal. The dorsal exposure of the prefrontal and the right-angled union with the lateral process is absent in other early diapsids (e.g. *Petrolacosaurus*; Reisz 1981 and pers. obs. KUVP 9952 and *Youngina*; pers. obs. BP/1/2871) but is in present in the varanopids *Mesenosaurus* (Reisz and Berman 2001) and *Elliotsmithia* (Reisz *et al.*1998).

The posterior process of the prefrontal is a thick, posteriorly tapering ramus of bone, which forms the anterodorsal margin of the orbit. The medial surface of this ramus is almost entirely occupied by a deep facet for the frontal. In ventral view the posterior process conjoins with the crista crani of the frontal, which transitions ventrally into the concave orbital rim of the prefrontal. This is best observed in OMNH 74607 (Fig. 7B).

The ventral process of the prefrontal forms the anterior margin of the orbit. Much of the ventrally tapering ramus is obscured in lateral view by the lacrimal and the suborbital process of the maxilla. Ventrally, the descending ramus remains in close contact with the medial surface of the orbital shelf of the lacrimal and extends ventrally to make a broad contact with the maxillary ramus of the palatine (Fig. 5B). A small foramen pierces the medial surface of the ventral tip of the prefrontal, which coincides with a foramen on the lateral surface of the maxillary ramus of the palatine. This would have carried blood vessels from the maxillary artery as is passed through the maxillary ramus of the palatine.

The posteromedially directed orbital rim serves as an attachment for the orbitonasal membrane, separating the orbital and nasal capsules. Laterally this rim extends to form the anteromedial wall of the orbit. This is best seen in medial view, where it joins with the dorsal and lateral regions in a deep concavity (Fig. 7B). This concavity

corresponds with the maximum transverse width of the antorbital region, and may have housed the laterally expanded flanges of the olfactory lobe.

Nasal. Only the partial left nasal of OMNH 74606 is preserved. It is an elongate, dorsoventrally thin sheet of bone posteriorly, and becomes curved anteriorly such that the dorsal surface is mildly convex posterior to the external naris. The anteromedial process, which would have contacted the dorsal process of the premaxilla medially, is not preserved. Given the morphology of the premaxillae it is likely that the nasals had a long anteromedial process, which separated the dorsal processes of the premaxillae and terminated far anteriorly, close to the tip of the snout. The median contact surface for the right nasal cannot be distinguished. The nasal is almost entirely exposed on the dorsal surface of the snout, with a limited lateral exposure of the anterior region.

The dorsoventrally narrow supranarial process of the nasal is elongate, comprising some 25% of the lateral length of the bone, reflecting to some degree the anteroposteriorly long external naris. This is unusual in early diapsids where the contribution of the nasal to the external naris is small compared to its anteroposterior length (e.g. *Youngina* and *Prolacerta*; Gow 1975 and *Lanthanolania*; Modesto and Reisz 2002). An elongate supranarial process of the nasal is associated with an anteroposteriorly elongate external naris in varanopids (Reisz and Dilkes 2003). In *Orovenator* the process is mediolaterally thin, and would have underlain the lateral margin of the dorsal process of the premaxilla.

A narrow shelf of bone extends from the lateral surface of the nasal for the lacrimal (anteriorly) and the prefrontal (posteriorly). The posterior-most region of the lateral surface of the nasal bears a slot recess that forms a tongue and groove contact with the prefrontal. Posteriorly the nasal overlaps a broad ‘V’ shaped shelf between the

anterolateral and anteromedial processes of the frontal (Fig. 7A). The suture between the paired nasals and frontals is 'W' shaped, with a broad posterolateral extension of the nasal. The posteromedial region of the dorsal surface of the nasal is slightly depressed such that it lies below the level of the posterolateral extension region, and would have been overlain by the anteromedial process of the frontal.

Skull roof and orbital region

The skull roof of *Orovenator,* as in many early diapsids, is mildly convex, sloping gently posteroventrally in the postorbital region, and sloping more steeply anteroventrally, anterior to the orbit (Fig. 3A). The postorbital region is anteroposteriorly short along the midline, and the parietals are deeply excavated posterodorsally. The large sub-circular pineal foramen is positioned on the midline within the posterior half of the parietals. The upper temporal fenestra, as indicated by the lateral excavation of the parietal, was probably the smaller of the two temporal openings. Because the postorbital, quadratojugal and squamosal are not preserved, it is not possible to confirm the completion of the ventral bar or the size and shape of the lower opening. Nevertheless, given the length of the dorsal and posterior processes of the jugal and the articular facets of the postfrontal and parietals for the postorbital, it is likely to have had at least twice the total area of the upper temporal fenestra. The orbits are large, subcircular and contain several articulated scleral ossicles. In the larger individual, OMNH 75607, the frontals, parietals, prefrontals and postfrontals bear a number of foramina, many of which are associated with small grooves in the bone surface.

Frontal. The frontals are anteroposteriorly long, paired elements of the skull roof. Only the anterior parts of the frontals of OMNH 74606 are preserved. The paired frontals of *Orovenator* are best represented in OMNH 74607, where both elements

are almost complete (Fig. 2). The frontals are relatively slender and elongate bones, as noted by Reisz *et al.* (2011). They contact the nasals anteriorly and prefrontals anterolaterally, extending into the antorbital region of the snout. Posteriorly they contact the parietals and posterolaterally the postorbitals. The frontals make anteroposteriorly broad contributions to the dorsal margins of the orbits. They are slightly concave along the orbital margin and do not possess a lateral lappet. The interorbital width of the frontals is narrow, being approximately 35% of their total median length. The maximum transverse width, approximately 44% of the median length, is level with the anterior margin of the orbit. Medially the paired frontals are sutured by a scarf joint, with the right frontal providing the dorsal overlap. The ventral surface of the frontal has a prominent *crista crani* extending along the dorsal margin of the orbit (Fig. 7B). The suture with the prefrontal consists of a tongue and groove anteriorly, and a dorsoventrally deep rugose articular surface posteriorly, which fits into a wedge-shaped facet on the medial surface of the anterior process of the prefrontal.

An anteromedial process and a smaller anterolateral process extend from the anterior region of the frontal (Fig. 7A). A thin sheet of bone extends from the ventral surface of the frontal between these two processes, and is overlain by the posterolateral process of the nasal. The anterior-most region of the anteromedial process of the frontal overlies a shallow depression on the posteromedial surface of the nasal. Consequently, contact between the frontal and nasal is distinctive: the nasal overlies the frontal laterally, and the frontal overlies the nasal medially. The prominent posterolateral process of the frontal extends at an acute angle to make contact with the entire dorsal margin of the postfrontal, thus excluding the parietal from contact with the dorsal margin of the postfrontal. A deep facet in the posterolateral margin of the frontal accommodates the postfrontal.

In the smaller individual, OMNH 74606, the dorsal surface of the frontal is relatively smooth, with only a few foramina evident. In the larger individual, OMNH 74607, the dorsal surface of the frontal exhibits several foramina (Fig. 7A). The absence of these from the smaller individual suggests that development of foramina and shallow grooves on the dermal bones developed during ontogeny. Foramina occupy the anterodorsal surface of the frontal and continue to the supraorbital area. Some of these foramina are associated with small anteriorly or laterally directed grooves. The grooves associated with the posterior foramina are more pronounced, such that a series of conspicuous posteriorly directed furrow-like grooves striate the posterodorsal surface of the frontal of OMNH 74607.

Parietal. The paired parietals make up the posterior skull roof. Only the left parietal of OMNH 74607 is completely preserved, together with a fragment of the right parietal. They have a prominent anteromedial process that contacts the frontals, a concave posterolateral margin to accommodate the upper temporal fenestra and a posterolateral process that contributes to a deeply embayed occipital margin. The dorsal surface of the parietal slopes posteroventrally and follows the curvature of the frontal.

The anteroposteriorly elongate anteromedial process of the parietal incises deeply into the frontal, extending into the supraorbital region and tapering anteriorly, as in the later diapsids *Youngina* and *Prolacerta* (pers. obs. BP/1/3859 and BP/1/4504) and varanopids (Reisz and Berman 2001). There is a small recess between the anterior tips of the paired anteromedial processes of the parietals into which fits a short posteromedial process of the frontals (Fig. 7A). Contact of the parietal with the postfrontal is limited to a weakly convex surface on the posterodorsal margin of the postfrontal. A deep notch separates the suture ventrally to accommodate the dorsal process of the postorbital.

The lateral surface of the parietal is embayed by the upper temporal fenestra posteriorly. This rim lacks the ventrolateral flange present in later diapsids such as *Prolacerta* (pers. obs. BP/1/3575), *Claudiosaurus* (Carroll 1981) and *Pamelina* (Evans 2009). The embayment of the lateral surface of the parietal is deeper than that of *Petrolacosaurus*, as noted by Reisz *et al.* (2011), and the upper temporal fenestra is visible in dorsal view. The posterolateral process extends posteriorly beyond the posterior margin of the upper temporal fenestra. Laterally this process bears a deep groove to receive the mediolaterally thin supratemporal and the dorsal ramus of the squamosal (Fig. 7A).

A large, subcircular pineal foramen is present on the median suture of the parietals. Its anterior margin is almost level with that of the upper temporal fenestra, as in *Petrolacosaurus* (Reisz 1981). However, the pineal foramen is situated entirely in the posterior half of the parietal midline, unlike *Petrolacosaurus* where the pineal foramen is positioned at the midpoint of the parietals (Fig. 7). A shallow raised platform of bone surrounds the pineal foramen. It is irregular in shape, and extends from a transversely narrow region at the posterior medial margin of the parietal to an extensive region lateral and anterolateral to the foramen.

The position of the pineal foramen varies amongst early amniotes and is phylogenetically informative (Reisz and Dilkes 2003, Reisz et al. 2010, Ezcurra 2014). In all early synapsids the pineal foramen is located posteriorly, with the exception of caseasaurs in which the foramen is anteriorly positioned. Indeed, a posteriorly located pineal foramen has been proposed as a synapomorphy of Eupelycosauria (i.e. all early synapsids except caseasaurs, and including varanopids; de Braga and Rieppel 1997). This condition, which can also be found in *Orovenator*,

is otherwise rare in eureptiles, with only *Paleothyris* (pers. obs. MCZ 3483) and *Youngina* (pers. obs. BP/1/ 3859) showing a similar morphology.

There is a deep bilateral embayment on the posterior margin of the parietals. A small, posteriorly directed spur extends from the posterior end of the parietal median suture, in the centre of this embayment. This may represent a nuchal crest. A thin lamina of bone extends posteroventrally from the embayed posterior margin of the parietal, identified as an occipital flange (Reisz *et al.* 2011)(Fig.8A). The surface of the flange is relatively smooth, with a transverse sulcus ventral to the posterior rim of the parietal, which probably accommodated the dorsal margin of the postparietal and tabular, neither of which is preserved. The flange extends posteroventrally at an angle of approximately 45° from the posterior rim of the parietal, suggesting that the occipital region may have sloped strongly posteroventrally.

Several small foramina are present on the dorsal surface of the parietal, medial to the margin of the upper temporal fenestra. On the ventral surface a small anteroposteriorly orientated ridge lies between the pineal foramen and the upper temporal fenestra (Fig. 7B). This corresponds to a similar ridge found in *Petrolacosaurus*, identified by Reisz (1981) as the point of attachment of the cartilaginous *taenia marginalis*, a dorsal extension of the chondrocranium, connecting the otic capsule with the braincase (Romer 1956).

The scan of *Orovenator* allows us, for the first time, to make a direct comparison between the left parietal of OMNH 74607 and a right parietal (YPM 4926) described as a diapsid from the fissure-fill limestone of Fort Sill, western Oklahoma (Carroll 1969). Whilst the general morphology is strikingly similar there are significant differences (Fig. 8). The pineal foramen in YPM 4926 is much larger and ovoid in shape. The embayment for the upper temporal fenestra is more extensive medially

and differs in the anterior curvature of OMNH 74606. Although only observed in the photograph provided as fig.1 (Carroll 1969) the surface appears quite smooth and lacks the raised platform of *Orovenator*. The posterolateral process of YPM 4926 is significantly narrower and more laterally orientated than OMNH 74607. We therefore agree with Reisz *et al.* (2011) that YPM 4926 is not attributable to *Orovenator mayorum* and therefore represents a different species.

Postfrontal. Both postfrontals are complete and preserved in articulation with the frontal and parietal in OMNH 75607 (Fig. 2). The postfrontal is a small triangular bone that forms the posterodorsal corner of the orbital margin, contacting the frontal dorsally, the parietal posterodorsally and the postorbital posteroventrally. The anterodorsal process is slightly longer than the ventral process, which it meets posteromedially at an angle of approximately 90°. The dorsolateral surface of the postfrontal bears more than a dozen foramina of various sizes distributed principally along its medial and posterior margins.

The medial articular surface of the postfrontal for the frontal is broad and rugose. It bears a narrow, anteroposteriorly-orientated ridge that fits into a deep recess on the posterolateral surface of the frontal. A small shelf of bone extends posteriorly from the ventral surface of the posterodorsal corner of the postfrontal and is overlain by the parietal. This is unlike the situation in *Petrolacosaurus,* in which a shelf on the parietal underlies the postfrontal (Reisz 1981). The postfrontal of *Orovenator* is prevented from contributing to the upper temporal fenestra by contact between the parietal and the postorbital, the dorsal ramus of which is accommodated by a deep notch formed between the ventrolateral processes of the postfrontal and parietal.

The exclusion of the postfrontal from the upper temporal fenestra by contact of the parietal and postorbital is plesiomorphic in diapsids. This morphology was present in

the earliest diapsids *Petrolacosaurus* (Reisz 1981) and *Araeoscelis* (Vaughn 1955), and in later neodiapsids (e.g. *Lanthanolania* and *Youngina* (Modesto and Reisz 2002, Reisz et al. 2000)). The plesiomorphic condition also appears in early archosauromorphs such as *Prolacerta* (Modesto and Sues 2004), *Macrocnemus* (pers. obs. C 111 (MCSNM)) and *Tanystropheus* (Nosotti 2007). In early non-diapsid amniotes (early synapsids, captorhinids and parareptiles) the parietal/postorbital contact is almost universal. Exceptionally, such contact is prevented by the postfrontal and supratemporal in the parareptile *Acleistorhinus* (de Braga and Reisz 1996).

The derived condition, where the postfrontal prevents contact between the parietal and postorbital, is first observed in *Acerosodontosaurus* and *Hovasaurus* (Currie 1980, 1981). Although Bickelmann *et al.* (2009) queried this interpretation in *Acerosodontosaurus* due to the poor preservation of the skull roof. It is present convergently in early lepidosauromorphs (Evans and Borsuk-Bialynicka 2009, Evans 1991) and extant lepidosaurs (Evans 2008).

Supratemporal: the anterior portion of the left supratemporal is preserved *in situ* in OMNH 74607, within a groove on the lateral surface of the posterolateral process of the parietal (Fig. 2D). It is a mediolaterally thin, anteroposteriorly elongate bone, which probably extended to the tip of the posterolateral process of the parietal, with a slight posteromedial curve. It is excluded from any participation in the upper temporal fenestra by the squamosal and parietal. A thin lamina of bone extends from the ventral margin of the supratemporal. Anteriorly this lamina fits into a small facet on the parietal, and posteriorly it would have been overlain by the squamosal.

Jugal. The right jugal of OMNH 74606 is almost completely preserved, with only the anterior region and dorsolateral surface of the suborbital process missing (Fig. 1D). A

deep sub-circular cavity of uncertain origin is located on the lateral surface of the dorsal process near its origin ventrally (Fig. 3A). Only the suborbital process of the left jugal of OMNH 74606 is preserved, in articulation with the maxilla and lacrimal. This element provides valuable data on the nature of the anterior contact and overall length of the jugal, which is absent on the right side.

The jugal is a distinctly triradiate bone. The suborbital process is anteroposteriorly elongate, and extends to the level of the anterior orbit margin. The posterior process attenuates posteriorly to a fine point and is orientated slightly posteromedially. This process provides the anteroventral bar to the lower temporal fenestra (in taxa with 'diapsid' or 'synapsid' skulls). The dorsal process of the jugal is anteroposteriorly broad at its origin in central region of the jugal. It is orientated posterodorsally and somewhat medially, tapering to a point along its length. The suborbital and dorsal processes jointly form the posteroventral margin of the orbit.

The suborbital process of the jugal is mediolaterally thin and blade-like, tapering slightly towards the anterior tip to terminate in a smoothly round point. The ventral surface of the posterior half of the process fits into a shallow recess on the posterior part of the maxilla. Only the posterior half of the suborbital process is visible in lateral view. The anterior half contacts the medial surface of the maxilla. The posterior process of the lacrimal overlies the anterior region of the jugal medially, such that it is enclosed between the maxilla and the lacrimal (Fig. 5).

The posterior or subtemporal process of the jugal is a slender, tapering component that terminates in a fine point. There is no evidence of a facet for contact with the quadratojugal on the lateral or medial surface of the posterior process, which is smooth and featureless. Nevertheless, in the absence of the preservation of the quadratojugal, the completion or non-completion of the ventral bar of the lower

temporal fenestra cannot be unequivocally determined. The dorsal process of the jugal is triangular in cross-section, with a mediolaterally broad orbital rim and a blade-like posterior margin. The lateral surface bears a shallow depression that probably received the ventral process of the postorbital.

Scleral ossicles. An articulated series of seven partially or completely preserved scleral ossicles, and two further disarticulated ossicles, lie within the orbit of OMNH 74606 (Fig. 1B). The more complete examples are thin irregular rectangular sheets of bone, approximately twice as long radially as wide circumferentially. Exteriorly the surface is convex along its long axis (i.e. radially). The lateral surface does not taper towards the aperture, unlike in ichthyosaurs (McGowan and Motani 2003), and inter-ossicular contact is entirely limited to unidirectional overlapping sutures rather than irregular overlapping or abutting sutures, particularly towards the aperture where the contact is most extensive. Both internal and external surfaces are smooth. Each ossicle overlaps its neighbour in a clockwise direction.

Although many groups of vertebrates possess scleral cartilage, fewer possess both the scleral cartilage and ossicles that form the sclerotic ring. The sclerotic ring is common in teleost fish, and several groups of extant sauropsids: testudines, birds and most squamates except snakes (Atkins and Franz-Odendaal 2016). In extinct taxa scleral ossicles were present in seymouriamorphs (Klembara 1997), early synapsids, therapsids and basal cynodonts (Angielczyk and Schmitz 2014), some captorhinids and many archosaurs, including dinosaurs (Romer 1956). Preserved examples amongst early fossil diapsids are quite rare. They are present in *Petrolacosaurus* (Reisz 1981) and some archosauromorphs (e.g. *Prolacerta*; Camp 1945 and *Tanystropheus;* Nosotti 2007).

Orovenator is estimated to have possessed 19 scleral plates, based on a virtual reconstruction of the orbit and sclerotic ring in the present study (see Supplement 1). This is a relatively high number of plates compared to estimates from other diapsids. Fourteen plates are reported in *Prolacerta* (Romer 1956), twelve in the Triassic marine reptile *Askeptosaurus* (Müller 2005) and twelve in the archosauromorph *Euparkeria* (Sookias and Butler 2013). However, the reduction in the number of scleral plates may be a derived feature of later diapsids, since up to 20 plates are reported in late Carboniferous tetrapod *Gephyrostegus bohemicus* (Klembara et al. 2014), up to 19 in the early Permian synapsid *Sphenacodon ferox* (Spielmann et al. 2010) and as many as 40 in the seymouriamorph *Discosauriscus* (Klembara 1997).

Palate, palatoquadrate and braincase

All elements of the palate are present in OMNH 74606, permitting an accurate reconstruction (Fig. 9). The choanae are extremely elongate, incising deeply into the anterior surface of the palatines. Although the medial surface of the left pterygoid is missing, the pterygoids probably contacted each other on the midline for approximately half the length of the palatal ramus, limiting the anterior extent of the interpterygoid vacuity. All elements of the palate bear teeth, including the ectopterygoids and the cultriform process of the parabasisphenoid. The suborbital fenestrae are very narrow mediolaterally, more so anteriorly where the lateral margin of the palatine closely approaches the maxilla. The presence of a suborbital opening has been proposed as an autapomorphy of sauropsids (de Braga and Rieppel 1997). It is generally present as a small foramen in captorhinids (Heaton 1979, Romer 1956), and is enlarged to a fenestra in diapsids (Laurin and Reisz 1995). It is absent in synapsids (Romer and Price 1940). In early diapsids such as *Petrolacosaurus* (Reisz 1981) and *Youngina* (Carroll 1981) the suborbital fenestra is anteroposteriorly

long and moderately broad. Therefore the narrow suborbital fenestra in *Orovenator* is somewhat anomalous for early diapsids.

Vomer. The paired vomers are unfused anterior elements of the palate that contact the premaxillae anteriorly, the palatines posteriorly, and the pterygoids posteromedially. Both vomers are preserved in OMNH 74606. In ventral view the vomers are anteroposteriorly elongate triangular bones. They bear two distinct longitudinal series of denticles: a medial series of larger denticles and lateral array of smaller denticles. The vomers form the medial margins of the choanae, and are joined along the midline of the palate for three quarters of their length. A narrow shelf extends medially from the right vomer and overlies the dorsal surface of the left vomer.

Anteriorly the vomer contacts the premaxilla in an asymmetrically bifurcated suture, consisting of a small anterolateral process and a larger anteromedial process, which joins its partner on the midline (Fig. 4C). The vomerine process of the premaxilla fits into the notch between these anterior processes of the vomer. The lateral surface of the vomer forms the medial margin of the choana along its entire length. Posteriorly it is overlain by the palatine dorsally forming a ‘V’ shaped suture. The tapering anterior palatal process of the pterygoid contacts the posteromedial margin of the vomer.

Two irregular rows of large denticles extend anteriorly from the contact with the pterygoid along the medial region of the ventral surface the vomer. An array of smaller denticles situated on a low ridge extends from the lateral contact with the palatine and converges anteriorly with the larger denticles. A longitudinal median ridge extends along the anterodorsal surface of the vomers, similar to that of *Petrolacosaurus* (Reisz 1981), where it probably supported the cartilage of the

internasal septum. A low dorsal ridge is also present laterally, resulting in a 'U' shaped cavity on the anterodorsal surface of the vomer.

Palatine. The palatines are paired, lateral bones, both of which are preserved in OMNH 74606. Each contacts the vomer anteriorly, the pterygoid medially and the ectopterygoid posteriorly. The palatine is a dorsoventrally thin, sheet-like bone that is trapezoidal in ventral view, with a lateral maxillary ramus that anchors the palate to the alveolar shelf of the maxilla (Figs 5B, 9). The palatine is deeply incised by the choana anterolaterally such that the posterior region of the choana is enclosed between the palatine medially and laterally. A narrow field of large denticles extends anterolaterally from the posterior border with the pterygoid to the maxillary ramus. Several denticles are also present on the anteromedial region of the ventral surface of the palatine, which continue on to the posterior region of the vomer.

The anterior portion of the palatine is a triangular sheet of bone that tapers anteriorly. It overlaps the dorsal surface of the vomer. The lateral margin of the anterior portion of the palatine bears a ventral ridge posteriorly where it meets the maxillary ramus. The palatine is inflected to slope posteroventrally posterior to the choana. The medial margin of the palatine contacts the pterygoid along its entire length. The posterior region of both palatines is missing, but the contact with the ectopterygoid can be inferred from the anterior extension of the medial margin of the suborbital fenestra, which in *Orovenator* is anteroposteriorly long and mediolaterally very narrow. The suborbital fenestra is enclosed by the alveolar shelf of the maxilla laterally and by the palatine and the ectopterygoid medially.

The maxillary ramus of the palatine is connected to the main body of the palatine by a robust, dorsally thickened flange of bone. Anteroposteriorly it is rather elongate, being approximately one third the estimated length of the palatine, as in

Petrolacosaurus (Reisz 1981). The lateral surface of the ramus is deeply concave, and consists of two elements; a vertically orientated ventral process that contacts the medial surface of the alveolar shelf of the maxilla, and a shorter but transversely broader, horizontally orientated dorsal process which overlies the dorsal surface of the alveolar shelf.

A canal, which opens via a foramen on the posterior surface of the maxillary ramus, accommodates the anterior progress of the maxillary artery and nerve (Fig. 5B). It is evident from the position of the infraorbital foramen on the maxilla that the infraorbital artery and nerve, a subsidiary of the maxillary artery and nerve, enters the infraorbital foramen immediately posterior to the suture with the maxillary ramus of the palatine. Within the maxillary ramus the canal divides into two branches, one exits the ramus anteriorly and houses the main maxillary artery and nerve, which extends along a sulcus in the alveolar shelf before entering the anterior opening of the alveolar canal. The other branch is directed dorsally where it divides again into two dorsomedially orientated branches emerging as grooves on the dorsal surface of the robust flange joining the maxillary ramus to the main body of the palatine (Fig. 5B). They extend across the posterodorsal surface of the anterior portion of the palatine, where they probably meet the palatine artery and nerve medially, similar to the anterior passage of these arteries and nerves in *Gephyrosaurus* (Evans 1980). The posterior dorsomedial branch has a ventral extension, which opens onto the lateral surface of the ramus adjacent to a foramen on the alveolar shelf that is overlain by the maxillary ramus. Several anastomosing capillaries are associated with the main canal.

Ectopterygoid. The ectopterygoid is an auriform posterolateral element of the palate. Both ectopterygoids are preserved in OMNH 74606. It consists of a dorsoventrally thin sheet of bone that overlies the medial part of the transverse flange of the pterygoid dorsally, contacts the posterior margin of the palatine and bears a flange

on the posterolateral surface, which expands in to an anteroposteriorly elongate but dorsoventrally narrow jugal ramus. Anterolaterally the ectopterygoid forms the posteromedial and posterior margin of the suborbital fenestra.

The posterior surface of the ectopterygoid forms the anterior boundary of the subtemporal fenestra and bears an arcuate ventral ridge that grades into the lateral rim of the transverse flange of the pterygoid. The ventral surface of the ectopterygoid bears several small denticles, some of which continue as a sparse cluster on to the surface of the pterygoid. The lateral margin of the jugal ramus, which contacts the medial surface of the jugal, is smooth and featureless. The nature of the suture with the palatine cannot be determined. Anterolaterally, a shallow emargination of the lateral margin encloses the posterior region of the suborbital fenestra.

Pterygoid. The pterygoids are the largest of the palatal elements and the longest bones in the cranium. Both pterygoids are present in OMNH 74606, with the right pterygoid the better preserved of the two, missing only the posterior portion of the quadrate ramus. They contact all other bones of the palate, as well as the basicranium and the quadrate. The pterygoids therefore play a key role in the structural integrity of the skull.

The pterygoid of *Orovenator* has an anteroposteriorly elongate palatal ramus, which tapers mediolaterally from the basal articulation to its anterior end, which contacts the medial surface of the vomer (Fig. 9). It slopes posteroventrally as is observed in the palatine. The palatal ramus of the pterygoid bears two distinctive fields of denticles on its ventral surface. The first series occupy a ventrally raised ridge, which extends from the basal articulation along the ventromedial surface of the ramus, tapering to a point anteriorly, before continuing on to the ventromedial surface of the vomer. The denticles are tightly but irregularly spaced and are confined to the ridge. A dorsally

inclined lamina extends from the denticle bearing ventromedial surface of the palatal ramus, where it probably met its partner medially. The second series of denticles are less densely clustered and extend anterolaterally from the basal articulation to the pterygoid contact with the palatine, continuing onto the ventral surface of the palatine.

The transverse flange is rectangular in outline, as in *Lanthanolania* (Modesto and Reisz 2002), and is posteroventrally orientated more steeply than the palatal ramus by an additional angle of 32°. The lateral and posterior margins of the transverse flange form an angle of approximately 85° in ventral view, and the process is orientated slightly posterolaterally, as in *Youngina* and *Prolacerta* (Carroll 1981, Gow 1975, Modesto and Sues 2004), but unlike in *Petrolacosaurus* and *Araeoscelis*, in which the transverse process extends anterolaterally (Reisz 1981, Vaughn 1955). Six large denticles, the largest of the palate, are attached to the rim of the posteroventral margin of the process, and three more extend anteriorly from the posterolateral corner. The anterior buttress of the basal articulation projects medially from the median junction of the palatal ramus and the quadrate ramus of the pterygoid, and is formed solely by the pterygoid. It is an anteroposteriorly thin sheet of bone, which slopes slightly anterodorsally. The recess of the basal articulation is directed posteromedially and slightly dorsally. Lateral to the basal articulation the dorsal surface of the pterygoid slopes ventrally to form a narrow neck of bone that joins the quadrate ramus to the transverse flange. This surface bears a shallow longitudinal depression, which accommodates the base of the epipterygoid.

The quadrate ramus of the pterygoid extends posterolaterally from the basal articulation and is somewhat dorsally inclined. It is composed of a mediolaterally thin, vertical sheet of bone with a thickened ventral rim, the dorsal flange (Fig. 10). A dorsoventrally thin arcuate flange is also present and extends medially from the

ventral rim of the dorsal flange at an angle of approximately 90°(Fig. 10B). Although missing its posterior region, the arcuate flange is mediolaterally broad, and the ventral surface is mildly concave. This is somewhat similar to the quadrate ramus in *Captorhinus laticeps,* where a tympanic membrane sheathed the concave ventral surface of the arcuate flange (Heaton 1979). This morphology of the quadrate ramus appears to be plesiomorphic for amniotes, and is seen in basal captorhinids, early diapsids and early synapsids (Müller and Reisz 2005, Vaughn 1955, Romer and Price 1940).

A mediolaterally thin, vertical septum of bone connects the dorsal flange to the arcuate flange of the anterior quadrate ramus, creating a deep posteriorly facing cavity. The smooth medial surface of this septum provides the posterior buttress for the basipterygoid process (Fig. 10B). Posteriorly, the lateral surface of the dorsal flange probably contacted the medial surface of the pterygoid wing of the quadrate, but the nature of the suture cannot be determined.

Epipterygoid. Both epipterygoids are preserved in OMNH 74606. The right epipterygoid is the more complete of the two. The epipterygoid consists of a triangular base, with a convex ventral margin in lateral view. The ventral surface is anteroposteriorly long, and tapers mediolaterally towards its posterior end. Anteriorly, a small lenticular facet extends anterodorsally from the ventral surface. A mediolaterally-compressed columella projects dorsally from the apex of the triangular base.

The ventral surface of the epipterygoid is rugose. Prior to disarticulation, it was attached, probably via a connective tissue, to a shallow depression on the dorsal surface of the quadrate ramus of the pterygoid, dorsolateral to the basal articulation (Fig. 10A). Contrary to Reisz *et al*. (2011) the anteroventral lenticular facet does not

contribute to the basal articulation, but instead contacts a small ridge of bone that extends anterolaterally from the anterior buttress of the basal articulation. The lateral and medial surfaces of the dorsal columella are smooth, the anterior margin almost straight and the posterior margin is mildly concave. The columella of the right epipterygoid is missing the dorsal tip, but it is likely that it continued to curve posteriorly, as in *C. laticeps* (Heaton 1979), terminating in a cartilaginous extension that contacted the ventral surface of the parietal.

The shape and position of the epipterygoid of *Orovenator* is similar to that of *Youngina* as figured in lateral view by Gow (1975:94 fig. E). Gow suggested that the morphology of the epipterygoid in *Youngina* might be similar to that of the late Permian parareptile *Milleretta,* in which a small anterior process of the base "roofs" the basal articulation, rather than participates in the recess for the basipterygoid (Gow 1972:236). In *Prolacerta* the epipterygoid overlies the basal articulation in a manner somewhat similar to *Milleretta* (Gow 1975). The base of the epipterygoid of *Orovenator* has a smooth, mildly convex lateral surface. The medial surface, which lies dorsolateral to the basal articulation, consists of unfinished bone in both epipterygoids (Fig. 10B). OMNH 74606 is an immature individual and, therefore, since other elements of the palatoquadrate of this specimen are finished in cartilage (cf. quadrate), it is possible that a cartilaginous extension to the medial surface of the base of the epipterygoid capped or participated in the basal articulation.

An anteromedial exposure of the base of the epipterygoid contributes partly or wholly to the basal articulation in captorhinids (*Captorhinus aguti*; Fox and Bowman 1966 and *C. laticeps*; Heaton 1979) and early diapsids (*Petrolacosaurus*; Reisz 1981). This has also been reported in the varanopid *Varanops* (Campione and Reisz 2010). Laurin (1991) notes the epipterygoid of the varanopid *Apsisaurus* probably did not participate in the basal articulation, an interpretation disputed by other authors

(Campione and Reisz 2010). In early lepidosauromorphs such as *Diphydontosaurus, Gephyrosaurus* and *Marmoretta* (Whiteside 1986, Evans 1980, Evans 1991), the epipterygoid does not participate in the basal articulation.

Quadrate. Only the right quadrate of OMNH 74606 is preserved (Fig. 11). It is a relatively short element, which is slightly taller dorsoventrally than long anteroposteriorly. The posteroventral condylar region is damaged or unfinished with much of the articular surface missing. A quadrate shaft extends dorsally from the condylar region. An anteroposteriorly broad and transversely narrow lamina or pterygoid wing extends anteromedially from the posterior shaft and condylar region. This lamina has a convex anterior margin of unfinished bone which slopes anteroventrally from the dorsal margin of the posterior shaft.

The posterior surface of the shaft is quite straight, with no evidence of the anterior curvature that is common to early members of the diapsid crown-group, Sauria (e.g. *Prolacerta;* Gow 1975, *Pamelina*; Evans 2009 and *Paliguana*; pers. obs. AM3585). A prominent shelf of bone extends from the medial surface of this shaft, transitioning ventrally into the anteromedial condyle (Fig. 11B). Reisz *et al.* (2011) suggest this received the distal region of the paroccipital process. However, it may alternatively have supported a cartilaginous extension of the columella of the stapes, which contacted a shallow recess in the medial surface of the quadrate shaft, similar to the structure found in *Captorhinus aguti* and *Araeoscelis* (Fox and Bowman 1966, Vaughn 1955). A small notch, the quadrate foramen, is present in the posterolateral surface of the quadrate shaft, immediately lateral to this shelf (Fig. 11B).

Orovenator has a single pterygoid wing extending anteromedially from the quadrate shaft, as in *Petrolacosaurus* and early synapsids (Reisz 1981, Romer and Price 1940). There is no lateral tympanic crest, unlike in *Prolacerta* (Modesto and Sues

2004), or anterolateral conch, as in early lepidosauromorphs (*Pamelina*; Evans 2009 and *Sophineta*; Evans and Borsuk-Bialynicka 2009). The lateral surface of the pterygoid wing is relatively smooth. The medial surface is slightly rugose. However, it does not bear the prominent scarring seen in some captorhinids, in which the medial surface of the pterygoid wing contacts the lateral surface of the quadrate ramus of the pterygoid (Fox and Bowman 1966, Heaton 1979). The transversely narrow, anteroventrally curving anterior surface of the lamina consists of a deeply concave groove of unfinished bone (fig. 11D). It is likely that a cartilaginous anterior extension of this surface provided the main region of contact with the pterygoid, and may, given the immature nature of OMNH 74606, have been in the process of ossification.

Parabasisphenoid. The ventral plate of the braincase (the basisphenoid) and the dermal bone that sheaths it ventrally (the parasphenoid) are difficult to delimit in *Orovenator*, and are here described as a single compound element, the parabasisphenoid (Fig. 12). This bone is composed of four principal structures, the elongate and narrow cultriform process anteriorly; the dorsal surface, which bears the pituitary fossa and clinoid processes; the anterolaterally directed basipterygoid processes; and the ventral surface enclosed laterally by the cristae ventrolaterales. OMNH 74606 preserves all of these structures, lacking only the posterior part of the ventral surface of the parabasisphenoid.

The cultriform process is formed of two anteroposteriorly elongate lateral laminae that meet ventrally to produce a deep ‘V’ shaped trough (Fig. 12). It extends anteriorly from the anterior margin of the pituitary fossa to the level of the choanae, attenuating gradually to a fine point. In doing so it bisects the interpterygoid vacuity, but does not contact the medial margin of the pterygoids. The cultriform process does not extend anteriorly beyond the anterior tip of the pterygoids, unlike in *Araeoscelis* (Vaughn 1955).

The ventral surface of the cultriform process bears approximately 24 small denticles posteriorly. Reisz *et al.* (2011), using a scanning electron microscope, also noted the bases of small denticles on the ventral surface of the parabasisphenoid and the cristae ventrolaterales. The presence of teeth on the parabasisphenoid is primitive for amniotes, and this trait is lost in early archosaurs, rhynchosaurs and lepidosaurs (Evans 1986). Its distribution amongst early amniotes, however, is not uniform. In captorhinids, a dentate parasphenoid is known in *Euconcordia* and *Captorhinus aguti* (Muller and Reisz 2005b, Fox and Bowman 1966*)*, but is absent in *Captorhinus laticeps*, *Romeria* and *Protocaptorhinus* (Heaton 1979). In diapsids, denticles on the cultriform process are reported in *Petrolacosaurus* and *Lanthanolania* (Reisz 1981, Modesto and Reisz 2003), but absent in *Araeoscelis* and *Youngina* (Vaughn 1955, Gow 1975). In synapsids both caseasaurs and varanopids have a dentate parasphenoid (Maddin *et al.* 2008, Reisz and Berman 2001, Spindler *et al.* 2018), although even within these groups the character state remains variable, as in the varanopid *Archaeovenator* where the parasphenoid is edentulous (Reisz and Dilkes 2003). Dentition is entirely absent in ophiacodontids, edaphosaurids and sphenacodontids where the parabasisphenoid is preserved (Benson 2012). The nyctiphruretid parareptile *Abyssomedon* has a few small denticles on the parasphenoid, whereas in its sister taxon *Nyctiphruretus* the cultriform parasphenoid is edentulous (MacDougall and Reisz 2014).

The dorsal surface of the parabasisphenoid anterior to the dorsum sellae is roughly pentagonal in dorsal view, with a short rostral process that narrows anteriorly from the level of the basipterygoid processes (Fig. 12B). The rostral process has a flat anterior surface that marks an abrupt anatomical transition to the dorsally hollow cultriform process. It therefore lacks the anterior projections of the *cristae trabeculares*. These are paired, small anteriorly tapering pedicels of bone on the

anterolateral surface of the rostral process of the parabasisphenoid that bear facets for the *trabeculae cranii,* and are present in *Petrolacosaurus* (Reisz 1981), *Gephyrosaurus, Youngina* and extant squamates (Evans 1980, Evans 1987, Evans 2008). Trabecular facets on the rostral process are also absent in early archosauromorphs, such as *Prolacerta* and *Tanystropheus*, and early archosaurs, in which the raised dorsolateral borders of the cultriform process may represent a composite ossification of the trabeculae (Evans 1986). However, the *cristae trabeculares* are posterior extensions of the cartilaginous *trabeculae cranii* (Evans 2008), and it is also possible that they were incompletely unossified in OMNH 74606 due to its juvenile status.

A deep ovoid pit is present on the midline of the dorsal surface of the rostral process, opening anteriorly into the cultriform recess through a 'V' shaped notch (Fig. 12B). This is the pituitary fossa, which contained the pituitary gland. A shallower, transversely broad depression for the retractor bulbi muscles is located just posterior to the pituitary fossa. The dorsum sellae, an anteriorly sloping transverse sheet of bone, rises from the posterior margin of the retractor depression, supported laterally by the clinoid processes. The left clinoid process is missing its dorsal tip and some of the dorsum sellae attached to it is incomplete. Nevertheless, it is clear from what remains that the dorsum sellae was rather low. The dorsoventrally low dorsum sellae of the parabasisphenoid suggests that the prootic contributed substantially to the dorsum sellae, a feature usually associated with early synapsids rather than sauropsids (Romer and Price 1940). The dorsal articular surface of the clinoid process would have supported both the prootic and a cartilaginous dorsal bar, the pila antotica (Romer 1956).

The basipterygoid processes are robust, finger-like projections that emerge anteroventrolaterally from the parabasisphenoid, between the bases of the clinoid

processes posteriorly and the rostral process anteriorly. They are somewhat ventrally orientated (Fig. 12E). Distally each process bears two facets, a semi-circular anterior facet that contacts the similarly shaped posterior surface of the anterior buttress on the basal articulation, and a dorsal facet that abuts the septum of bone bridging the anterior dorsal and arcuate flanges of the quadrate ramus of the pterygoid. The resulting contact would have been quite rigid and permitted little flexibility between the palate and the braincase. Posteriorly and ventrally the basipterygoid process consists of a robust shaft of smooth bone, with minimal constriction at the point of connection with the main body of the parabasisphenoid.

The ventral surface of the parabasisphenoid is smooth concave surface, confined laterally by the *crista ventrolateralis,* a thickened, ventrally rounded ridge of bone that extends posterolaterally from the ventral surface of the basipterygoid process (Fig. 12 D). Much of the shelf of bone connecting the cristae posterior to the dorsum sellae is missing in OMNH 74606.

The vidian sulcus can be seen on both lateral surfaces of the parabasisphenoid. It begins as a shallow groove, becoming progressively deeper, that extends along the lateral surface of the parabasisphenoid anteroventrally from the base of the clinoid process. It passes below the basipterygoid process, where it forms a deep groove between the ventrolaterally projecting ridge of the parasphenoidal plate and the ventral surface of the basipterygoid process. The vidian sulcus traces the route of the palatine branch of the facial nerve and the internal carotid artery (Romer 1956). A large foramen opens along the sulcus ventral to the anteroventral surface of the basipterygoid process (Fig. 12A) At this point the internal carotid artery divides into the palatine artery, which continues anterodorsally along the surface of the parabasisphenoid, and the cerebral carotid, which enters the foramen (Rieppel 1993). The cerebral artery extends dorsolaterally through the body of the

parabasisphenoid to open on to the dorsal surface via paired foramina at the posterior base of the pituitary fossa (Figs 12B, C). Between the cerebral carotid foramina, a third foramen opens into the pituitary fossa. The canal leading from this foramen ends abruptly a short way into the body of the parabasisphenoid.

In OMNH 74606 the course of the left sulcus can be clearly traced along the lateral surface of the parabasisphenoid. The right sulcus, however, enters an enclosed canal ventral to the basipterygoid process before entering the foramen, which is also located within the canal. It is probable that the thin septum of bone enclosing the canal was not preserved on the left sulcus, and that in life a short vidian canal was present on both sides of the parabasisphenoid, ventral to the basipterygoid processes. The septum of bone enclosing the canal derives from the ventrolateral ridge of the parasphenoid plate. The vidian canal is formed by the fusion of the lateral margin of the parasphenoid with the overlying lateral margin of the basisphenoid during development (Evans 1980). Complete closure of the vidian canal is a squamate synapomorphy (Rieppel 1993), although it is present in some parareptiles (Gow 1972, Spencer 2000). Closure of the vidian canal remains incomplete in early eureptiles (e.g. *Captorhinus laticeps*; Heaton 1979 and the diapsids *Prolacerta* and *Sphenodon*; Evans 1986). In early synapsids the grooves for the internal carotid arteries extend anteriorly along a narrow area of the ventral surface of the parasphenoid between or just posterior to the basipterygoid processes, where they enter foramina situated on the ventral surface of the parasphenoid. These foramina can clearly be seen in ventral view (Fig. 21A-D). The vidian canal is absent (Romer and Price 1940). This may differ, however, in some varanopids, in which the course of the internal carotid artery is similar to that of *Orovenator* (see Discussion).

Stapes. The footplate and part of the columella of the stapes are preserved in OMNH 74606, in close proximity to the right quadrate. The footplate is broadly ovoid in

shape with a deeply concave articular surface (Fig. 11F). The rim of the footplate is thickened, apart from what is probably the ventral region where a groove accommodates the passage of the stapedial artery. The base of the columella is damaged. There is a short pedicel of bone projecting distally from the footplate (Fig. 11G), originally interpreted as the dorsal process (Reisz et al. 2011). However, this may be the base of the bridge of bone forming the stapedial foramen with the columella. The presence or absence of a dorsal process, which is present in captorhinids (Heaton 1979, Fox and Bowman 1966), synapsids (Romer and Price 1940) and early diapsids (Vaughn 1955, Reisz 1981), cannot be clearly determined due to the damage to the base of the columella.

Mandible

The lower jaw of *Orovenator* is a slender element, with a tooth row that terminates near the level of the posterior margin of the orbit. (Figs 3A, B). The dentary is the longest bone in the mandible and covers most of its lateral surface. The posterior region of the mandible, including the adductor fossa, is relatively low and elongate, and the increase in dorsoventral height from the posterior tooth row to the posterior surangular is moderate, enhancing the somewhat gracile impression of the mandible. There are two inframeckelian fossae on the medial surface. The ventral margin, in lateral view, is rather straight, and there is a slight posteromedial inflection of the surangular.

Dentary. Both dentaries are preserved in OMNH 74606. The right has an eroded anterior tip and is missing the posterodorsal process. The left dentary is complete. The dentary is a dorsoventrally narrow and elongate bone, covering a substantial area of the lateral surface of the mandible (Fig. 13A). It bears 42 alveoli on its dorsal surface. A tapering posterodorsal process terminates posteriorly level with and

ventral to the inferred midpoint of the postorbital region of the skull, and bears an extensive edentulous region. More than 12 conspicuous foramina line the anterior half of the lateral surface, some associated with deep posteriorly directed grooves. An elongate groove, present on the lateral surface of both dentaries, extends posteriorly from a large foramen ventral to the 24th alveolus (Fig. 13A). The dentary provides the lateral and dorsal wall to the Meckelian canal.

The anteroposterior length of the dentary accentuates its slender lateral profile, with the ratio of length to maximum dorsoventral depth approximately 12:1. Extensive sutural surfaces on the angular and surangular support the dentary medially. Anteriorly the dentary gradually tapers dorsoventrally from the 31st alveolus, ending in a narrow, smoothly rounded symphyseal tip. Posteriorly, the dentary tapers in dorsoventral height sharply from the 31st alveolus, forming the posterodorsal process, which terminates in a point ventral to the mid-temporal region. The ventral margin of the posterodorsal process contacts the angular anteriorly and the surangular posteriorly. Most of the edentulous region of the posterodorsal process lies within a posteriorly tapering recess on the dorsolateral surface of the surangular, where a transversely narrow ridge of the surangular separates the dentary from the coronoid dorsally. The ventromedial surface of the dentary overlies a narrow, anteriorly tapering lateral flange on the splenial, and excludes the splenial from the lateral surface of the mandible.

A broad alveolar shelf extends medially from the dorsal surface of the dentary to support the marginal dentition. It has a high lateral lamina and a low medial ridge, which extends ventrally to form the dorsomedial wall of the Meckelian canal. The symphyseal surface is a small, semi-lunate area, which lies anterior to the anteroventral extension of the splenial. Posterior to the mandibular symphysis, the dentary is exposed dorsomedially to the level of the 9th alveolus (Fig. 13B).

Posteriorly the medial surface of the dentary contacts an anterodorsal process of the prearticular. A narrow spur of the alveolar shelf separates the coronoid from the anterior tip of the prearticular (Fig. 13B).

There are spaces for 42 teeth in the left dentary of OMNH 74606, 30 of which are occupied by small homodont teeth, similar to the marginal dentition of the maxilla. The two anterior teeth are slightly smaller than the subsequent teeth, which remain roughly isodont until the 26th tooth position, where the teeth gradually reduce in size, with the ultimate alveolus bearing the smallest tooth of the entire marginal dentition. The labial wall of the dentary is considerably taller than the lingual wall, which is reduced to a low ridge formed by thin paradental plates. The implantation remains basically 'subthecodont', although the alveoli are shallower than those of the maxilla, and the interdental plates are less prominent. The high marginal tooth count in the dentary is the highest known for a Palaeozoic neodiapsid (Reisz *et al.* 2011).

Angular. In OMNH 74606 the right angular is missing the medial and posterior regions. The left angular is essentially complete. The angular is an anteriorly tapering sheet of bone, exposed posterolaterally on the mandible, where it provides the ventral half of the surface, and posteromedially where only a narrow region is exposed ventral to the prearticular.

Anterolaterally the angular has an elongate anteriorly attenuating articular surface that underlies the dentary. The exposed posterolateral surface overlies a narrow shelf on the ventral surface of the surangular, and provides the thin ventral ridge of the mandible for the posterior third of its length. Medially the dorsoventrally narrow exposed surface has a shallow excavation along its dorsal margin, which forms the ventral rim of the posterior inframeckelian foramen (foramen intermandibularis caudalis of Reisz *et al.* 2011) (Fig. 13B). Anteromedially, a narrow sheet of bone

provides sutural contact for the posterior splenial. Posteromedially it overlies the posteromedial margin of the prearticular and forms a narrow ridge of bone ventrally. Since the articular is missing from both mandibles, it is not possible to determine whether the angular contacted the articular ventrally. The narrow ridge of bone that overlies the prearticular is similar to that seen in *Archaeovenator*, but is absent in later varanopids (Reisz and Dilkes 2003, Reisz and Berman 2001). The angular also bears a ventral keel in the early diapsid *Petrolacosaurus* (Reisz 1981).

Surangular. Both surangulars are preserved in OMNH 74606, with the posterior region and articular facet present only on the right surangular. The surangular forms the dorsal region of the posterolateral surface of the mandible and the lateral wall of the adductor fossa. It is a sheet-like bone ventrally, but thickens dorsally to form a distinctive anterodorsal ridge and a transverse expansion forming a broad medial platform, the dorsomedial shelf (Fig. 13D). It contacts the articular along its posterior margin.

The surangular attenuates anteriorly between its dorsal and ventral articulation with the dentary and angular respectively (Fig. 13A). The articular surface for the dentary extends posteriorly to form a tapering recess on the dorsolateral surface of the surangular. The narrow anterodorsal extension of the surangular provides the dorsal margin to this recess, and substantially separates the posterior dentary from the coronoid (Fig. 13D). The dorsomedial shelf is mediolaterally broad and bears a deep central anterior groove, which accommodates the posterodorsal process of the coronoid, and thus the low coronoid eminence. Posterior to the coronoid, a much shallower groove continues along the dorsal surface of the shelf. The purpose is uncertain, but it may have provided a sulcus for blood vessels or nerves. The dorsomedial shelf overhangs the lateral wall of the adductor fossa (Fig. 13B).

Posteriorly the surangular curves medially from the point where the dentary terminates. A flange of thin, vertically orientated bone extends medially from the posterodorsal region of the surangular (Fig. 14B). Both the antrerior and posterior surfaces of this flange form are smoothly concave. The posterior margin of the surangular is rugose and probably contacted the articular.

Splenial. Both splenials are present in OMNH 74606, only the left splenial is complete. Most of the anteromedial surface of the mandible, and therefore the medial wall of the Meckelian canal, is formed by the splenial. There is a small foramen, the anterior inframeckelian foramen (*foramen intermandibularis oralis*) close to the ventral margin, level with the 18th alveolus (Fig. 13B). A similar foramen can be seen on the medial surface of the splenial assigned to a mycterosaurine varanopid (gen. et sp. indet.) from the Capitanian, middle Permian, of South Africa, and in a undescribed mycterosaurine from the early Permian of Richards Spur, Oklahoma (Modesto *et al.* 2011). It is absent, however, in the varanopids *Aerosaurus* (Langston and Reisz 1981), *Varanops* (Campione and Reisz 2010) and *Varanodon* (Modesto et al. 2011), and indeed, in all other 'pelycosaur'- grade synapsids current known (Modesto et al. 2011). Posteriorly, the splenial overlies the prearticular and the angular.

The splenial is a long dorsoventrally thin bone that tapers anteriorly from the 14th alveolus to a narrow ventromedial process that provides a medial wall to the anterior Meckelian canal (Fig 13B). This process terminates ventral to the 2nd alveolus, and therefore does not participate in the symphyseal joint. Dorsally the splenial contacts the medial surface of the alveolar shelf at the 14th alveolus, and continues posteriorly until it meets the anterior process of the prearticular, from which point it tapers posteroventrally. It does not contact the anterolateral surface of the coronoid.

A dorsoventrally thin lateral process of the splenial extends posteriorly from a point level with the 8th dentary alveolus. This is overlain by the ventromedial surface of the dentary, and is therefore not visible in lateral view. A narrow keel joining the medial and lateral processes of the splenial provides the floor to the Meckelian canal. The splenial tapers posteroventrally, where it overlies the prearticular and the angular. *Orovenator* does not possess a posterior splenial, a bone present in seymouriamorphs (Klembara 1997, Klembara and Ruta 2005) but not reported in any amniotes with the exception of *Petrolacosaurus* (Reisz 1981).

Prearticular. Both prearticulars are well preserved in OMNH 74606. The prearticular is the central element in the posteromedial surface of the mandible, forming the medial wall of the adductor fossa and providing ventral support for the coronoid (Fig. 13B). It a dorsoventrally narrow bone, attenuating anteriorly. There is a thickened dorsal margin along much of its length. Posteriorly a distinct ventromedial surface is overlain by the posteromedial exposure of the angular.

The anterior portion of the prearticular is a very finely tapering thin sheet of bone that is overlain by the splenial. A thickened dorsal rim develops medial to and in contact with the narrow spur of alveolar shelf of the dentary that borders the anterior coronoid. The dorsal rim thickens posteriorly and contacts the medial margin of the coronoid posterior to the spur of the alveolar shelf. An elongate triangular lamina extends dorsomedially from the dorsal rim of the prearticular, which, along with a similar lamina on the dentary, provides support for the coronoid ventrally.

Immediately posterior to the dorsomedial lamina, the dorsal rim rises gradually to form a low eminence. The posteroventral margin of the coronoid contacts the apex of this eminence, and together they form the anterior margin of the adductor fossa.

Posteriorly from this point the dorsal rim of the prearticular provides the dorsomedial margin of the adductor fossa.

The posterior region of the prearticular is strongly inclined dorsoventrally, where it overlies the posteromedial flange of the angular. Anterior to this the ventral surface of the prearticular is free and forms the dorsal margin of posterior inframeckelian foramen (Fig. 13B). Because the articular is not preserved, the nature of the prearticular/ articular contact cannot be determined.

Coronoid. Both coronoids are preserved in OMNH 74606. The left coronoid, and its contact with the surrounding bones, is particularly well represented. The single coronoid is a mediolaterally thin bone with an anteriorly tapering anterior process and a thickened rim along its dorsal margin that develops into a posterodorsal process (Fig. 14B). Almost all of the exposure is medial, apart from the low coronoid eminence of the posterodorsal process, which is visible in lateral view. Both coronoids are edentulous.

The anterior process of the coronoid has an elongate blade-like appearance, tapering anteriorly to a point. The lateral surface of the blade overlies two thin laminae of bone; anteriorly a shelf of bone recessed into a medial extension of the alveolar shelf of the dentary and posteriorly a flange projecting from the dorsal rim of the prearticular. The anterior process contacts the dentary along its dorsal margin and the prearticular along its ventral margin apart from the anterior-most region, which is bordered ventrally by a small spur of bone from the dentary. This prevents contact between the coronoid and the splenial (Fig. 13B).

The thickened posterodorsal process extends from the dorsal rim of the coronoid. It bears a broad ventral facet that fits into a deep groove in the dorsomedial shelf of the

surangular. A concavity on the posterior margin of the bone marks the anteromedial rim of the adductor fossa.

Post-cranial skeleton

Four vertebrae are partially preserved in OMNH 74607 (Figs 2B, D); three have been identified as cervicals, including the axis, and the fourth as a caudal (Reisz *et al.* 2011). They represent the only post-cranial bones known for *Orovenator*. The axis and the 3rd cervical are in semi-articulation. The left pedicel of the neural arch, which is exposed to the surface of the specimen, has been completely eroded in all three cervicals.

Cervical vertebrae. All centra are amphicoelous and notochordal. They are sharply keeled and deeply excavated ventrolaterally, such that in anterior or posterior view the notochordal canal is considerably offset towards the dorsal rim of the centrum (Fig. 15A). They are relatively short anteroposteriorly, and tall in relation to their length (ratio approximately 0.60).(Fig. 15B)The zygopophyses extend slightly lateral to the centrum, and the zygopophyseal facet is inclined at an angle of approximately 27°. The pedicels of the neural arch are lateromedially narrow and firmly sutured to the centrum. The neural arch is broad and tall (Figs. 15A,B).

The axis is the anterior of the two semi-articulated vertebrae, and is identified by the anteroposteriorly elongate neural spine in relation to the subsequent or 3rd cervical vertebra (Reisz *et al.* 2011). The anterior and dorsal region of the neural spine is missing. The posteroventral margin of the neural spine bears a notch leading to a small foramen. The neural spine of the 3rd cervical is missing the dorsal and posterior region. The only evidence of a transverse process is on the disarticulated cervical, which is possibly the 4th cervical, where a slightly raised hourglass shaped facet lies

ventral to the prezygopophysis. There is no evidence of an accessory articulating process on the anterior or posterior margins of the neural spines (Fig. 15D).

The cervical vertebrae of *Orovenator* differ from those of earlier diapsids, particularly in the length of the centra (Reisz 1981, Vaughn 1955, Reisz *et al.* 1984). There is, however, some similarity in shape of the 3rd cervical with cervical vertebra of *Acerosodontosaurus* (Currie 1980). The dorsoventrally low neural spine and tall neural arch of the axis in *Orovenator* differs from ophiacodontid synapsids where the neural spine is tall and the neural arch somewhat narrow and short (Sumida 1989). A 'massive' neural arch is present in the varanopid *Archaeovenator* (Reisz *et al.* 2011), and a low axial neural spine is present in *Ascendonanus* and other small varanopids (Spindler et al. 2018).

Caudal vertebra. A small caudal vertebra is poorly preserved, particularly the lateral wall of the centrum, which has completely eroded ventral to the neurocentral suture. The neural spine is reduced to a posterodorsally inclined nub of bone, with an anterior margin that slopes steeply anteroventral to a deep 'V' shaped recess between the prominent prezygopophyses. Reisz *et al.* (2011) considered that this element was ontogenetically separate from the cervicals, and was therefore probably not associated with the other material in OMNH 74607.

DISCUSSION

Palaeobiology and palaeoecology

Diel activity in Orovenator. The preservation of articulated scleral ossicles in the left orbit of *Orovenator*, a rare occurrence in early amniote fossils, allows a virtual

reconstruction of the orbit and scleral ring (see Supplement 1). Measurements of the orbit and scleral ring can be used as palaeoecological indicators of patterns of diel activity using a derivative of Generalised Discriminant Analysis modified for phylogenetic bias (Motani and Schmitz 2011, Schmitz and Motani 2011a). There has been some debate on the efficacy of this method in extinct taxa (Hall et al. 2011, Schmitz and Motani 2011b). Nevertheless, phylogenetically flexible discriminant analysis (PFDA) has also been used to investigate diel patterns in non-mammalian synapsids (Angielczyk and Schmitz 2014).

We added our measurements of *Orovenator* to the dataset of Angielczyk and Schmitz (2014), inserting *Orovenator* into their time calibrated phylogeny as a sister taxon to the 'pelycosaur'- grade synapsids (*Aerosaurus, Heleosaurus, Dimetrodon* and *Sphenacodon*), thus reflecting the synapsid/sauropsid relationship, with a terminal branch length equal to that of *Aerosaurus*, from the Abo/Cutler Formation of New Mexico (=Wolfcampian) (Langston and Reisz 1981). The PFDA of a sample of 164 extant terrestrial diapsids provides a discriminant function that can be used to infer patterns of diel activity in extinct specimens as being photopic (diurnal; prior probability = 58.6%), scotopic (nocturnal; 27.1%) or mesopic (cathemeral; 14.3%). This analysis, conducted by Angielczyk and Schmitz (2014), has an estimated phylogenetic signal parameter (Pagel's lambda) of 0.08, indicating that the relationship is essentially free from phylogenetic signal. Our data for *Orovenator* is principally based on elements from a juvenile individual some 67% the size of the adult specimen, and the effects of ontogenetic status on inferences from this type of analysis have not been fully explored. Nevertheless, Angielczyk and Schmitz (2014) found the results of the two best-preserved specimens of the therapsid *Cyonosaurus* were consistently congruent despite one of them being the smallest specimen in the dataset (46% of maximum size). Furthermore, 21 of the 33 specimens included in the

original study were 50% of the maximum size or larger, so our findings should be comparable to those of the original work (Angielczyk and Schmitz 2014).

Our results show a 98.61% posterior probability of a scotopic ocular function in *Orovenator*, which we interpret as a strong indication of nocturnality (see Supplement 1). This represents the earliest example of nocturnality in diapsid evolution. Inferences of nocturnality in extinct amniotes were initially proposed as a predominantly mammaliaform trait that evolved in conjunction with homeothermy in Mesozoic mammals (Crompton et al. 1978). Studies have since suggested that a nocturnal life style may have been prevalent in middle Permian parareptiles with impedance-matching hearing (Müller and Tsuji 2007) and in Mesozoic archosaurs (Schmitz and Motani 2011a), as well as early synapsids (Angielczyk and Schmitz 2014). Although the current data on diel activity in early amniotes is insufficient to imply whether nocturnality evolved independently or was homologous in the synapsid and sauropsid lineages, our findings do indicate that amniotes occupied a range of diel activity patterns quite early in their history.

Burrowing behaviour in Orovenator. In both general morphology and internal structure, *Orovenator* possesses a suite of features consistent with use of the snout in burrowing behaviour., which are absent in other Permian diapsids (Vaughn 1955, Reisz 1981, Bickelmann et al. 2009, Modesto and Reisz 2003, Gow 1975) Although the large orbits and external nares of *Orovenator* do not suggest a fully fossorial or subterranean life style, a rostral process and a broad, anteriorly tapering dorsal surface of a wedge-shaped snout (Fig. 16) are traits associated with burrowing in extant squamates (Wake 1993). Further, *Orovenator* possesses several features that imply mechanical reinforcement of the snout, and may be associated with burrowing. The extent to which the skull is strengthened by complex articulations and thus able

to withstand greater stress can infer a propensity towards fossoriality (Roscito and Rodrigues 2010). Such features are present in *Orovenator,* notably*:* (1) the anteroposteriorly long maxillary and dorsal processes of the premaxillae, and dorsoventrally thick maxillary plate, all of which serve to strengthen the anterior snout; (2) the interlocking fronto-nasal suture that braces the posterior part of the snout against lateral torsion; (3) the mutually supporting arrangement of the anterior circumorbital elements and the palate; (4) the medial buttress and crest of the maxilla which provides a firm platform for the ventromedial ridge of the lacrimal. Some other early amniotes also possess a medial buttress on the maxilla, such as ophiacodontids and sphenacodontians (Berman et al. 1995, Romer and Price 1940). However, in these taxa it is associated with the caniniform dentition ('supracanine' buttress), suggesting it functioned as resistance to bite forces. This is not the case in *Orovenator*, which lacked caniniform teeth and possessed a shelf on the posterodorsal crest of the medial alveolar buttress that supported the ventromedial surface of the lacrimal, thus reinforcing the snout against vertical stress.

The similarity of the skull shape of *Orovenator* with the sandfish skink (*Scincus scincus*), an extremely efficient burrower, is particularly striking (Fig. 17), and a rostral process is a common feature of burrowing amphisbaenians and snakes (e.g. the North American worm lizard; *Rhineura floridana* and the Mexican burrowing snake; *Loxocemus bicolor*). A rostral process is also present in all caseasaurian synapsids (Romer and Price 1940). The morphology of the terminal phalanges in caseasaurs has lead some authors to suggest a functional correlate with the rostral process, implying a digging behaviour in some caseid taxa (Olson 1968, Maddin and Reisz 2007). A recent study on the long bone scaling of caseids suggests that allometric changes in forelimb morphology, even in smaller taxa, may support this hypothesis (Romano 2017). A moderate rostral process has also been suggested in

the varanopids *Varanops* and *Aerosaurus* (Brinkman and Eberth 1983, though subsequently disputed by Reisz 1986).

The origin of burrowing in terrestrial vertebrates is at best obscure. Burrowing activity, particularly amongst faunivorous tetrapods, could have been used incidentally to explore the substrate for food. Exploitation of subsurface prey may have lead to selection for adaptations that strengthened the structural integrity of the snout and improved prey capture (Wake 1993). Direct evidence of burrowing is rare in early Permian (Cisuralian) terrestrial vertebrates. The skull morphology of recumbirostran 'microsaurs' from the Artinskian of Oklahoma and Texas is strongly suggestive of a burrowing life-style (Maddin *et al.* 2011, Anderson *et al.* 2009), an observation supported by burrows containing the putative recumbirostran *Brachydectes newberryi* (Pardo and Anderson 2016). Otherwise there are several examples of burrowing associated with therapsids from the middle to late Permian (Guadalupian/Lopingian) e.g. helical burrows containing specimens of Diictodon (Smith 1987), fossorial adaptations in cistecephalid dicynodonts (Nasterlack et al. 2012), cynodont burrows from the Permo-Triassic boundary of South Africa (Damiani et al. 2003) and *Lystrosaurus* burrows from the Lower Triassic Karoo Basin (Botha-Brink 2017). Sauropsid examples include an aggregation of five immature diapsid skeletons, referred to *Youngina*, in a possible underground burrow from the late Permian of South Africa (Smith and Evans 1996) and potential facultative fossoriality in the stem-turtle *Eunotosaurus* (Lyson et al. 2016).

Paranasal air sinus and the origins of antorbital fenestration. The contact of the lacrimal and maxilla in *Orovenator* forms a cavity on the medial surface of the snout, bounded posteriorly and dorsally by the ventromedial ridge of the nasolacrimal canal, and anteriorly by the 'supracanine' buttress and crest of the maxilla (Fig. 5). This is topologically similar to the antorbital cavity of extant archosaurs, (i.e. birds and

crocodilians), which takes the form of an internal space, rostral to the orbit, external to the nasal capsule, and bounded dorsally by the nasolacrimal canal (Witmer 1995). Based on its associations in extant archosaurs, the antorbital cavity has been proposed as an osteological correlate of an epithelial paranasal air sinus among crown-group archosaurs (Witmer 1995, 1997). Furthermore, a similar morphology is present in the early Triassic stem-group archosaur *Prolacerta*, which possesses a 'supracanine' buttress and crest on the medial surface of the maxilla (Gow 1975). The morphology seen in *Prolacerta* is highly similar to that of *Orovenator* (Fig. 18A, B). One key difference between these taxa, and the structures seen in birds/dinosaurs and most stem-group crocodylians is the absence of an antorbital fenestra that opens from the internal antorbital cavity laterally to external space (the antorbital fenestra is secondarily closed in the crown-group of crocodylians and in some extinct groups). Witmer (1997) suggested that the origin of paranasal pneumaticity (indicated by the internal cavity) preceded the origin of crown-group Archosauria, and this is supported by the morphology of the medial surface of the snout in *Prolacerta* (Fig. 18B). Witmer (1995,1997) further hypothesised that the antorbital fenestra of early archosaurs derived from a fontanelle that failed to close during development in bones lateral to the pre-existing paranasal sinus.

The morphology of the snout in *Orovenator* is therefore consistent with the presence of paranasal pneumaticity. This is further supported in *Orovenator* by the presence of a small canaliculus that connects the nasolacrimal canal with the antorbital cavity (Fig. 5B), somewhat similar to that found in birds and theropod dinosaurs (Witmer and Ridgely 2008). In contrast, this morphology is absent in the late Permian neodiapsid *Acerosodontosaurus* (Currie 1980). Furthermore, the antorbital cavity is absent in extant lepidosaurs (Witmer 1997) and fossil lepidosauromorphs (e.g. *Marmoretta*, *Gephyrosaurus*, *Sophineta*), where a shallow depression in the medial surface of the maxilla is associated with the nasal gland cavity (Evans 1980, 1991,

Evans and Borsuk-Bialynicka 2009), a feature homologous with the archosaurian nasal gland rather the paranasal air sinus (Witmer 1997). In addition, the lacrimal does not extend anterodorsal to the nasal gland cavity in these taxa, as it does in the antorbital cavity in *Orovenator.* Consequently the hypothesis of the antorbital cavity in *Orovenator* as a homologue of the paranasal sinus of archosaurs requires the secondary loss of this feature in lepidosaurs. The osteological evidence present in *Orovenator,* however, remains sufficiently compelling to expand this area of research in future studies.

Similarities between Orovenator *and varanopids*

Morphological similarities between diapsids and varanopids have long been noted, and have been the basis of protracted taxonomic and phylogenetic rearrangements (Reisz 1981, Reisz *et al.* 2010). Despite these similarities, varanopids have been assigned to Synapsida, the total-group of mammals, due to the presence of a single, lateral temporal opening (the synapsid condition). This contrasts with the presence of two temporal openings in early diapsids: the upper temporal fenestra and lower temporal fenestra or arch (the diapsid or euryapsid conditions).

The first varanopid to be described, *Varanops brevirostris*, was assigned to the Ophiacodontidae (Poliosauridae of Williston 1911). Romer and Price later erected the family ‘Varanopsidae’ as ‘primitive sphenacodonts, retaining many ophiacodont features’ (Romer and Price 1940:268). Four of the fifteen genera currently recognised as varanopids were originally or secondarily described as diapsids (see Table 1). Furthermore, early diapsids have also been misidentified as synapsids: *Petrolacosaurus* was initially referred to the Synapsida by several authors (Lane 1945, Romer 1956, Stovall *et al.* 1966), before being comprehensively reassessed as a diapsid (Reisz 1977), and the early diapsid *Lanthanolania* was originally catalogued

as a referred specimen of the varanopid *Mesenosaurus* (Modesto and Reisz 2003). One of the difficulties faced by researchers of early amniotes is that cranial characters used to distinguish between the two clades, such as the absence of the upper temporal opening and suborbital fenestra, are often not preserved or are obscured. In the case of *Apsisaurus* and *Heleosaurus* the presence of tubercles on the lateral surface of the jugal has been a significant factor in their reassessment as varanopids rather than diapsids (Reisz et al. 2010, Reisz and Modesto 2007), although circumorbital ornamentation is absent in the basal varanopid *Ascendonanus nestleri* (Spindler *et al.* 2018). Altogether, it is clear that the hypothesised highly distinct phylogenetic positions of varanopids (as synapsids) and early diapsids (as sauropsids) are supported by only a small number of character states.

In contrast, numerous similarities shared between early diapsids and varanopids have already been noted, including a triradiate jugal with a dorsoventrally thin subtemporal process, a sigmoidal femur, osteoderms and serrations on the mesial edges of marginal teeth (Reisz and Modesto 2007, Reisz *et al.* 2010). In non-varanodontine varanopids similarities also include slender limbs, relatively small body size and recurved conical teeth, as in the basal varanopids *Archaeovenator and Ascendonanus* (Reisz and Dilkes 2003, Spindler *et al.* 2018). Within the current paradigm (Reisz and Modesto 2007, Reisz and Dilkes 2010) these similarities are interpreted as the result of convergent evolution. However, they have also been used to support alternative hypotheses of early amniote phylogeny. Reig (1967) noted a series of features shared by varanopids and ‘proterosuchians’ (early Triassic stem-group archosaurs), and suggested that archosaurs evolved from varanopids in the late Permian. He subsequently listed 13 cranial and 16 post-cranial similarities (Reig 1970), which Romer (1971) dismissed essentially as being plesiomorphies. Only the putative antorbital fenestra reported in the varanopid *Varanodon* (Olson 1965) appeared to support any derived affinity of varanopids with proterosuchians. This

feature, however, was later interpreted as post-mortem damage to a region of thin antorbital lamina (Langston and Reisz 1981).

In our re-examination of *Orovenator* we have identified 16 additional similarities that varanopids share with *Orovenator* and other sauropsids. This additional evidence for a clade comprising varanopids plus *Orovenator* prompted an assessment of the support for this clade, and its affinities with either synapsids or diapsids. Moreover, since this hypothesis is incongruent with the current paradigm of early amniote phylogeny, we discuss each relevant character state below. These similarities may be summarised as follows: (1) potential synapomorphies of varanopids that are also present in *Orovenator* – the rounded sub-narial shelf of the premaxilla, the posterodorsal extension of the external naris , the extensive dorsal exposure of the prefrontal with a sharp angle between the dorsal and lateral surfaces, the ventral process of the prefrontal that contacts the palatine, the prominent dorsomedial shelf of the surangular, the narrow anterodorsal extension of the surangular, the asymmetric bifurcation of the anterior vomers; (2) similarities shared by *Orovenator* and the early varanopid *Archaeovenator* – the medial 'supracanine buttress' of maxilla and absence of caniniform dentition, the dorsolateral inclination of the suborbital ramus of the maxilla, the posteroventral ridge of the angular, absence of contact between the coronoid and splenial; (3) potential synapomorphies of sauropsids that are present in varanopids – the posterolateral process of the frontal and the anteromedian process of the parietal, teeth on the cultriform process of the parasphenoid, the adductor crest and fourth trochanter of the femur absent; (4) potential synapomorphies of synapsids that are absent in most sauropsids and in varanopids -a distinct lateral lappet of the frontal (as also found in lanthanosuchoid parareptiles), the pathway of the cerebral carotid artery on the ventral surface of the parabasisphenoid and absence of the vidian sulcus.

Potential synapomorphies of varanopids that are also present in Orovenator.

The character states described in this section support the inclusion of *Orovenator* in a clade with varanopids. As such, their distributions are incongruent with the presence of a diapsid or euryapsid pattern of temporal fenestration in *Orovenator.* This contrasts with the presence of a single lateral temporal fenestra in varanopids (the synapsid condition).

Rounded sub-narial shelf of the premaxilla: a broadly rounded transition between the dorsal surface of the body of the premaxilla, which forms the sub-narial shelf, and the lateral surface of the premaxilla ventral to it is a proposed unique synapomorphy of varanopids in respect to synapsids (Reisz and Dilkes 2003, Maddin et al. 2006) and other Paleozoic amniotes (Reisz and Berman 2001). It differs from the situation in other taxa, in which this transition is marked by a sharp, well-defined margin. Both premaxillae in *Orovenator* exhibit the rounded morphology shared with varanopids (Fig. 4A).

Posterodorsal extension of the external naris: in *Orovenator* the posterodorsal corner of the external naris is extended posteriorly, and is 'pinched' between the maxilla ventrally and the nasal dorsally (Figs. 3A, B). The dorsoventrally narrow anterior process of the lacrimal forms the posterior margin of this extended region of the external naris. A similar posterodorsal expansion of the external naris between the maxilla and the nasal is present in most basal and mycterosaurine varanopids where observable, with the exception of *Ascendonanus*, which possessed a small naris with no posterodorsal extension (Spindler et al. 2018). This feature is also absent in other synapsids (Botha-Brink and Modesto 2009, Reisz *et al.* 2010) and early amniotes, including diapsids (Clark and Carroll 1973, Reisz 1981, Carroll 1981). In varanodontine varanopids the posterodorsal expansion is greatly enlarged (Maddin

et al. 2006). Other than in varanopids and *Orovenator*, this morphology may also be present in weigeltisaurids,in which the posterodorsal expansion was scored as present in the taxon/character matrix of Reisz *et al.* (2010), although specimens of this group were not examined during the present study.

Extensive dorsal exposure of the prefrontal, with a sharp angle between the dorsal and lateral surfaces: the mediolaterally broad subtriangular dorsal exposure of the prefrontal in *Orovenator* forms a right angle with the lateral surface of the snout (Figs 3A, C). This abrupt transition is also seen in the varanopids *Mesenosaurus* and *Elliotsmithia* (Reisz and Berman 2001, Reisz et al. 1998), and in specimens of *Varanodon* (FMNH UR 986) and *Varanops* (MCZ 1926), in which the mediolateral width of the skull roof across the prefrontals is twice the interorbital width in dorsal view. In synapsids this feature is also present in the ophiacodontids such as *Varanosaurus* (Berman et al. 1995). This differs from the condition in other synapsids (e.g. *Dimetrodon*; Romer and Price, *Edaphosaurus*; Modesto 1995), in basal eureptiles such as *Paleothyris*, *Euconcordia* and *Romeria texana* (Carroll 1969, Müller and Reisz 2005b, pers. obs. MCZ 1480), and in the diapsid *Youngina* (pers. obs. BP/1/2871), in which the transition from the dorsal to lateral surface is gradual, and the mediolateral width of the skull roof across the prefrontals is less than twice the interorbital width.

Ventral process of the prefrontal contacts the palatine: A broad contact between the prefrontal and the maxillary ramus of the palatine is present in the varanopids *Elliotsmithia* (Modesto *et al.* 2001) and *Mesenosaurus* (Reisz and Berman 2001). A µCT scan of *Mycterosaurus* (FMNH UC 692), conducted for the present study, also shows evidence of this contact, confirming the scoring of this state in the analysis of Reisz *et al.* (1998, character 7). This contact is absent in early synapsids in which the medial surface of the antorbital region is known (e.g. *Dimetrodon* and *Ophiacodon*:

Romer and Price 1940, *Haptodus*, Laurin 1993, *Ennatosaurus*; Maddin *et al.* 2008), other than *Edaphosaurus* (Modesto 1995). In *Orovenator* the prefrontal also bears a robust ventral process that lies across the medial surface of the lacrimal and makes a broad contact with the palatine (Fig. 5B). *Orovenator* is the only Permian diapsid known to possess this morphology. Otherwise a broad prefrontal/palatine contact is considered an independently acquired synapomorphy of parareptiles, lepidosauromorphs and rhynchosaurs (de Braga and Rieppel 1997). It is also present in stem and extant turtles (Gaffney 1979).

Prominent dorsomedial shelf of the surangular: A broad dorsomedial shelf of the angular overlies the adductor fossa dorsally, and provides a platform for the posterodorsal process of the coronoid in *Orovenator* (Fig. 11C). This is also present in the varanopids *Apsisaurus* (Reisz et al. 2010b), *Mycterosaurus* (µCT scan of FMNH UC 692, Fig. 13B), *Varanops* (Campione and Reisz 2010), *Varanodon* (Reisz et al. 2010) and *Aerosaurus* (Campione and Reisz 2010). In *Archaeovenator* there is a dorsomedial thickening of the posterior region of the surangular of the right mandible, which is exposed in medial view in the holotype (pers. obs. KUVP 12483). The same morphology is seen in *Mesenosaurus* (Reisz and Berman 2001). This shelf is absent in all non-varanopid synapsids in which the dorsomedial margin of the mandible is known (e.g. *Dimetrodon* and *Ophiacodon;* Romer and Price 1940, *Varanosaurus;* Berman et al. 1995, *Edaphosaurus*; Modesto 1995, *Ennatosaurus;* Maddin et al. 2008, *Eothyris*; Reisz et al. 2009 and *Haptodus*; Laurin 1993). A prominent dorsomedial shelf of the surangular is also present in the parareptile *Belebey*, in which the shelf overhangs the adductor fossa (Reisz *et al.* 2007). In other early sauropsids this feature is less pronounced than in *Orovenator*, forming a thickened dorsomedial ridge of the surangular (e.g. *Acerosodontosaurus*; Currie 1980, *Petrolacosaurus*; Reisz 1981 and *Delorhynchus*; Reisz *et al.* 2014). However, it is absent in most early sauropsids in which this region can be examined (e.g.

Araeoscelis; pers. obs. MCZ 4380, *Prolacerta*; Modesto and Sues 2004, *Captorhinus laticeps*; Heaton 1979 and *Labidosaurus*; Modesto *et al.* 2007).

Narrow anterodorsal extension of the surangular: In *Orovenator* the posterodorsal part of the dentary lies in a shallow recess on the lateral surface of the surangular. A transversely narrow and dorsoventrally thin process of the surangular extends dorsal to the dentary, substantially separating the posterior region of the dentary from the coronoid (Fig. 13D) (Reisz *et al.* 2011, fig.3). Varanopids also exhibit this morphology where the relevant region can be examined (*Mesenosaurus*; Reisz and Berman 2001, *Apsisaurus*; pers. obs. MCZ 1474, *Mycterosaurus*; µCT scan of FMNH UC 692 (Fig. 13C) and *Aerosaurus*; Langston and Reisz 1981). A similar morphology can also be seen in the ophiacodontids *Ophiacodon* (Romer and Price 1940) and *Varanosaurus* (Berman et al. 1995), the parareptile *Delorhynchus* (Reisz et al. 2014), the captorhinids *Captorhinus laticeps* and *Reiszorhinus* (Sumida et al. 2010) and proterosuchid archosauriforms (Welman 1998, Ezcurra and Butler 2015). However, in these taxa the anterodorsal extension is dorsoventrally deeper than that of *Orovenator* and the varanopids noted above. Furthermore, the anterodorsal extension of the surangular is entirely absent in other synapsids (e.g. *Ennatosaurus*; Maddin et al. 2008, *Edaphosaurus*; Modesto 1995 and *Dimetrodon*; Romer and Price 1940) and in other sauropsids: the basal eureptiles *Paleothyris* (Carroll 1969) and *Protorothyris* (Clark and Carroll 1973), araeoscelidian diapsids (Reisz 1981, Vaughn 1955), in the neodiapsids *Lanthanolania* (Modesto and Reisz 2002), *Claudiosaurus* (Carroll 1981) and *Youngina* (Reisz *et al.* 2000) and in *Prolacerta* (Modesto and Sues 2004).

Asymmetrical bifurcation of the anterior vomers: In *Orovenator* the vomerine process of the premaxilla is incised deeply into the anterior surface of the vomer, which is bifurcated anteriorly into a short lateral process and an elongate medial process (Fig.

4C). This morphology can also be found in *Paleothyris* (pers. obs. MCZ 3481 and Reisz 1981), *Petrolacosaurus* (pers. obs. KUVP 8351) and in the varanopids *Mesenosaurus* (Reisz and Berman 2001) and *Archaeovenator* (Reisz and Dilkes 2003) (Fig. 19). The anterior region of the vomer is insufficiently exposed or not preserved in other varanopids. A notch on the anterior surface of the vomer where it articulates with the vomerine process of the premaxilla is also present in the diadectomorph *Limnoscelis* (Berman *et al.* 2010), in the synapsids *Dimetrodon milleri* (Brink and Reisz 2012) and *Edaphosaurus boanerges* (Modesto 1995), and the parareptile *Colobomycter pholeter* (MacDougall *et al.* 2017). However, the notch is shallow in all these taxa, and the lateral and medial processes that form the notch are short. The notch is altogether absent in more derived diapsids, such as *Prolacerta* (Gow 1975), captorhinids (*Captorhinus laticeps*; Heaton 1979, *C. aguti*; Fox and Bowman 1966 and *Labidosaurus*; Modesto et al. 2007), and early sphenodontians (*Clevosaurus;* Fraser 1988 and *Gephyrosaurus*; Evans 1980). A bifid anterior vomer is present in the archosauriform *Proterosuchus fergusi,* although the notch is 'U' shaped and the lateral and medial processes are of equal length (Ezcurra and Butler 2015).

Similarities of Orovenator *and the early varanopid* Archaeovenator

Orovenator shares several cranial similarities with *Archaeovenator* that are not present in more derived varanopids or other sauropsids. As such, they may support a sister taxon relationship of *Orovenator* with *Archaeovenator*, or be primitive morphologies for a clade of *Orovenator* and Varanopidae.

Presence of a medial 'supracanine buttress' of maxilla combined with the absence of caniniform teeth: Orovenator possesses a thickened dorsal eminence of the alveolar

shelf that extends dorsally into a triangular, tapering buttress at the level of the 9th alveolus (Figs 5A, B). *Archaeovenator* also possesses a similar buttress (Reisz and Dilkes 2003 fig. 2b), (pers. obs. KUVP 12483, right maxilla Fig. 18C), which appears to taper dorsally. This morphology is also present in ophiacodontids (Reisz 1972, Romer and Price 1940, Brinkman and Eberth 1986) and sphenacodontians (Romer and Price 1940, Reisz et al. 1992), and is termed a 'supracanine' buttress because members of both these groups possess caniniform teeth ventral to the maxillary buttress. Unlike in ophiacodontids and sphenacodontians, caniniform teeth are absent in both *Orovenator* and *Archaeovenator* (Reisz and Dilkes 2003). The buttress is absent in *Aerosaurus* (Langston and Reisz, 1981) and its presence or absence cannot be determined in other varanopids.

Dorsolateral inclination of the suborbital portion of the maxilla: The lateral surface of the suborbital portion of the maxilla is dorsolaterally inclined by approximately 12° laterally in *Orovenator*, such that it overhangs the alveolar margin (Fig. 3A, Supplement 1, Fig. 1A). This also occurs in *Archaeovenator* (Reisz and Dilkes 2003), but is not found, to our knowledge, in any other early synapsid or sauropsid.

Posteroventral ridge of the angular: the posteroventral region of the angular in *Orovenator* forms a narrow ridge of bone that overlies the prearticular. Anterior to this, the ventral surface of the angular is smoothly rounded (Fig. 13E). The ventral surface of the angular in *Archaeovenator* also bears a ridge posteriorly (Reisz and Dilkes 2003). In *Ascendonanus* the ventral ridge extends along the entire mandibular ramus (Spindler et al. 2018). This ridge is absent in derived varanopids such as *Mesenosaurus* (Reisz and Berman 2001), in which the ventral margin of the angular is rounded. Amongst synapsids the ventral margin of the angular bears a thin keel in caseasaurs (e.g. *Ennatosaurus* and *Cotylorhynchus;* Maddin et al. 2008). In ophiacodontids, edaphosaurs and basal sphenacodontians (e.g. *Haptodus*) the

posteroventral margin of the angular is expanded ventrally and transversely compressed forming a deep keel (Brinkman and Eberth 1983, Benson 2012). In derived sphenacodontians this keel is expanded ventrally to form a sheet-like lamina (Reisz 1986), a precursor of the reflected lamina of therapsids. In early eureptiles there is no posteroventral keel of the angular, which appears to be smoothly rounded in *Paleothyris*, *Protorothyris* and *Protocaptorhinus* (pers. obs. MCZ 3483, MCZ 1532, and MCZ 1478). Amongst diapsids the angular bears a deep posteroventral keel in the *Petrolacosaurus* (Reisz 1981), but is rounded in the neodiapsid *Youngina* (pers. obs. BP/1/2871).

Absence of contact between the coronoid and splenial: the morphology of the single coronoid in *Orovenator* is similar to that found in captorhinids, basal diapsids and the posterior coronoid in early synapsids (Heaton 1979, Reisz 1981, Romer and Price 1940). In captorhinids, diapsids and archosauromorphs the splenial makes contact with the coronoid (e.g. *Captorhinus laticeps*; Heaton 1979*, Labidosaurus*; Modesto *et al.* 2007*, Petrolacosaurus*; Reisz 1981 and *Prolacerta*; Gow 1975). In contrast, the coronoid in *Orovenator* is prevented from contacting the splenial by a thin extension of the dentary (Fig. 20B). This is almost identical to the condition found in *Archaeovenator,* in which the dentary also prevents contact between the coronoid and splenial (Reisz and Dilkes 2003, pers. obs. KUVP 12483 (Fig. 20A)). In more derived varanopids, e.g. *Mesenosaurus*, the splenial contacts the anterior region of the (single) coronoid (Reisz and Berman 2001).

Potential synapomorphies of sauropsids that are present in varanopids and absent in other synapsids

In this section we examine character traits found in sauropsids as a whole or in clades within the Sauropsida (e.g. diapsids) that are also present in varanopids, but absent in other early synapsid groups. These observations potentially support the existence of a clade inclusive of varanopids and diapsids.

Posterolateral process of the frontal and anterior median process of the parietal: In *Orovenator* and other early diapsids (e.g. *Araeoscelis*; Vaughn 1955, *Youngina*; pers. obs. BP/1/3859 and *Prolacerta*; pers. obs. BP/1/5375) an elongate posterolateral process of the frontal extends along the medial margin of the postfrontal at an acute angle (Fig. 7A). This morphology of the frontal creates a deep 'V' shaped embayment in the posterior margin of the paired frontals. An anterior median process of the parietal occupies this embayment, incising into the supraorbital region of the skull roof. The posterolateral process of the frontal and the anteromedial process of the parietal were viewed as individual synapomorphies of varanopids by Reisz and Berman (2001). Here we consider these features as correlated, and note that both are present in *Orovenator* and varanopids (e.g. *Archaeovenator;* Reisz and Dilkes 2003, *Heleosaurus;* Botha-Brink and Modesto 2009, *Elliotsmithia*; Reisz *et al.* 1998, *Mycterosaurus*; Berman and Reisz 1982, *Mesenosaurus;* Reisz and Berman 2001 and *Varanodon*; pers. obs. FMNH UR 986). In non-varanopid synapsids this morphology is either absent (e.g. *Dimetrodon limbatus*; Romer and Price 1940, *Ennatosaurus*; Maddin *et al.* 2008, *Sphenacodon ferox*; Spielmann *et al.* 2010) or much reduced, with the posterolateral process of the frontal being relatively shorter, and not covering the entire medial margin of the postfrontal (e.g. *Haptodus*; Laurin 1993, *Varanosaurus*; Berman *et al.* 1995, *Edaphosaurus;* Modesto 1995). It is also absent in stem amniotes (e.g. *Limnoscelis*; Berman et al. 2010, *Seymouria*; Laurin 1996 and *Tseajaia*; Moss 1972), in captorhinids (Heaton 1979, Fox and Bowman 1966, Müller and Reisz 2005, Modesto *et al.* 2007, Sumida *et al.* 2010), parareptiles

(*Macroleter poezicus*; Tsuji 2006) and basal eureptiles (Carroll 1964,1969, Clark and Carroll 1973).

Teeth on the cultriform process of the parasphenoid: The presence of cultriform teeth is a derived and widespread (but variable) condition in early sauropsids. Cultriform teeth are present in *Orovenator* and other eureptiles (e.g. *Paleothyris*; Carroll 1969, *Petrolacosaurus*; Reisz 1981, *Lanthanolania*; Modesto and Reisz 2003 and *Captorhinus aguti*; Fox and Bowman 1966), but absent in *Youngina* (Gardner et al. 2010) and *Captorhinus laticeps* (Heaton 1979). In parareptiles they are present in *Acleistorhinus* (de Braga and Reisz 1996) and *Milleretta* (Gow 1972), but absent in *Belebey* (Reisz *et al.* 2007). Teeth on the ventral surface of the cultriform process of the parasphenoid are also present in varanopids (Langston and Reisz 1981, Reisz and Modesto 2007, Reisz and Berman 2001, Berman and Reisz 1982, Spindler *et al.* 2018). They are absent in stem-group amniotes (e.g. *Limnoscelis paludis;* Fracasso 1987, Berman et al. 2010, *Tseajaia campi*; Moss 1972 and *Seymouria sanjuanensis;* Klembara et al. 2005). They are also absent in most early synapsids (e.g. ophiacodontids; Berman et al. 1995, sphenacodontians; Romer and Price 1940, Laurin 1993 and edaphosaurids; Modesto 1995), except for caseasaurs (Maddin *et al.* 2008).

Adductor crest and fourth trochanter of the femur absent: In many early amniotes a prominent ridge of bone extends diagonally along the ventral surface of the femur from the internal trochanter proximally to the popliteal area of the posterior condyle distally. This ridge, the adductor crest, is interrupted approximately midshaft by the fourth trochanter when present. The fourth trochanter and adductor crest are absent in most varanopids in which the ventral surface of the femur is known (e.g. *Archaeovenator;* Reisz and Dilkes 2003, *Apsisaurus*; Laurin 1991, *Mycterosaurus*; Berman and Reisz 1982 and *Heleosaurus*; Botha-Brink and Modesto 2009). In

Varanops, uniquely amongst varanopids, there is a moderately developed fourth trochanter (Campione and Reisz 2010). Both features are also absent in araeoscelidian diapsids (*Petrolacosaurus*; Reisz 1981 and *Araeoscelis;* Vaughn 1955), 'younginiforms' (Laurin and Reisz 1995), the archosauromorphs *Prolacerta* (Gow 1975) and *Proterosuchus* (Ezcurra *et al.* 2013), and early sphenodontians (e.g. *Clevosaurus*; Fraser 1988). The fourth trochanter and adductor crest are present in caseasaurs, ophiacodontids and edaphosaurids (Romer and Price 1940, Reisz 1986). In sphenacodontians, these features are relatively weaker but still present, for example in *Haptodus* (Laurin 1993) or as a rugose line with a fourth trochanter in *Dimetrodon* (Reisz 1986). Both traits are also known in captorhinids (*Captorhinus aguti*; Fox and Bowman 1966), and procolophonid parareptiles (*Procolophon*; de Braga 2003). The presence of the adductor crest and fourth trochanter may be plesiomorphic for amniotes since they are present in the Permian reptiliomorphs *Limnoscelis* (Romer 1946), and *Seymouria* (White 1939)

Potential synapomorphies of synapsids that are absent in most sauropsids and varanopids

Lateral lappet of the frontal absent: A distinct lateral lappet of the frontal contributing to the orbital margin is absent in varanopids (Reisz and Dilkes 2003, Reisz et al. 1998, Langston and Reisz 1981), although a small lateral lappet has been noted in *Ascendonanus* (Spindler *et al.* 2018). It is also absent in *Orovenator* and early diapsids, such as *Petrolacosaurus* (Reisz 1981), *Acerosodontosaurus* (Bickelmann et al. 2009) and *Lanthanolania* (Modesto and Reisz 2003). The absence of this feature is considered to be the primitive state for amniotes (de Braga and Reisz 1997) as noted in early eureptiles (*Hylonomus lyelli*; Carroll 1964, *Paleothyris*; Carroll 1969, *Captorhinus laticeps*; Heaton 1979 and *Romeria;* Clark and Carroll 1973). In synapsids, the contribution of the frontal to the orbital margin is formed by a distinct

lateral lappet (e.g. *Euromycter rutenus*; Sigogneau-Russell and Russell 1974, *Ophiacodon uniformis* and *Dimetrodon limbatus;* Romer and Price 1940, *Haptodus garnettensis*; Laurin 1993, *Ianthasaurus hardestiorum*; Modesto and Reisz 1990 and *Edaphosaurus boanerges*; Modesto 1995). It is also present in lanthanosuchoid parareptiles, such as *Colobomycter pholeter* (MacDougall *et al.* 2017) and *Delorhynchus* (Reisz *et al.* 2014). It is therefore an autapomorphy of Lanthanosuchoidea that was independently acquired in Synapsida (de Braga and Reisz 1997).

Pathway of the cerebral carotid artery in the parabasisphenoid: The cerebral branch of the internal carotid artery (CBCA) extends through the basisphenoid from a position ventral to the basicranium into the endocranial cavity. However, its course thorough the basicranium varies among early amniotes. In particular, the condition in varanopids, stem-group amniotes, and sauropsids differs from that in synapsids. In synapsids (e.g. sphenacodontians, ophiacodontids and edaphosaurids*)* the point of entry of the CBCA into the endocranial cavity is located on the ventral surface of the parasphenoid medial to the basipterygoid processes, and is clearly visible in ventral view (Brinkman and Eberth 1983, Müller et al. 2011, Brink and Reisz 2012) (Figs. 21A-D). The internal carotid artery extends along grooves on the ventral surface of the parasphenoid rather than a deep trough on ventral surface of the basipterygoid process (Romer and Price 1940).

In contrast, the varanopid *Mycterosaurus* (= *Basicranodon*, Reisz *et al.* 1997) possesses a pathway of the CBCA very similar to that of *Orovenator* (Figs. 21E, F)), with the entry point via a foramen in a deep trough or vidian sulcus formed by the lateral ridge of the parasphenoidal plate and the ventral surface the basipterygoid process, effectively obscuring the foramen in ventral view (Vaughn 1958). In the varanopid *Aerosaurus*, it has been suggested that the entry point for the CBCA is

situated on the lateral surface of the basisphenoid, posterior to the clinoid process, rather than via the vidian sulcus ventral to the basipterygoid process (Langston and Reisz 1981). A similar condition is only otherwise seen in taxa with vidian canals where the division of the carotid artery into the cerebral and palatine branches occurs internally (e.g. in parareptiles, squamates, crown-group turtles and birds) rather than externally as in early synapsids, early turtles and eureptiles (Müller *et al.* 2011). The pathway of the CBCA is located in a vidian sulcus ventral to the basipterygoid process in all early eureptiles in which the parabasisphenoid is preserved, for example *Prolacerta* (Evans 1986), *Youngina* (Evans 1987, Gardner et al. 2010), *Captorhinus laticeps* (Heaton 1979), *Gephyrosaurus* (Evans 1980), *Sphenodon* and basal lepidosaurs (Evans 2008). It is similarly located in the stem amniotes *Chroniosuchus* and *Seymouria baylorensis* (White 1939, Shishkin 1968) suggesting this feature may be plesiomorphic for amniotes.

PHYLOGENETIC ANALYSIS

Orovenator has so far been regarded as a diapsid, because of its diapsid-like temporal fenestration (Reisz *et al.* 2011). Reisz *et al.* (2011) therefore investigated the phylogenetic position of *Orovenator* within the framework of early diapsid evolution, using 29 neodiapsid and diapsid taxa with four out-groups. This analysis recovered *Orovenator* as the most basal member of Neodiapsida (Fig. 13A). However, our new data and comparisons (discussed above) includes many more observations of similarity between *Orovenator* and varanopids, which have classically been regarded as synapsids (Romer & Price 1940, Reisz 1986, Reisz and Laurin 2004, Benson 2012, Reisz and Fröbisch 2014). We therefore elected to test whether the relationship between *Orovenator* and varanopids might differ from the current consensus. For this purpose we scored *Orovenator* into the character/taxon matrix of Reisz *et al.* (2010) designed to differentiate between diapsids and varanopids, and

previously used to reassess the phylogenetic position of *Apsisaurus witteri* (Figs. 22A, B).

One change was made to the matrix. The score of character 60 (number of coronoids) was changed from two (state 0) to one (state 1) for *Mesenosaurus*, based on the absence of an anterior coronoid (Berman and Reisz 2001). This change made no difference to the tree topology prior to the inclusion of *Orovenator.* All ordered (additive) characters were analysed as such, following Reisz et al. (2010). The scores for *Orovenator* are given in Supplement 2. The matrix was run in TNT v.1.5 (Goloboff *et al.* 2008) using New Technology search with drift, tree fusing, parsimony ratchet and sectorial search. The initial search level was set at 60 and additional sequence replicates at 500. Minimum length search was 30. Zero length branches are collapsed as default in TNT v.1.5. All resultant trees were subjected to final TBR branch swapping (bbreak=tbr). This analysis resulted in 3 MPT's with tree length of 386 (Fig. 23).

The inclusion of *Orovenator* into the matrix of Reisz *et al.* (2010) results in a fundamental change to tree topology. Varanopids were previously found as synapsids, but are now instead recovered within the diapsid clade as a monophyletic group, with *Orovenator* as the basal-most member. This group is placed crownward to araeoscelidian diapsids and is the sister group of all remaining neodiapsids. Bremer support, however, is poor with only one additional step required to collapse all major nodes (i.e. Synapsida, Sauropsida and Diapsida). Furthermore, only one additional step is required to recover varanopids as synapsids to the exclusion of *Orovenator*. This result occurs in spite of the fact that only five of the 16 similarities or synapomorphies between *Orovenator*/sauropsids and *Archaeovenator*/varanopids documented above are included in the character list used in this analysis. Therefore, this phylogenetic hypothesis test is conservative - the finding of an early diapsid

clade comprising *Orovenator* plus varanopids occurs in the absence of the addition of extra characters that are consistent with that hypothesis. To test hypotheses of the phylogenetic position of varanopids further requires a broad-based approach to early amniote phylogeny, incorporating a comprehensive character/taxon matrix that may be applied across all established groups of early amniotes. This is currently not available and such an undertaking is beyond the scope of this study. It will be addressed in future work currently in preparation.

Nevertheless, these results imply that, contrary to the current paradigm, varanopids may represent a monophyletic clade of early non-araeoscelidian diapsids that diverged from its sister group, the neodiapsids, during or prior to the late Carboniferous (Upper Pennsylvanian). The scarcity of diapsids during the early Permian (Reisz *et al.* 2011) is to some extent rectified by this hypothesis, in which varanopids represent a previously unrecognised clade of early Permian diapsids. However, it also extends the ghost lineage for neodiapsids from the late Carboniferous to the appearance of *Lanthanolania* in the late middle Permian (Modesto and Reisz 2003). This hypothesis, if correct, makes several characters that were highly congruent with previous phylogenetic hypotheses (in which varanopids are synapsids) incongruent. These are discussed below.

Character states that are incongruent with the hypothesis that varanopids are sauropsids.

Varanopids possess only a single, lateral temporal fenestra as seen in synapsids. In contrast, *Orovenator* and all diapsids possess upper and lower temporal openings - although in some taxa the lower temporal bar is not completed, meaning that the lower temporal fenestra takes the form of an arch or emargination. Indeed, the condition of the lower temporal opening is not known in *Orovenator,* despite the

elongate subtemporal process of the jugal (see Description). If the topology recovered by our analysis is correct, then diapsid or euryapsid temporal fenestration was primitively present in the clade comprising *Orovenator* + varanopids, as indicated by the anatomy of *Orovenator*. However, the upper temporal fenestra was subsequently lost in this group, as it is absent in varanopids where the posterior process of the postorbital has closed with the lateral margin of the parietal, resulting in a dorsoventral enlargement of the lower temporal fenestra.

Hypotheses of early amniote phylogeny have placed substantial emphasis on temporal fenestration (Gauthier *et al.* 1988, Laurin and Reisz 1995, de Braga and Rieppel 1997), despite the recognition of widespread plasticity of temporal fenestrae in early amniotes (Frazetta 1968, Müller 2003). Many examples of homoplasy have been reported relating to the loss or acquisition of temporal fenestration, suggesting a high degree of plasticity even amongst closely related taxa, with multiple independent modifications of temporal fenestration amongst parareptiles (Piñeiro *et al.* 2012, MacDougall and Reisz 2014) or the opportunistic development of lower temporal fenestration in the early synapsid *Ophiacodon* (Romer and Price 1940, Frazetta 1968). There is also good evidence for local-scale homoplasy in temporal fenestration amongst diapsids. For example, the araeoscelidian diapsid *Petrolacosaurus* has a lower temporal fenestra with a complete ventral bar (the diapsid condition), whereas its sister taxon *Araeoscelis* lacks a lower temporal opening entirely (Reisz *et al.* 1984, Vaughn 1955). Furthermore, the euryapsid condition is widespread among late Permian neodiapsids (*Claudiosaurus*; Carroll 1981 and *Acerosodontosaurus*; Bickelmann et al. 2009), archosauromorphs (*Prolacerta*; Modesto and Sues 2004 and *Tanystropheus;* Nosotti 2007), sauropterygians (Rieppel 1993), and is present in all extant squamates (Evans 2008). It has even been proposed that turtles are modified diapsids, which implies the secondary closure of the upper and lower temporal fenestrae and the

emargination of the posterior and ventral temporal region (Rieppel 1993, Bever et al. 2015). Recent work on the patterns of ontogenetic change in the temporal region of early amniotes may provide some clues on the mechanisms of closure of fenestrae (Haridy *et al.* 2016). However, it is evident that temporal fenestration can be readily lost or gained within closely related groups of early amniotes.

In addition to temporal fenestration, there are other morphologies that would appear to contradict the grouping of varanopids within Diapsida. However, when the presence or absence of such morphologies is reviewed for each taxon we find that their occurrence in varanopids is variable. For example, *Orovenator* possesses a single coronoid in the mandible, a widely recognised synapomorphy of Sauropsida (de Braga and Rieppel 1997). The presence of multiple coronoids is plesiomorphic for amniotes (Moss 1972, Laurin 1996, Berman *et al.* 2010), and early synapsids possess two coronoids (anterior and posterior coronoids; Romer and Price 1940, Romer 1956). This condition has also been stated to be present in varanopids (Reisz 1986). However, although varanopids, such as *Mesenosaurus, Mycterosaurus, Varanodon* and *Varanops* have been scored as possessing two coronoids in some phylogenetic studies (e.g. Reisz *et al.* 2010), we are aware of only one specimen of *Varanops* (TMM 43628-1 Campione and Reisz 2010) in which evidence of an anterior coronoid has been unequivocally documented. Moreover, the anterior coronoid is absent in *Mesenosaurus* (Reisz and Berman 2001), and it also appears to be absent in the right mandible of *Archaeovenator* (pers. obs. KUVP 12483, Reisz and Dilkes 2003). There is no evidence of an anterior coronoid in the mandible assigned to a mycterosaurine varanopid from the middle Permian of South Africa (Modesto *et al.* 2011). In *Aerosaurus*, the coronoid is not preserved, but a groove on the anteromedial surface of the dentary is interpreted as accommodating the anterior coronoid (Langston and Reisz 1981). A “probable” anterior coronoid was identified in *Heleosaurus* (Reisz and Modesto 2007:736), although this is not conclusive. In

consequence, the number of coronoids cannot be determined in many varanopids, and seems to be variable. The variable nature of the coronoid count in amniotes is further exemplified in the early diapsid *Araeoscelis*, which possesses an anterior and posterior coronoid (Vaughn 1955).

The suborbital fenestra in the suborbital region of the palate between the maxilla, palatine, pterygoid and ectopterygoid is a synapomorphy of sauropsids (de Braga and Rieppel 1997). In captorhinids and parareptiles it is present as a small gap or foramen (e.g. *Captorhinus laticeps*; Heaton 1979 and *Belebey vegrandis*; Reisz et al. 2007). In diapsids it commonly takes the form of an anteroposteriorly elongate and transversely broad fenestra, as seen in the earliest members of the clade (e.g. araeoscelidian diapsids; Vaughn 1955, Reisz 1981) and more derived taxa (e.g. *Prolacerta*; Gow 1975, *Youngina*; Carroll 1981 and *Gephyrosaurus*; Evans 1980). *Orovenator* possesses a slender, transversely narrow, slot-like suborbital fenestra that is particularly narrow anteriorly where the lateral margin of the palatine is dorsoventrally thin and almost contacts the maxilla (Fig.9).

The absence of a suborbital fenestra is likely primitive for amniotes since it is also absent in basal eureptiles (e.g. *Paleothyris*; Carroll 1969, *Protorothyris* and *Romeria*; Clark and Carroll 1973). All ‘pelycosaur’ – grade synapsids also lack the suborbital fenestra (de Braga and Rieppel 1997). In fact, many of them possess a dorsoventrally deep, firmly sutured contact between the maxilla and the palate. Although varanopids have been scored as lacking a subtemporal fenestra in phylogenetic analyses (Reisz *et al.* 2010), in fact this region is damaged or otherwise unobservable in most taxa. In *Mesenosaurus* the anterior process of the ectopterygoid contacts the jugal laterally and the palatine medially thus effectively eliminating the possibility of a suborbital opening in the palate (Reisz and Berman 2001). In *Elliotsmithia*, only a small region of the medial margin of the right palatine is

exposed (Reisz et al. 1998). This is mildly concave and the nature of its contact with the maxilla cannot be ascertained. In *Heleosaurus*, the right palatine was considered too wide posteriorly to accommodate a suborbital fenestra (Reisz and Modesto 2007), although this is almost identical to the right palatine of *Orovenator*. The suborbital region of the palate is not observable in *Mycterosaurus*, *Pyozia*, *Apsisaurus*, *Ascendonanus, Aerosaurus*, *Varanodon*, *Watongia* and *Varanops*.

In summary, we find that the character states that are incongruent with the hypothesis of varanopids as sauropsids are either highly homoplastic amongst early amniotes (temporal fenestration), variably present or absent amongst varanopids (single or multiple coronoids) or cannot be unequivocally scored in most varanopid taxa (the absence of a suborbital fenestra).

CONCLUSIONS

We review the anatomy of the oldest non-araeoscelidian diapsid, *Orovenator mayorum*, using high resolution μCT scanning and reconstruction. We find at least 16 similarities, many of which previously unrecognised, between *Orovenator*/sauropsids and varanopids, which are typically considered to be synapsids. We therefore propose a hypothesis that *Orovenator* forms a clade with varanopids, raising questions about whether this clade belongs to Synapsida or Sauropsida. The further evidence presented in our study supports a relationship between sauropsids and varanopids that is incongruent with the current paradigm of early amniote phylogeny. However, our findings clearly emphasise the need for further scrutiny of the base of the amniote tree, including more comprehensive character and taxon sampling across the diversity of early amniotes. We also concur with early studies that highlight the highly homoplastic nature of temporal fenestration amongst early amniotes. Finally, the present study illustrates the potential advantages in

reassessing early amniote taxa using µCT scanning. Many of the earliest fossil amniotes are small-bodied taxa, for which only external cranial anatomy has been visible until now. Our work on *Orovenator* demonstrates that high resolution µCT scanning can create new insights on the comparative anatomy of the earliest amniotes. We expect that this may stimulate further debate on the systematics of amniote evolution.

Acknowledgements

Our grateful thanks go to the curators and collection managers for allowing access to the specimens under their care: Rich Cifelli and Jennifer Larson (OMNH), Stephanie Pierce and Jessica Cundiff (MCZ), Bill Simpson and Ken Angielczyk (FMNH), Jonah Choiniere and Sifelani Jirah (ESI), Chris Beard and Desui Miao (KUVP) and Cristiano Dal Sasso (MCSNM). Thanks also to Roger Burkhalter (OMNH) for his stacked photography of OMNH 74606 and 74607, which are used in this study and to Jessie Maisano (University of Texas, Austin) and April Isch (University of Chicago) for the µCT scans. We further thank Ken Angielczyk and Christian Kammerer for their insightful comments and suggestions, which greatly improved this manuscript. DPF has benefited from the help and support of his colleagues in the Dept. of Earth Sciences, University of Oxford: Mimi Beckett, Gemma Benevento, Neil Brocklehurst, Serjoscha Evers and James Neenan. This research was supported by a NERC studentship for DPF from the DTP Environmental Research Council, UK (NE/L0021612/1).

DATA ARCHIVING STATEMENT

The µCT data for this study, including all mesh files in .ply format generated from the µCT data together with the tiff stacks for each specimen are available for download

through MorphoSource (http://www.MorphoSource.org/) as project 'Orovenator_DPF/RBJB'.

Supplementary data for this study, including notes on the virtual construction of the scleral ring and optical measurements (Supplement 1), phylogenetic matrix scores based on Reisz *et al.* 2010 and accompanying notes (Supplement 2) and specimen measurements (Supplement 3) are available in the Dryad Digital Repository: https://datadryad.org/review?doi=doi:10.5061/dryad.n62t1hm

REFERENCES

ANDERSON, J. S., SCOTT, D. and REISZ, R. R. 2009. *Nannaroter mckinziei*, a new ostodolepid 'microsaur'(Tetrapoda, Lepospondyli, Recumbirostra) from the Early Permian of Richards Spur (Ft. Sill), Oklahoma. *Journal of Vertebrate Paleontology*, **29**, 379-388.

ANGIELCZYK, K. and SCHMITZ, L. 2014. Nocturnality in synapsids predates the origin of mammals by over 100 million years. **1642** *Proc. R. Soc. B*. The Royal Society.

ANGIELCZYK, K. D. and KAMMERER, C. F. In Press. Non-mammalian synapsids: the deep roots of the mammalian family tree. In Handbook of Zoology: Mammalia: Mammalian Evolution, Diversity and Systematics (F. E. Zachos and R. J. Asher, eds.) *De Gruyter, Berlin.*

ATKINS, J. B. and FRANZ□ODENDAAL, T. A. 2016. The sclerotic ring of squamates: an evo□devo□eco perspective. *Journal of anatomy*, **229**, 503-513.

AUGE, M. and SMITH, R. 2009. An assemblage of early Oligocene lizards (Squamata) from the locality of Boutersem (Belgium), with comments on the Eocene-Oligocene transition. *Zoological Journal of the Linnean Society*, **155**, 148-170.

BENOIT, J., ANGIELCZYK, K. D., MIYAMAE, J. A., MANGER, P., FERNANDEZ, V. and RUBIDGE, B. 2018. Evolution of facial innervation in anomodont therapsids (Synapsida): Insights from X-ray computerized microtomography. *Journal of morphology*, **279**(5), 673-701.

BENSON, R. B. 2012. Interrelationships of basal synapsids: cranial and postcranial morphological partitions suggest different topologies. *Journal of Systematic Palaeontology*, **10**, 601-624.

BENTON, M. J. 1985. Classification and phylogeny of the diapsid reptiles. *Zoological Journal of the Linnean Society*, ***84***(2), 97-164.

BENTON, M. J., DONOGHUE, P. C. J., ASHER, R. J., FREIDMAN, M., NEAR, T. J., and VINTHER, J. 2015. Constraints on the timescale of animal evolutionary history. *Palaeontologia Electronica* **18**.1.1FC; 1-106. https://doi.org/10.26879/424

BERMAN, D., REISZ, R.R., BOLT, J. and SCOTT, D. 1995. The cranial anatomy and relationships of the synapsid *Varanosaurus* (Eupelycosauria, Ophiacodontidae) from the Early Permian of Texas and Oklahoma. *Annals of Carnegie Museum*, **64**, 99-133.

BERMAN, D., REISZ, R. and SCOTT, D. 2010. Redescription of the skull of *Limnoscelis paludis* Williston (Diadectomorpha: Limnoscelidae) from the Pennsylvanian of Canon del Cobre, northern New Mexico. *New Mexico Mus. Nat. Hist. Sci. Bull.*, **49**, 185-210.

BERMAN, D. S. and REISZ, R. R. 1982. Restudy of *Mycterosaurus Longiceps* (Reptilia, Pelycosauria): From the Lower Permian of Texas. *Annals of the Carnegie Museum*, **51**, 423-453.

BERTMAR, G. 1981. Evolution of vomeronasal organs in vertebrates. *Evolution*, **35**, 359-366.

BEVER, G., LYSON, T. R., FIELD, D. J. and BHULLAR, B. A. S. 2015. Evolutionary origin of the turtle skull. *Nature*, **525**, 239.

BICKELMANN, C., MÜLLER, J. and REISZ, R. R. 2009. The enigmatic diapsid *Acerosodontosaurus piveteaui* (Reptilia: Neodiapsida) from the Upper Permian of Madagascar and the paraphyly of "younginiform" reptiles. *Canadian Journal of Earth Sciences*, **46**, 651-661.

BOTHA-BRINK, J. and MODESTO, S. P. 2009. Anatomy and relationships of the Middle Permian varanopid *Heleosaurus scholtz*i based on a social aggregation from the Karoo Basin of South Africa. *Journal of Vertebrate Paleontology*, **29**, 389-400.

BRINK, K. S. and REISZ, R. R. 2012. Morphology of the palate and braincase of *Dimetrodon milleri*. *Historical Biology*, **24**, 453-459.

BRINKMAN, D. and EBERTH, D. A. 1983. The interrelationships of pelycosaurs. *Breviora*, Museum of Comparative Zoology, Harvard University, **473**, 35 pp.

--- --- 1986. The anatomy and relationships of *Stereophallodon* and *Baldwinonus* (Reptilia, Pelycosauria). *Breviora*, Museum of Comparative Zoology, Harvard University, **485**, 34 pp.

BROOM, R. 1907. On some new fossil reptiles from the Karroo beds of Victoria West, South Africa. *Transactions of the South African Philosophical Society*, **18**(1), 31-42.

CAMP, C. L. 1945. Prolacerta and the protorosaurian reptiles; Part I. *American Journal of Science*, **243**, 17-32.

CAMPIONE, N. E. and REISZ, R. R. 2010. *Varanops brevirostris* (Eupelycosauria: Varanopidae) from the Lower Permian of Texas, with discussion of varanopid morphology and interrelationships. *Journal of Vertebrate Paleontology*, **30**, 724-746.

CARROLL, R. L. 1964. The earliest reptiles. *Zoological Journal of the Linnean Society*, **45**, 61-83.

--- 1968. A ?Diapsid (Reptilia) Perietal from the Lower Permian of Oklahoma. *Postilla,* Peabody Museum of Natural History, Yale University, **117**, pp.7

--- 1969. A Middle Pennsylvanian captorhinomorph, and the interrelationships of primitive reptiles. *Journal of Paleontology*, **43**(1), 151-170.

--- 1976. Eosuchians and the origin of archosaurs. *In* Essays on Paleontology in Honour of Loris Shano Russell, (CHURCHER C.S ed). Miscellaneous Publications of the Royal Ontario Museum, Toronto, 58-79

--- 1981. Plesiosaur ancestors from the Upper Permian of Madagascar. *Phil. Trans. R. Soc. Lond. B*, **293**, 315-383.

ČERŇANSKÝ, A. and AUGE, M. L. 2013. New species of the genus *Plesiolacerta* (Squamata: Lacertidae) from the Upper Oligocene (MP28) of southern Germany and a revision of the type species Plesiolacerta lydekkeri. *Palaeontology*, **56**, 79-94.

CHEN, X.-H., MOTANI, R., CHENG, L., JIANG, D.-Y. and RIEPPEL, O. 2014. The enigmatic marine reptile *Nanchangosaurus* from the Lower Triassic of Hubei, China and the phylogenetic affinities of Hupehsuchia. *PLoS One*, **9**, e102361.

CISNEROS, J. C., DAMIANI, R., SCHULTZ, C., DA ROSA, A., SCHWANKE, C., NETO, L. W. and AURÉLIO, P. L. 2004. A procolophonoid reptile with temporal fenestration from the Middle Triassic of Brazil. *Proceedings of the Royal Society of London B: Biological Sciences*, **271**, 1541-1546.

CLARK, J. and CARROLL, R. L. 1973. Romeriid reptiles from the Lower Permian. *The Bulletin of the Museum of Comparative Zoology*, Harvard University, **144**(5), 353-407.

CROMPTON, A., TAYLOR, C. R. and JAGGER, J. A. 1978. Evolution of homeothermy in mammals. *Nature*, **272**, 333.

CURRIE, P. J. 1980. A new younginid (Reptilia: Eosuchia) from the Upper Permian of Madagascar. *Canadian Journal of Earth Sciences*, **17**, 500-511.

--- 1981. *Hovasaurus boulei*, an aquatic eosuchian from the Upper Permian of Madagascar. *Palaeontologica Africana*, **24**, 99-168.

DAMIANI, R., MODESTO, S., YATES, A. and NEVELING, J. 2003. Earliest evidence of cynodont burrowing. *Proceedings of the Royal Society of London B: Biological Sciences*, **270**, 1747-1751.

DEBRAGA, M. 2003. The postcranial skeleton, phylogenetic position, and probable lifestyle of the Early Triassic reptile Procolophon trigoniceps. *Canadian Journal of Earth Sciences*, **40**, 527-556.

DEBRAGA, M. and REISZ, R. R. 1995. A new diapsid reptile form the uppermost carboniferous (Stephanian) of Kansas. *Palaeontology*, **38**, 199-212.

--- --- 1996. The Early Permian reptile *Acleistorhinus pteroticus* and its phylogenetic position. *Journal of Vertebrate Paleontology*, **16**, 384-395.

DEBRAGA, M. and RIEPPEL, O. 1997. Reptile phylogeny and the interrelationships of turtles. *Zoological Journal of the Linnean Society*, **120**, 281-354.

EFREMOV, J. A. 1940. Preliminary description of the new Permian and Triassic Tetrapoda from USSR. *Trudy Paleontologicheskogo Instituta*, ***10***, 1-140.

EVANS, S. E. 1980. The skull of a new eosuchian reptile from the Lower Jurassic of South Wales. *Zoological journal of the Linnean Society*, **70**, 203-264.

--- 1986. The braincase of *Prolacerta broomi* (Reptilia: Triassic). *Neues Jahrbuch fur Geologie und Palaontologie Abhandlungen*, **173**, 181-200.

--- 1987. The braincase of *Youngina capensis* (Reptilia: Diapsida; Permian). *Neues Jahrbuch für Geologie und Paläontologie Monatshefte*, **1987**(4), 193-203.

--- 1991. A new lizard□like reptile (Diapsida: Lepidosauromorpha) from the Middle Jurassic of England. *Zoological Journal of the Linnean Society*, **103**, 391-412.

--- 2008. The skull of lizards and tuatara. *In* Biology of the Reptilia, (The Skull of Lepidosauria) (C. Gans, A. S. Gaunt, and K. Adler, eds.). *Society for the Study of Amphibians and Reptiles, Ithaca, New York*, **20**, 1-347.

--- 2009. An early kuehneosaurid reptile from the Early Triassic of Poland. *Palaeontologia Polonica*, **65**, 145-178.

EVANS, S. E. and BORSUK-BIAŁYNICKA, M. 2009. A small lepidosauromorph reptile from the Early Triassic of Poland. *Palaeontologia Polonica*, **65**, 179-202.

EZCURRA, M. D. and BUTLER, R. J. 2015. Taxonomy of the proterosuchid archosauriforms (Diapsida: Archosauromorpha) from the earliest Triassic of South Africa, and implications for the early archosauriform radiation. *Palaeontology*, **58**, 141-170.

EZCURRA, M. D., BUTLER, R. J. and GOWER, D. J. 2013. 'Proterosuchia': the origin and early history of Archosauriformes. *Geological Society, London, Special Publications*, **379**, 9-33.

EZCURRA, M. D., SCHEYER, T. M. and BUTLER, R. J. 2014. The origin and early evolution of Sauria: reassessing the Permian saurian fossil record and the timing of the crocodile-lizard divergence. *PLoS One*, **9**, e89165.

FOX, R. C. and BOWMAN, M. C. 1966. Osteology and relationships of C*aptorhinus aguti* (Cope)(Reptilia: Captorhinomorpha). *The University of Kansas Paleontological Contributions, Vertebrata*, **11**, 1-79.

FRACASSO, M. A. 1987. Braincase of *Limnoscelis paludis* Williston. *Postilla*, Peabody Museum of Natural History, **201**, pp.22.

FRASER, N. and SHELTON, C. 1988. Studies of tooth implantation in fossil tetrapods using high-resolution X-radiography. *Geological Magazine*, **125**, 117-122.

FRASER, N. C. 1988. The osteology and relationships of *Clevosaurus* (Reptilia: Sphenodontida). *Phil. Trans. R. Soc. Lond. B*, **321**, 125-178.

FRAZZETTA, T. 1968. Adaptive problems and possibilities in the temporal fenestration of tetrapod skulls. *Journal of Morphology*, **125**, 145-157.

GAFFNEY, E. S. 1979. Comparative cranial morphology of recent and fossil turtles. . *Bulletin of the American Museum of Natural History* **164(2)**, 65-376.

GARDNER, N. M., HOLLIDAY, C. M. and O'KEEFE, F. R. 2010. The braincase of *Youngina capensis* (Reptilia, Diapsida): new insights from high-resolution CT scanning of the holotype. *Palaeontologica Electronica*, **13**, 16.

GAUTHIER, J., KLUGE, A. G. and ROWE, T. 1988. Amniote phylogeny and the importance of fossils. *Cladistics*, **4**, 105-209.

GOW, C. E. 1972. The osteology and relationships of the Millerettidae (Reptilia: Cotylosauria). *Journal of Zoology*, **167**, 219-264.

--- 1975. The morphology and relationships of *Youngina capensis* Broom and *Prolacerta broomi* Parrington. *Palaeontologia Africana*, **18**, 89-131.

HAECKEL E. 1866. Generelle Morphologie der Organismen: Allgemeine Grundzüge der organischen Formen-Wissenschaft, mechanisch begrundet durch die von Charles Darwin reformirte Descendenz-Theorie: *II Allgemeine Entwickelungsgeschichte der Organismen*.

HALL, M. I., KIRK, E. CHRISTOPHER, KAMILAR, JASON M., CARRANO, MATTHEW T. 2011. Comment on "Nocturnality in Dinosaurs Inferred from Scleral Ring and Orbit Morphology". *Science*, **334(6063)**, 1641.

HARIDY, Y., MACDOUGALL, M. J., SCOTT, D. and REISZ, R. R. 2016. Ontogenetic Change in the Temporal Region of the Early Permian Parareptile

Delorhynchus cifellii and the Implications for Closure of the Temporal Fenestra in Amniotes. *PloS one*, **11**, e0166819.

HEATON, M. J. 1979. Cranial anatomy of primitive captorhinid reptiles from the Late Pennsylvanian and Early Permian, Oklahoma and Texas. Oklahoma Geological Survey, University of Oklahoma, **127**, i-iv, 84.pp.

IVAKHNENKO, M.F. and KURZANOV, S.M., 1979. *Mesenosaurus*, a primitive archosaur. *Paleontological Journal* **12**, 131-141.

HILLENIUS, W. J. 2000. Septomaxilla of nonmammalian synapsids: Soft□tissue correlates and a new functional interpretation. *Journal of Morphology*, **245**, 29-50.

HILLENIUS, W. J. and REHOREK, S. J. 2005. From the eye to the nose: ancient orbital to vomeronasal communication in tetrapods? 228-241. *Chemical signals in vertebrates **10**.* Springer, 228-241.

HUXLEY, T.H. 1864. The Structure and Classification of the Mammalia. Hunterian lectures, presented in *Medical Times and Gazette,*

KLEMBARA, J. 1997. The cranial anatomy of *Discosauricsus* Kuhn, a seymouriamorph tetrapod from the Lower Permian of the Boskovice Furrow (Czech Republic). *Philosophical Transactions of the Royal Society B: Biological Sciences*, **352**, 257-302.

KLEMBARA, J., CLACK, J. A., MILNER, A. R. and RUTA, M. 2014. Cranial anatomy, ontogeny, and relationships of the Late Carboniferous tetrapod *Gephyrostegus bohemicus* Jaekel, 1902. *Journal of Vertebrate Paleontology*, **34**, 774-792.

KLEMBARA, J. and RUTA, M. 2005. The seymouriamorph tetrapod *Ariekanerpeton sigalovi* from the Lower Permian of Tadzhikistan. Part I: Cranial anatomy and ontogeny. *Earth and Environmental Science Transactions of The Royal Society of Edinburgh*, **96**, 43-70.

LANE, H. 1945. New mid-Pennsylvanian reptiles from Kansas. *Transactions of the Kansas Academy of Science*, **47**, 381-390.

LANGSTON JR, W. and REISZ, R. R. 1981. *Aerosaurus wellesi*, new species, a varanopseid mammal-like reptile (Synapsida: Pelycosauria) from the Lower Permian of New Mexico. *Journal of Vertebrate Paleontology*, **1**, 73-96.

LAURIN, M. 1991. The osteology of a Lower Permian eosuchian from Texas and a review of diapsid phylogeny. *Zoological Journal of the Linnean Society*, **101**, 59-95.

--- 1993. Anatomy and relationships of *Haptodus garnettensis*, a Pennsylvanian synapsid from Kansas. *Journal of Vertebrate Paleontology*, **13**, 200-229.

--- 1996. A reevaluation of *Ariekanerpeton*, a lower Permian seymouriamorph (Vertebrata: Seymouriamorpha) from Tadzhikistan. *Journal of Vertebrate Paleontology*, **16**, 653-665.

LAURIN, M. and REISZ, R. R. 1995. A reevaluation of early amniote phylogeny. *Zoological Journal of the Linnean Society*, **113**, 165-223.

LYSON, T.R., RUBIDGE, B.S., SCHEYER, T.M., DE QUEIROZ, K., SCHACHNER, E.R., SMITH, R.M., BOTHA-BRINK, J. and BEVER, G.S. 2016. Fossorial origin of the turtle shell. *Current Biology*, ***26***(14), 1887-1894.

MACDOUGALL, M. J., MODESTO, S. P. and REISZ, R. R. 2016. A new reptile from the Richards Spur Locality, Oklahoma, USA, and patterns of Early Permian parareptile diversification. *Journal of Vertebrate Paleontology*, **36**, e1179641.

MACDOUGALL, M. J. and REISZ, R. R. 2014. The first record of a nyctiphruretid parareptile from the Early Permian of North America, with a discussion of parareptilian temporal fenestration. *Zoological Journal of the Linnean Society*, **172**, 616-630.

MACDOUGALL, M. J., SCOTT, D., MODESTO, S. P., WILLIAMS, S. A. and REISZ, R. R. 2017a. New material of the reptile *Colobomycter pholeter* (Parareptilia:

Lanthanosuchoidea) and the diversity of reptiles during the Early Permian (Cisuralian). *Zoological Journal of the Linnean Society*, **180**, 661-671.

MACDOUGALL, M. J., TABOR, N. J., WOODHEAD, J., DAOUST, A. R. and REISZ, R. R. 2017b. The unique preservational environment of the Early Permian (Cisuralian) fossiliferous cave deposits of the Richards Spur locality, Oklahoma. *Palaeogeography, Palaeoclimatology, Palaeoecology*, **475**, 1-11.

MADDIN, H. C., EVANS, D. C. and REISZ, R. R. 2006. An Early Permian varanodontine varanopid (Synapsida: Eupelycosauria) from the Richards Spur locality, Oklahoma. *Journal of Vertebrate Paleontology*, **26**, 957-966.

MADDIN, H. C., OLORI, J. C. and ANDERSON, J. S. 2011. A redescription of *Carrolla craddocki* (Lepospondyli: Brachystelechidae) based on high□ resolution CT, and the impacts of miniaturization and fossoriality on morphology. *Journal of Morphology*, **272**, 722-743.

MADDIN, H. C. and REISZ, R. R. 2007. The morphology of the terminal phalanges in Permo-Carboniferous synapsids: an evolutionary perspective. *Canadian Journal of Earth Sciences*, *44*(2), 267-274.

MADDIN, H. C., SIDOR, C. A. and REISZ, R. R. 2008. Cranial anatomy of *Ennatosaurus tecton* (Synapsida: Caseidae) from the Middle Permian of Russia and the evolutionary relationships of Caseidae. *Journal of Vertebrate Paleontology*, **28**, 160-180.

MAISANO, J. A., KEARNEY, M. and ROWE, T. 2006. Cranial anatomy of the spade□ headed amphisbaenian *Diplometopon zarudnyi* (Squamata, amphisbaenia) based on high□resolution X□ray computed tomography. *Journal of Morphology*, **267**, 70-102.

MCGOWAN, C. and MOTANI, R. 2003. Handbook of Paleoherpetology: Ichthyopterygia. Part **8**, Friedrich Pfeil, Munich.

MODESTO, S. 1995. The skull of the herbivorous synapsid *Edaphosaurus boanerge*s from the Lower Permian of Texas. *Palaeontology*, **38**, 213.

MODESTO, S. and REISZ, R. 1990. A new skeleton of *Ianthasaurus hardestii*, a primitive edaphosaur (Synapsida: Pelycosauria) from the Upper Pennsylvanian of Kansas. *Canadian Journal of Earth Sciences*, **27**, 834-844.

MODESTO, S., SIDOR, C. A., RUBIDGE, B. S. and WELMAN, J. 2001. A second varanopseid skull from the Upper Permian of South Africa: implications for Late Permian 'pelycosaur'evolution. *Lethaia*, **34**, 249-259.

MODESTO, S. P. and REISZ, R. R. 2002. An enigmatic new diapsid reptile from the Upper Permian of Eastern Europe. *Journal of Vertebrate Paleontology*, **22**, 851-855.

MODESTO, S. P., SCOTT, D. M., BERMAN, D. S., MÜLLER, J. and REISZ, R. R. 2007. The skull and the palaeoecological significance of *Labidosaurus hamatus*, a captorhinid reptile from the Lower Permian of Texas. *Zoological Journal of the Linnean Society*, **149**, 237-262.

MODESTO, S.P., SCOTT, D.M., MACDOUGALL, M. J., SUES, H-D, EVANS, D. C. and REISZ, R. R. 2015. The oldest parareptile and the early diversification of the reptiles. *Philosophical Transactions of the Royal Society B: Biological Sciences*, **282**, (1801), 20141912

MODESTO, S. P. and SMITH, R. M. 2001. A new Late Permian captorhinid reptile: a first record from the South African Karoo. *Journal of Vertebrate Paleontology*, **21**, 405-409.

MODESTO, S. P., SMITH, R. M., CAMPIONE, N. E. and REISZ, R. R. 2011. The last "pelycosaur": a varanopid synapsid from the *Pristerognathus* Assemblage Zone, Middle Permian of South Africa. *Naturwissenschaften*, **98**, 1027-1034.

MODESTO, S. P. and SUES, H. D. 2004. The skull of the Early Triassic archosauromorph reptile *Prolacerta broomi* and its phylogenetic significance. *Zoological Journal of the Linnean Society*, **140**, 335-351.

MOSS, J. L. 1972.The Morphology and Phylogenetic Relationship of the Lower Permian Tetrapod *Tseajaia Campi* Vaughn (Amphibia: Seymouriamorpha). *University of California Publications in Geological Sciences,* University of California Press.

MOTANI, R. and SCHMITZ, L. 2011. Phylogenetic versus functional signals in the evolution of form–function relationships in terrestrial vision. *Evolution*, **65**, 2245-2257.

MÜLLER, J. 2003. Early loss and multiple return of the lower temporal arcade in diapsid reptiles. *Naturwissenschaften*, **90**, 473-476.

--- 2005. The anatomy of *Askeptosaurus italicus* from the Middle Triassic of Monte San Giorgio and the interrelationships of thalattosaurs (Reptilia, Diapsida). *Canadian Journal of Earth Sciences*, **42**, 1347-1367.

MÜLLER, J. and REISZ, R. R. 2005a. Four well□constrained calibration points from the vertebrate fossil record for molecular clock estimates. *BioEssays*, **27**, 1069-1075.

--- --- 2005b. An early captorhinid reptile (Amniota, Eureptilia) from the Upper Carboniferous of Hamilton, Kansas. *Journal of Vertebrate Paleontology*, **25**, 561-568.

MÜLLER, J., STERLI, J. and ANQUETIN, J. 2011. Carotid circulation in amniotes and its implications for turtle relationships. *Neues Jahrbuch für Geologie und Paläontologie-Abhandlungen*, **261**, 289-297.

MÜLLER, J. and TSUJI, L. A. 2007. Impedance-matching hearing in Paleozoic reptiles: evidence of advanced sensory perception at an early stage of amniote evolution. *Plos One*, **2**, e889.

NASTERLACK, T., CANOVILLE, A. and CHINSAMY, A. 2012. New insights into the biology of the Permian genus Cistecephalus (Therapsida, Dicynodontia). *Journal of Vertebrate Paleontology*, ***32***(6), 1396-1410.

NOSOTTI, S. 2007. *Tanystropheus longobardicus* (Reptilia, Protorosauria): Re-interpretations of the Anatomy Based on New Specimens from the Middle Triassic of Besano (Lombardy, Northern Italy). *Memorie della Società Italiana di Scienze Naturali e Museo Civico di Storia Naturale di Milano, **34**(3).*

OLORI, J. C. and BELL, C. J. 2012. Comparative skull morphology of uropeltid snakes (Alethinophidia: Uropeltidae) with special reference to disarticulated elements and variation. *PLoS One*, **7**, e32450.

OLSON, E. C. 1965. New Permian vertebrates from the Chickasha Formation in Oklahoma. *Circ. Okla. Geol. Surv.,* University of Oklahoma.

OLSON, E. C. 1968. The family Caseidae. *Fieldiana: Geology*. Field Museum of Natural History. **17**(3)

OSBORN, H. F. 1903. On the primary division of the Reptilia into two sub-classes, Synapsida and Diapsida. *Science*, **17**, 275-276.

PARDO, J.D. and ANDERSON, J.S. 2016. Cranial Morphology of the Carboniferous-Permian tetrapod *Brachydectes newberryi* (Lepospondyli, Lysorophia): New data from μCT. *PloS one*, ***11***(8), p.e0161823.

PIÑEIRO, G., FERIGOLO, J., RAMOS, A. and LAURIN, M. 2012. Cranial morphology of the Early Permian mesosaurid *Mesosaurus tenuidens* and the evolution of the lower temporal fenestration reassessed. *Comptes Rendus Palevol*, **11**, 379-391.

PRITCHARD, A. C. and NESBITT, S. J. 2017. A bird-like skull in a Triassic diapsid reptile increases heterogeneity of the morphological and phylogenetic radiation of Diapsida. *Royal Society open science*, **4**, 170499.

REIG, O. A. 1967. Archosaurian reptiles: a new hypothesis on their origins. *Science*, **157**, 565-568.

--- 1970. The Proterosuchia and the early evolution of the archosaurs; an essay about the origin of a major taxon. *Bulletin of the Museum of Comparative Zoology, Harvard University*, **139**, 229-292.

REISZ, R. R. 1972. Pelycosaurian reptiles from the middle Pennsylvanian of North America. *The Bulletin of the Museum of Comparative Zoology, Harvard University,* ***114***(2*),* 27-61.

--- 1977. Petrolacosaurus, the oldest known diapsid reptile. *Science*, **196**, 1091-1093.

--- 1981. A diapsid reptile from the Pennsylvanian of Kansas. *Special Publication of the Museum of Natural History, University of Kansas*. No.**7**

--- 1986. Handbook of Paleoherpetology: Pelycosauria. G*ustav Fisher Verlag*, Part **17a**, 102 pp.

--- 1989. Two small reptiles from a Late Pennsylvanian quarry near Hamilton, Kansas. *In* Regional geology and paleontology of Upper Paleozoic Hamilton Quarry area in southeastern Kansa*s (MAPES G.K. and MAPES R.H eds.). Kansas Geological Survey, University of Kansas*, **6**, 189-194.

--- 2005. *Oromycter*, a new caseid from the Lower Permian of Oklahoma. *Journal of Vertebrate Paleontology*, **25**, 905-910.

--- 2014. “Pelycosaur”- Grade Synapsids: Introduction. . 3-5. *In* KAMMERER, C. F., ANGIELCZYK, K. D. AND FRÖBISCH, J. (EDS). (ed.) *Early evolutionary history of the Synapsida*. Vertebrate Paleobiology and Paleoanthropology Series, Springer Science and Business Media, Dordrecht.

REISZ, R. R. and BERMAN, D. S. 2001. The skull of *Mesenosaurus romeri*, a small varanopseid (Synapsida: Eupelycosauria) from the Upper Permian of the Mezen River Basin, northern Russia. *Annals of the Carnegie Museum, Pittsburg*. **70**, 113-132.

REISZ, R. R., BERMAN, D. S. and SCOTT, D. 1984. The anatomy and relationships of the Lower Permian reptile *Araeoscelis*. *Journal of Vertebrate Paleontology*, **4**, 57-67.

--- --- --- 1992. The cranial anatomy and relationships of *Secodontosaurus*, an unusual mammal-like reptile (Synapsida: Sphenacodontidae) from the Early Permian of Texas. *Zoological Journal of the Linnean Society*, **104**, 127-184.

REISZ, R. R. and DILKES, D. W. 2003. *Archaeovenator hamiltonensis*, a new varanopid (Synapsida: Eupelycosauria) from the Upper Carboniferous of Kansas. *Canadian Journal of Earth Sciences*, **40**, 667-678.

REISZ, R. R., DILKES, D. W. and BERMAN, D. S. 1998. Anatomy and relationships of *Elliotsmithia longiceps* Broom, a small synapsid (Eupelycosauria: Varanopseidae) from the Late Permian of South Africa. *Journal of Vertebrate Paleontology*, **18**, 602-611.

REISZ, R. R. and FRÖBISCH, J. 2014. The oldest caseid synapsid from the Late Pennsylvanian of Kansas, and the evolution of herbivory in terrestrial vertebrates. *Plos One*, **9**, e94518.

REISZ, R. R., GODFREY, S. J. and SCOTT, D. 2009. *Eothyris* and *Oedaleops*: do these early Permian synapsids from Texas and New Mexico form a clade? *Journal of Vertebrate Paleontology*, **29**, 39-47.

REISZ, R. R., HARIDY, Y. and MÜLLER, J. 2016. *Euconcordia* nom. nov., a replacement name for the captorhinid eureptile *Concordia* Müller and Reisz, 2005 (non Kingsley, 1880), with new data on its dentition. *Vertebrate Anatomy Morphology Palaeontology*, **3**.

REISZ, R. R. and LAURIN, M. 2004. A reevaluation of the enigmatic Permian synapsid *Watongia* and of its stratigraphic significance. *Canadian Journal of Earth Sciences*, **41**, 377-386.

REISZ, R. R., LAURIN, M. and MARJANOVIĆ, D. 2010. *Apsisaurus witteri* from the Lower Permian of Texas: yet another small varanopid synapsid, not a diapsid. *Journal of Vertebrate Paleontology*, **30**, 1628-1631.

REISZ, R. R., LEBLANC, A. R., SIDOR, C. A., SCOTT, D. and MAY, W. 2015. A new captorhinid reptile from the Lower Permian of Oklahoma showing remarkable dental and mandibular convergence with microsaurian tetrapods. *The Science of Nature*, **102**, 50.

REISZ, R. R., MADDIN, H. C., FRÖBISCH, J, and FALCONNET, J. 2011. A new

large caseid (Synapsida, Caseasauria) from the Permian of Rodez (France), including a reappraisal of “Casea” rutena Sigogneau-Russell & Russell, 1974. *Geodiversitas*, ***33***(2), pp.227-246.

REISZ, R. R., MACDOUGALL, M. J. and MODESTO, S. P. 2014. A new species of the parareptile genus *Delorhynchus*, based on articulated skeletal remains from Richards Spur, Lower Permian of Oklahoma. *Journal of Vertebrate Paleontology*, **34**, 1033-1043.

REISZ, R. R. and MODESTO, S. P. 2007. *Heleosaurus scholtzi* from the Permian of South Africa: a varanopid synapsid, not a diapsid reptile. *Journal of Vertebrate Paleontology*, **27**, 734-739.

REISZ, R. R., MODESTO, S. P. and SCOTT, D. M. 2000. *Acanthotoposaurus bremneri* and the origin of the Triassic archosauromorph reptile fauna of South Africa. *South African Journal of Science*, **96**, 443-445.

--- --- --- 2011. A new Early Permian reptile and its significance in early diapsid evolution. 3731-3737. *Proc. R. Soc. B*. The Royal Society,

REISZ, R. R., MÜLLER, J., TSUJI, L. and SCOTT, D. 2007. The cranial osteology of *Belebey vegrandis* (Parareptilia: Bolosauridae), from the Middle Permian of Russia, and its bearing on reptilian evolution. *Zoological Journal of the Linnean Society*, **151**, 191-214.

REISZ, R. R. and MÜLLER, J. 2004. Molecular timescales and the fossil record: a paleontological perspective. *TRENDS in Genetics*, **20**, 237-241.

REISZ, R. R., WILSON, H. and SCOTT D. 1997. Varanopseid synapsid skeletal elements from Richards Spur, a lower Permian fissure fill near Fort Sill, Oklahoma. *Oklahoma Geology*, **57** (5), 160-170.

RIEPPEL, O. 1993. Patterns of diversity in the reptilian skull. *In* The Skull volume 2,Patterns of Structural and Systematic Diversity *(James Hanken and Brian K. Hall eds), University of Chicago Press, Chicago*, **2**, 344-390.

--- 2007. The naso-frontal joint in snakes as revealed by high-resolution X-ray computed tomography of intact and complete skulls. *Zoologischer Anzeiger-A Journal of Comparative Zoology*, **246**, 177-191.

RIEPPEL, O., GAUTHIER, J. and MAISANO, J. 2008. Comparative morphology of the dermal palate in squamate reptiles, with comments on phylogenetic implications. *Zoological Journal of the Linnean Society*, **152**, 131-152.

ROMANO, M. 2017. Long bone scaling of caseid synapsids: a combined morphometric and cladistic approach. *Lethaia*, ***50***(4), 511-526.

ROMER, A. S. 1946. The primitive reptile *Limnoscelis* restudied. *American Journal of Science*, **244**, 149-188.

--- 1956. Osteology of the Reptiles. University of Chicago Press.

--- 1971. Unorthodoxies in reptilian phylogeny. *Evolution*, **25**, 103-112.

ROMER, A. S. and PRICE, L. W. 1940. Review of the Pelycosauria. *Geological Society of America Special Papers*, **28**, 1-534.

ROSCITO, J. G. and RODRIGUES, M. T. 2010. Comparative cranial osteology of fossorial lizards from the tribe Gymnophthalmini (Squamata, Gymnophthalmidae). *Journal of morphology*, **271**, 1352-1365.

SCHMITZ, L. and MOTANI, R. 2010. Morphological differences between the eyeballs of nocturnal and diurnal amniotes revisited from optical perspectives of visual environments. *Vision research*, **50**, 936-946.

--- --- 2011a. Nocturnality in dinosaurs inferred from scleral ring and orbit morphology. *Science*, **332**, 705-708.

--- --- 2011b. Response to comment on “Nocturnality in dinosaurs inferred from scleral ring and orbit morphology”. *Science*, **334**, 1641-1641.

SHISHKIN, M. 1968. On the cranial arterial system of the labyrinthodonts. *Acta Zoologica*, **49**, 1-22.

SIGOGNEAU-RUSSELL, D. and RUSSELL, D. 1974. Étude du premier caséidé (Reptilia, Pelycosauria) d'Europe occidentale. *Bulletin du Museum national d'Histoire naturelle*, **230**, 145-216.

SMITH, R.M. 1987. Helical burrow casts of therapsid origin from the Beaufort Group (Permian) of South Africa. *Palaeogeography, Palaeoclimatology, Palaeoecology*, ***60***,155-169.

SMITH, R. M. and EVANS, S. E. 1996. New material of *Youngina*: evidence of juvenile aggregation in Permian diapsid reptiles. *Palaeontology*, **39**, 289-303.

SOOKIAS, R. B. and BUTLER, R. J. 2013. Euparkeriidae. *Geological Society, London, Special Publications*, **379**, 35-48.

SPENCER, P. S. 2000. The braincase structure of *Leptopleuron lacertinum* Owen (Parareptilia: Procolophonidae). *Journal of Vertebrate Paleontology*, **20**, 21-30.

SPIELMANN, J., RINEHART, L. F., LUCAS, S., BERMAN, D. S., HENRICI, A. and HARRIS, S. 2010. Redescription of the cranial amatomy of *Sphenacodon ferox* Marsh (Eupelycosauria: Sphenaocontidae) from the Late Pennsylvanian-Early Permian of New Mexico. *New Mexico Mus. Nat. Hist. Sci. Bull*, **49**, 159-184.

STOVALL, J. W., PRICE, L. I. and ROMER, A. S. 1966. The postcranial skeleton of the giant Permian pelycosaur *Cotylorhynchus romeri. The Bulletin of the Museum of Comparative Zoology*, Harvard University.

SUMIDA, S. S. 1989. Reinterpretation of vertebral structure in the Early Permian pelycosaur *Varanosaurus acutirostris* (Amniota, Synapsida). *Journal of Vertebrate Paleontology*, ***9***(4), 451-458.

SUMIDA, S. S., DODICK, J., METCALF, A. and ALBRIGHT, G. 2010. *Reiszorhinus olsoni*, a new single-tooth-rowed captorhinid reptile from the Lower Permian of Texas. *Journal of Vertebrate Paleontology*, **30**, 704-714.

TSUJI, L. A. 2006. Cranial anatomy and phylogenetic affinities of the Permian parareptile *Macroleter poezicus*. *Journal of Vertebrate Paleontology*, **26**, 849-865.

TSUJI, L. A., MÜLLER, J. and REISZ, R. R. 2010. *Microleter mckinzieorum* gen. et sp. nov. from the Lower Permian of Oklahoma: the basalmost parareptile from Laurasia. *Journal of Systematic Palaeontology*, **8**, 245-255.

VAUGHN, P. P. 1955. The Permian reptile *Araeoscelis* restudied. *The Bulletin of the Museum of Comparative Zoology*, Harvard. **113**(5), 304-467.

--- 1958. A pelycosaur with subsphenoidal teeth from the Lower Permian of Oklahoma. *Journal of the Washington Academy of Sciences*, **48**, 44-47.

WAKE, M. H. 1993. The skull as a locomotor organ. *In* The Skull volume 3, Functional and Evolutionary Mechanisms *(James Hanken and Brian K. Hall eds), University of Chicago Press, Chicago*, **3**, 197-240.

WATSON, D. 1914. The Deinoceplialia, an Order of Mammal□like Reptiles. *Journal of Zoology*, **84**, 749-786.

WELMAN, J. 1998. The taxonomy of the South African proterosuchids (Reptilia, Archosauromorpha). *Journal of Vertebrate Paleontology*, **18**, 340-347.

WHITE, T. E. 1939. Osteology of *Seymouria baylorensis* Broili. *Bulletin of the Museum of Comparative Zoology, Harvard College*, **85**, 325-409.

WHITESIDE, D. 1986. The head skeleton of the Rhaetian sphenodontid *Diphydontosaurus avonis* gen. et sp. nov. and the modernizing of a living fossil. *Phil. Trans. R. Soc. Lond. B*, **312**, 379-430.

WILLISTON, S. W. 1911. American Permian vertebrates. *University of Chicago Press,* Chicago, Illinois.

WITMER, L. M. 1995. Homology of facial structures in extant archosaurs (birds and crocodilians), with special reference to paranasal pneumaticity and nasal conchae. *Journal of morphology*, **225**, 269-327.

--- 1997. The evolution of the antorbital cavity of archosaurs: a study in soft-tissue reconstruction in the fossil record with an analysis of the function of pneumaticity. *Journal of Vertebrate Paleontology*, **17**, 1-76.

WITMER, L. M. and RIDGELY, R. C. 2008. The paranasal air sinuses of predatory and armored dinosaurs (Archosauria: Theropoda and Ankylosauria) and their contribution to cephalic structure. *The Anatomical Record*, **291**, 1362-1388.

WOODHEAD, J., REISZ, R., FOX, D., DRYSDALE, R., HELLSTROM, J., MAAS, R., CHENG, H. and EDWARDS, R. L. 2010. Speleothem climate records from deep time? Exploring the potential with an example from the Permian. *Geology*, **38**, 455-458.

Figure and Table captions

FIG. 1. OMNH 74606, holotype of *Orovenator mayorum*. A, left lateral view; B, segmented elements from µCT scan of specimen in left lateral view; C, right lateral view; D, segmented elements from µCT scan of specimen in right lateral view. *Abbreviations:* an, angular; co, coronoid; d, dentary; ec, ectopterygoid; ep, epipterygoid; f, frontal; j, jugal; lac, lacrimal; m, maxilla; n, nasal; pa, prearticular; pal, palatine; pbs, parabasisphenoid; pm, premaxilla; prf, prefrontal; pt, pterygoid; q, quadrate; sa, surangular; scl, scleral plates; sm, septomaxilla; sp, splenial; sta, stapes; v, vomer. Scale bar represents 1cm.

FIG. 2. OMNH 74607, referred specimen of *Orovenator mayorum*. A, right lateral view; B, segmented elements from µCT scan of specimen in right lateral view; C, left lateral view; D, segmented elements from µCT scan of specimen in left lateral view. *Abbreviations;* ax.v, axial vertebra; ca.v, caudal vertebra, ce.v, cervical vertebra; f, frontal; lac, lacrimal; n, nasal; p, parietal; pal, palatine; pof, postfrontal; prf, prefrontal; pt, pterygoid; scl, scleral plate; st, supratemporal; v, vomer. Scale bar represents 1cm.

FIG. 3. Composite reconstruction of the skull of *Orovenator mayorum*. A, left lateral view; B, interpretive drawing of A, highlighting hypothetical morphology of missing elements, elements taken from OMNH 74606, elements taken from OMNH 74607 and mirrored or duplicated elements; C, dorsal view; D, interpretive drawing of C, with hypothetical morphology of missing elements, elements taken from OMNH 74606, elements taken from OMNH 74607, mirrored elements and palatal elements from OMNH 74606. *Abbreviations;* an, angular; ar, articular; co, coronoid; d, dentary; ec, ectopterygoid; f, frontal; j, jugal; lac, lacrimal; m, maxilla; n, nasal; p, parietal; pal, palatine; pf, pineal foramen; pm, premaxilla; po, postorbital; pof, postfrontal; prf, prefrontal; pt, pterygoid; pt(qr), quadrate ramus of pterygoid; qj, quadratojugal; sa, surangular; scl, scleral plates; sm, septomaxilla; sq, squamosal; st, supratemporal. Scale bar represents 1cm.

FIG. 4. OMNH 74606, premaxillae and left vomer. A, left premaxilla oblique lateral view; B, reconstruction of articulated premaxillae in ventral view, with addition of right vomerine process; C, left vomer, anterior region in ventral view. *Abbreviations;* for, foramina; pm(mp), maxillary process of premaxilla; pm(vp), vomerine process of premaxilla; v(am), anteromedial process of vomer; v(al), anterolateral process of vomer. Scale bars represent 1mm.

FIG. 5. OMNH 74606, left preorbital region, with all elements *in situ* except for premaxilla and septomaxilla (reconstructed). A, medial view; B, oblique medial view, with partially transparent lacrimal. *Abbreviations;* aaf, anterior alveolar foramen; j(st), subtemporal process of jugal; lac, lacrimal; lac.p, lacrimal puncti; m, maxilla; med.but, medial buttress; med.cr, medial crest; nlc, nasolacrimal canal; nld, nasolacrimal duct; nld(db), dorsal branch of nasolacrimal duct; nld(vb), ventral branch of nasolacrimal duct; paf, posterior alveolar foramen; pal(mrc), maxillary ramus canal of palatine; pm, premaxilla; prf, prefrontal; sm, septomaxilla; sm.c, septomaxillary canal. Scale bar represents 2mm.

FIG. 6. OMNH 74606, left septomaxilla. A, posterior view; B, lateral view; C, anterior view; D, medial view. *Abbreviations;* sm.ap, anterior process of septomaxilla, sm.c, septomaxillary canal; sm.dp, dorsal process of septomaxilla, sm.vp, ventral plate of septomaxilla. Scale bar represents 0.5 mm.

FIG. 7. OMNH 74607, reconstruction of skull roof. A, dorsal view; B, ventral view. *Abbreviations;* f, frontal; cr.c, *crista cranii*; f(ns), narial shelf of frontal; p, parietal; pf, pineal foramen; pof, postfrontal; prf, prefrontal; r(tm), ridge for *taenia marginalis*; st, supratemporal, utf(m), medial margin of upper temporal fenestra. Scale bar represents 5mm.

FIG. 8. Comparison of diapsid-like parietals. A, left parietal of OMNH 74607; B, right parietal (YPM 4926). *Abbreviations*; pf, pineal foramen; pl.p, posterolateral process; po.p, postorbital process; utf(m), medial margin of upper temporal fenestra. Image of YPM 4926 from Carroll (1968).

FIG. 9. OMNH 74606, reconstruction of palate. A, ventral view; B, interpretive drawing of A, highlighting hypothetical morphology of missing elements, palatal elements, basicranial elements, mirrored elements and dermal elements. Abbreviations; ec, ectopterygoid; int.n, internal naris (choana), j, jugal; m, maxilla, pal, palatine; pbs, parabasisphenoid; pm, premaxilla; pt, pterygoid; pt(qr), quadrate ramus of the pterygoid; sof, suborbital fenestra; v, vomer. Scale bar represents 5mm.

FIG. 10. OMNH 74606, reconstruction of articulation of right pterygoid and epipterygoid. A, lateral view; B, medial view. *Abbreviations;* ba.r, recess for basal articulation; ep, epipterygoid; pt, pterygoid; pt(qr), quadrate ramus of pterygoid; pt(qraf), arcuate flange of quadrate ramus of pterygoid; pt(qtdf), dorsal flange of quadrate ramus of pterygoid; pt(t), transverse process of pterygoid. Scale bar represent 2mm.

FIG. 11. OMNH 74606**,** right quadrate (A-D) and stapes (E-G). A, quadrate in lateral view; B, quadrate in medial view; C, quadrate in posterior view; D, quadrate in anteromedial view; E, stapes in posterior view; F, footplate of stapes in proximal view; E, stapes in ventral view. *Abbreviations*; (A-D) as(u), anterior surface (unfinished); cr, condylar region; ps, posterior shaft; pw, pterygoid wing; qf, quadrate foramen; scs, shelf for columella of stapes; (E-G) col., columella; col.b(?), possible base of bridge of stapedial foramen; fp, footplate; s.for(?), possible stapedial foramen. Scale bars represent 2mm.

FIG. 12. OMNH 74606, parabasisphenoid, with pathway of internal carotid and cerebral arteries. A, ventrolateral view; B, dorsal view; C, dorsal view with partial transparency of parabasisphenoid; D, ventral view with cultriform process; E, left lateral view with cultriform process. *Abbreviations;* bpp, basipterygoid process; cbi(p), pathway of cerebral branch of internal carotid artery through parabasisphenoid; cl.p, clinoid process; cp, cultriform process; c.vl, *crista ventrolaterales*; d.re.bul, depression for retractor bulbi muscle; ds, *dorsum sellae*; ent.f, entry foramen for cerebral branch of internal carotid artery; ex.f, exit foramen for cerebral branch of internal carotid artery; ica, internal carotid artery; pit.fos, pituitary fossa; pp, parasphenoidal plate; vs.(a), anterior egress of vidian sulcus; vs.(p), posterior vidian sulcus. Scale bar represents 5mm.

FIG. 13. Mandibles of OMNH 74606 and *Mycterosaurus longiceps* (FMNH UC 692 holotype). A, OMNH 74606, reconstruction of left mandible in lateral view; B, OMNH 74606, reconstruction of left mandible in medial view; C, *Mycterosaurus longiceps*, posterior right mandible in dorsolateral view (image reversed); D, OMNH 74606, reconstruction of posterior left mandible in dorsolateral view; E, OMNH 74606, reconstruction of posterior left mandible in ventral view. *Abbreviations;* aif, anterior inframeckelian foramen; an, angular; an(pvr), posteroventral ridge of angular; co, coronoid; d, dentary; for, foramina; for.g, foramen and groove; pa, prearticular; pif, posterior inframeckelian foramen; sa, surangular; sa(ae), anterodorsal extension of surangular; sa(ds), dorsomedial shelf of surangular; sp, splenial. Scale bars represent 5mm, except for fig. E which represents 2mm.

FIG. 14. OMNH 74606, right mandible. A, right mandible in medial view; B, right surangular and coronoid in medial view (inset from A). *Abbreviations*; an, angular; co, coronoid; d, dentary; pa, prearticular; sa, surangular; sa(ds), dorsal shelf of surangular; sa(mf), medial flange of surangular; sp, splenial. Scale bars represent 2mm.

FIG. 15. OMNH 75607, cervical vertebrae. A, first post-axial vertebra (3rd cervical) in anterior view; B, 3rd cervical in right lateral view; C, 3rd cervical in posterior view; D, reconstruction of cervical vertebrae (2-4) in articulation, including possible 4th cervical (anterior to right). *Abbreviations*; ans, axial neural spine; na, neural arch; nc, notochordal canal; ns, neural spine; posz, postzygopophysis; prez, prezygopophysis; 2v(ax), 2nd cervical (axial) vertebra; 3v, 3rd cervical vertebra; 4v(?), possible 4th cervical vertebra. Scale bars represent 5mm.

FIG. 16. Composite reconstruction of the skull of *Orovenator mayorum*, with mirrored or duplicated elements in grey. A, left oblique dorsolateral view; B, anterodorsal view. Scale bar represents 5mm.

FIG. 17. Crania in anterolateral view. A, composite reconstruction of *Orovenator mayorum*; B, North African sandfish (*Scincus scincus*). Scale bars represent 5mm. CT reconstruction of *Scincus scincus* courtesy of DigiMorph.org.

FIG. 18. Maxillae in medial view. A, OMNH 74606; B, *Prolacerta broomi* (BP/I/2675); C, *Archaeovenator hamiltonensis* (KUVP 12483) (image reversed). *Abbreviations*; med.cav, medial cavity of maxilla; med.cr, medial crest; med.but, medial buttress; pm.f, facet for maxillary process of premaxilla. Scale bars represent 5mm.

FIG. 19. Asymmetric processes of anterior vomers. A, *Petrolacosaurus kansensis* (KUVP 8351); B, *Paleothyris acadiana* (MCZ 3481); C, *Archaeovenator hamiltonensis* (from Reisz and Dilkes 2003); *Mesenosaurus romeri* (from Reisz and Berman 2001)(image reversed). *Abbreviations*; v(am), anteromedial process of vomer; v(al), anterolateral process of vomer. Scale bars represent 2mm.

FIG.20. Coronoids in medial view. A, *Archaeovenator hamiltonensis* (KUVP 12483) right mandible; B, OMNH 74606 reconstruction of left mandible (image reversed). *Abbreviations*; an, angular; co, coronoid; d, dentary; pa, prearticular; sa, surangular; sp, splenial. Scale bars represent 2mm.

FIG.21. Parabasisphenoids in ventral view. A, *Ophiacodon retroversus* (MCZ 5792); B, *Edaphosaurus boanerges* (MCZ 1762); C, *Ophiacodon retroversus* (MCZ 4820); D, *Secodontosaurus obtusidens* (MCZ 2028); E, *Orovenator mayorum* (OMNH 74606); F, 'Basicranodon fortsillensis' (= *Mycterosaurus longiceps*) from Vaughn (1958). Arrows indicate position of entry foramina for cerebral branch of internal carotid arteries. Scale bars represent 2mm.

FIG. 22. Phylogenetic analyses of the character/taxon matrices of: A, Reisz *et al.* (2011); B, Reisz *et al.* (2010). Taxa recovered as Sauria in both datasets have been condensed to a single operational taxonomic unit.

FIG. 23. Time calibrated strict consensus of the three most-parsimonious trees recovered from the dataset of Reisz *et al.* (2010) after the inclusion of *Orovenator mayorum* into the character/taxon matrix. White circles denote first appearance datum, lines ending with vertical bars denote range. Taxa recovered as Sauria in have been condensed to a single operational taxonomic unit. *Abbreviations;* Coelurosaur. = *Coelurosauravus*, Acerosodont. = *Acerosodontosaurus*.

Table 1. Taxa originally or secondarily assignment to Diapsida and later revised to Varanopidae.

Fig. 1 (Supp.1). Reconstruction of the circumorbital elements and scleral ring of *Orovenator mayorum. A,* orbit and scleral ring, with dotted line denoting estimated position of the orbital margin of postorbital. B, ring of 19 scleral plates, articulated *in situ* plates in blue, duplicated plates in grey. *Abbreviations;* ext (yellow bar), maximum external diameter of scleral ring; ol (red bar), maximum orbital length; int (blue bar), maximum internal diameter of scleral ring.

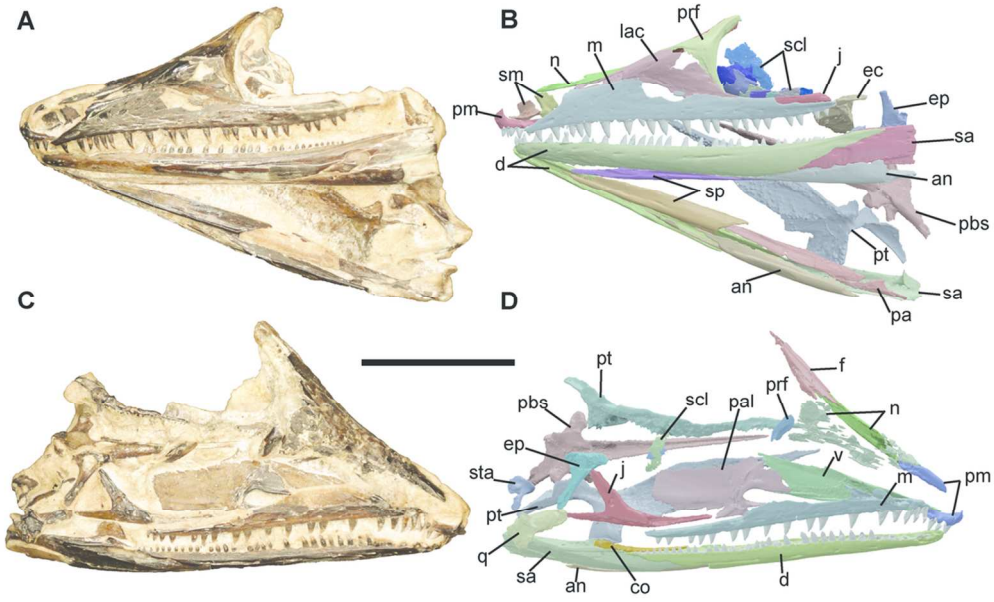

FIG. 1. OMNH 74606, holotype of Orovenator mayorum. A, left lateral view; B, segmented elements from µCT scan of specimen in left lateral view; C, right lateral view; D, segmented elements from µCT scan of specimen in right lateral view. Abbreviations: an, angular; co, coronoid; d, dentary; ec, ectopterygoid; ep, epipterygoid; f, frontal; j, jugal; lac, lacrimal; m, maxilla; n, nasal; pa, prearticular; pal, palatine; pbs, parabasisphenoid; pm, premaxilla; prf, prefrontal; pt, pterygoid; q, quadrate; sa, surangular; scl, scleral plates; sm, septomaxilla; sp, splenial; sta, stapes; v, vomer. Scale bar represents 1cm.

106x67mm (300 x 300 DPI)

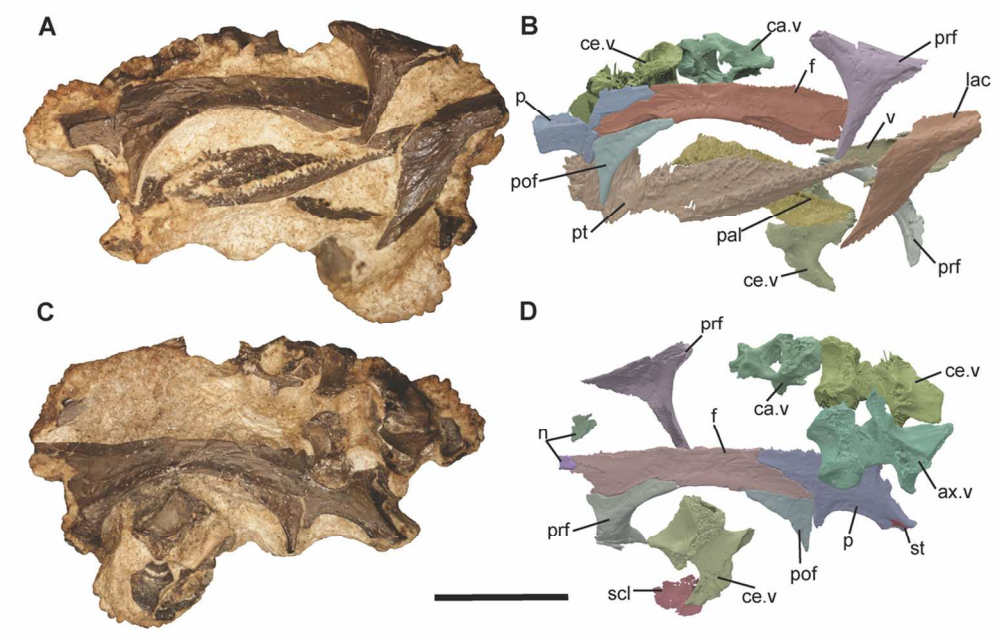

FIG. 2. OMNH 74607, referred specimen of Orovenator mayorum. A, right lateral view; B, segmented elements from µCT scan of specimen in right lateral view; C, left lateral view; D, segmented elements from µCT scan of specimen in left lateral view. Abbreviations; ax.v, axial vertebra; ca.v, caudal vertebra, ce.v, cervical vertebra; f, frontal; lac, lacrimal; n, nasal; p, parietal; pal, palatine; pof, postfrontal; prf, prefrontal; pt, pterygoid; scl, scleral plate; st, supratemporal; v, vomer. Scale bar represents 1cm.

106x67mm (300 x 300 DPI)

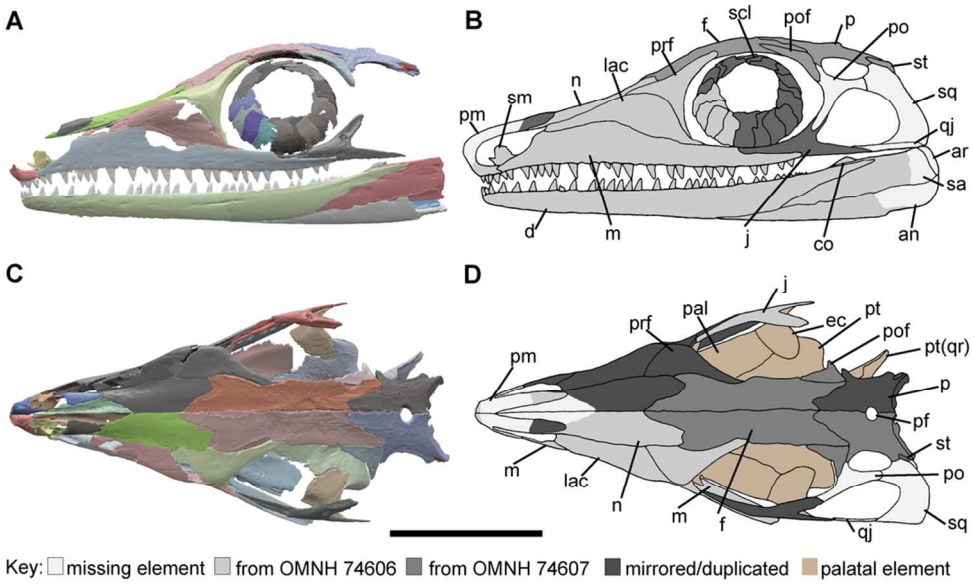

FIG. 3. Composite reconstruction of the skull of Orovenator mayorum. A, left lateral view; B, interpretive drawing of A, highlighting hypothetical morphology of missing elements, elements taken from OMNH 74606, elements taken from OMNH 74607 and mirrored or duplicated elements; C, dorsal view; D, interpretive drawing of C, with hypothetical morphology of missing elements, elements taken from OMNH 74606, elements taken from OMNH 74607, mirrored elements and palatal elements from OMNH 74606. Abbreviations; an, angular; ar, articular; co, coronoid; d, dentary; ec, ectopterygoid; f, frontal; j, jugal; lac, lacrimal; m, maxilla; n, nasal; p, parietal; pal, palatine; pf, pineal foramen; pm, premaxilla; po, postorbital; pof, postfrontal; prf, prefrontal; pt, pterygoid; pt(qr), quadrate ramus of pterygoid; qj, quadratojugal; sa, surangular; scl, scleral plates; sm, septomaxilla; sq, squamosal; st, supratemporal. Scale bar represents 1cm.

96x55mm (300 x 300 DPI)

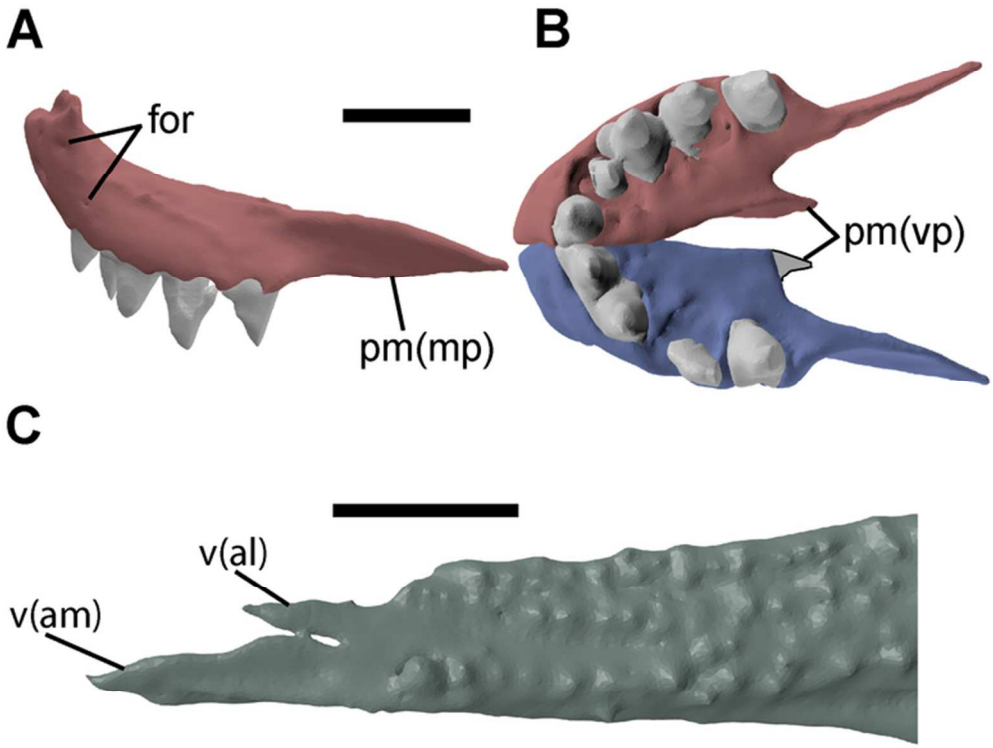

FIG. 4. OMNH 74606, premaxillae and left vomer. A, left premaxilla oblique lateral view; B, reconstruction of articulated premaxillae in ventral view, with addition of right vomerine process; C, left vomer, anterior region in ventral view. Abbreviations; for, foramina; pm(mp), maxillary process of premaxilla; pm(vp), vomerine process of premaxilla; v(am), anteromedial process of vomer; v(al), anterolateral process of vomer. Scale bars represent 1mm.

66x54mm (300 x 300 DPI)

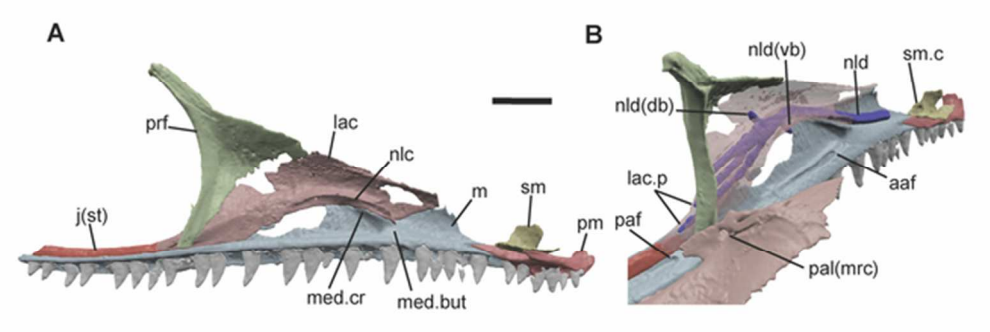

FIG. 5. OMNH 74606, left preorbital region, with all elements in situ except for premaxilla and septomaxilla (reconstructed). A, medial view; B, oblique medial view, with partially transparent lacrimal. Abbreviations; aaf, anterior alveolar foramen; j(st), subtemporal process of jugal; lac, lacrimal; lac.p, lacrimal puncti; m, maxilla; med.but, medial buttress; med.cr, medial crest; nlc, nasolacrimal canal; nld, nasolacrimal duct; nld(db), dorsal branch of nasolacrimal duct; nld(vb), ventral branch of nasolacrimal duct; paf, posterior alveolar foramen; pal(mrc), maxillary ramus canal of palatine; pm, premaxilla; prf, prefrontal; sm, septomaxilla; sm.c, septomaxillary canal. Scale bar represents 2mm.

56x18mm (300 x 300 DPI)

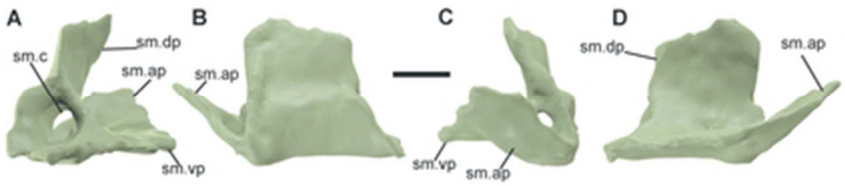

FIG. 6. OMNH 74606, left septomaxilla. A, posterior view; B, lateral view; C, anterior view; D, medial view. Abbreviations; sm.ap, anterior process of septomaxilla, sm.c, septomaxillary canal; sm.dp, dorsal process of septomaxilla, sm.vp, ventral plate of septomaxilla. Scale bar represents 0.5 mm.

35x7mm (300 x 300 DPI)

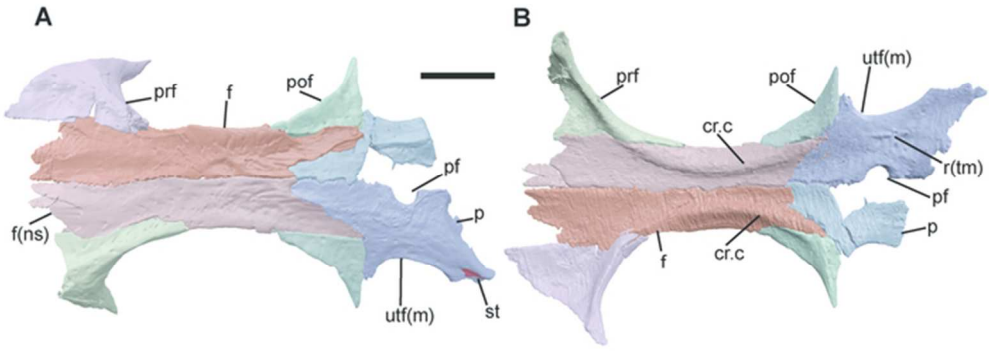

FIG. 7. OMNH 74607, reconstruction of skull roof. A, dorsal view; B, ventral view. Abbreviations; f, frontal; cr.c, crista cranii; f(ns), narial shelf of frontal; p, parietal; pf, pineal foramen; pof, postfrontal; prf, prefrontal; r(tm), ridge for taenia marginalis; st, supratemporal, utf(m), medial margin of upper temporal fenestra. Scale bar represents 5mm.

60x21mm (300 x 300 DPI)

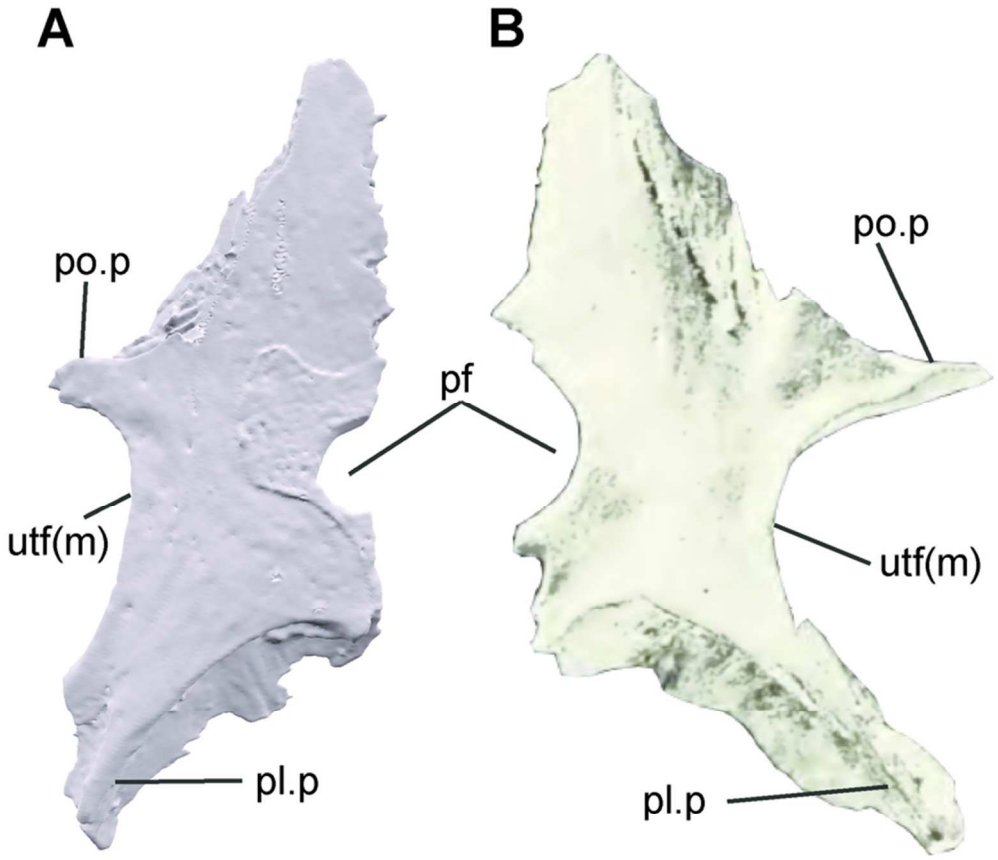

FIG. 8. Comparison of diapsid-like parietals. A, left parietal of OMNH 74607; B, right parietal (YPM 4926). Abbreviations; pf, pineal foramen; pl.p, posterolateral process; po.p, postorbital process; utf(m), medial margin of upper temporal fenestra. Image of YPM 4926 from Carroll (1968).

73x68mm (300 x 300 DPI)

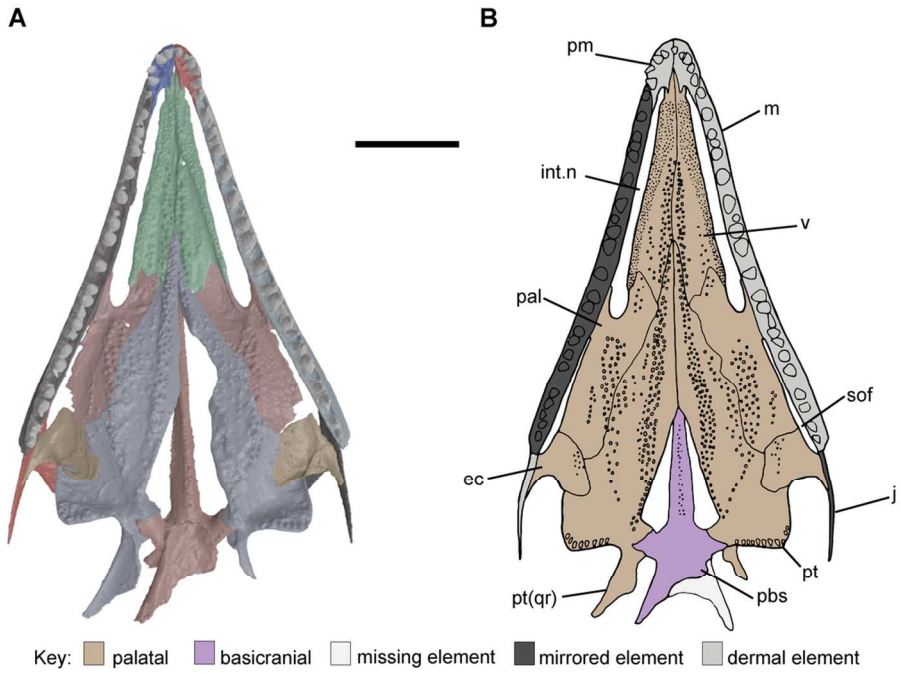

FIG. 9. OMNH 74606, reconstruction of palate. A, ventral view; B, interpretive drawing of A, highlighting hypothetical morphology of missing elements, palatal elements, basicranial elements, mirrored elements and dermal elements. Abbreviations; ec, ectopterygoid; int.n, internal naris (choana), j, jugal; m, maxilla, pal, palatine; pbs, parabasisphenoid; pm, premaxilla; pt, pterygoid; pt(qr), quadrate ramus of the pterygoid; sof, suborbital fenestra; v, vomer. Scale bar represents 5mm.

111x74mm (300 x 300 DPI)

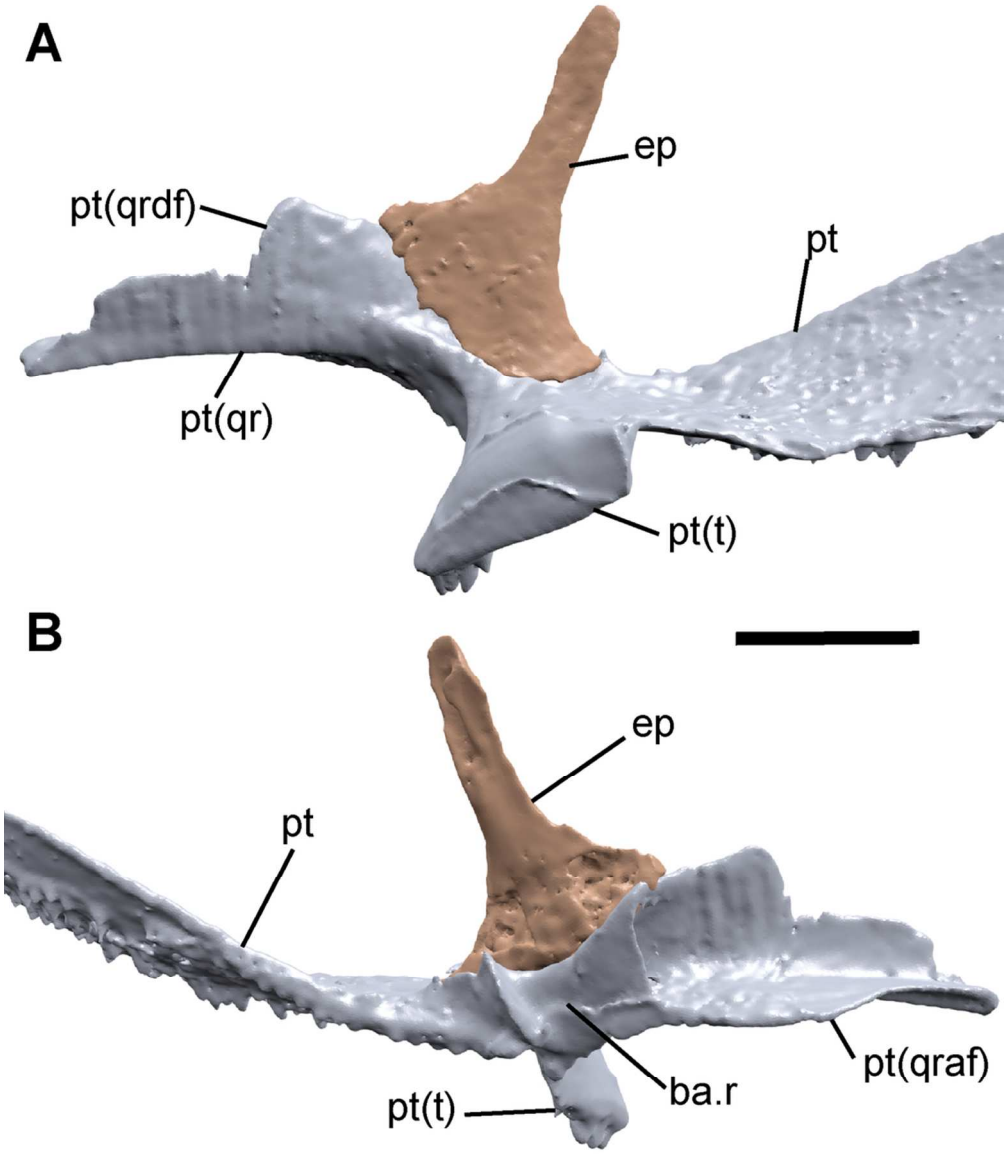

FIG. 10. OMNH 74606, reconstruction of articulation of right pterygoid and epipterygoid. A, lateral view; B, medial view. Abbreviations; ba.r, recess for basal articulation; ep, epipterygoid; pt, pterygoid; pt(qr), quadrate ramus of pterygoid; pt(qraf), arcuate flange of quadrate ramus of pterygoid; pt(qtdf), dorsal flange of quadrate ramus of pterygoid; pt(t), transverse process of pterygoid. Scale bar represent 2mm.

96x115mm (300 x 300 DPI)

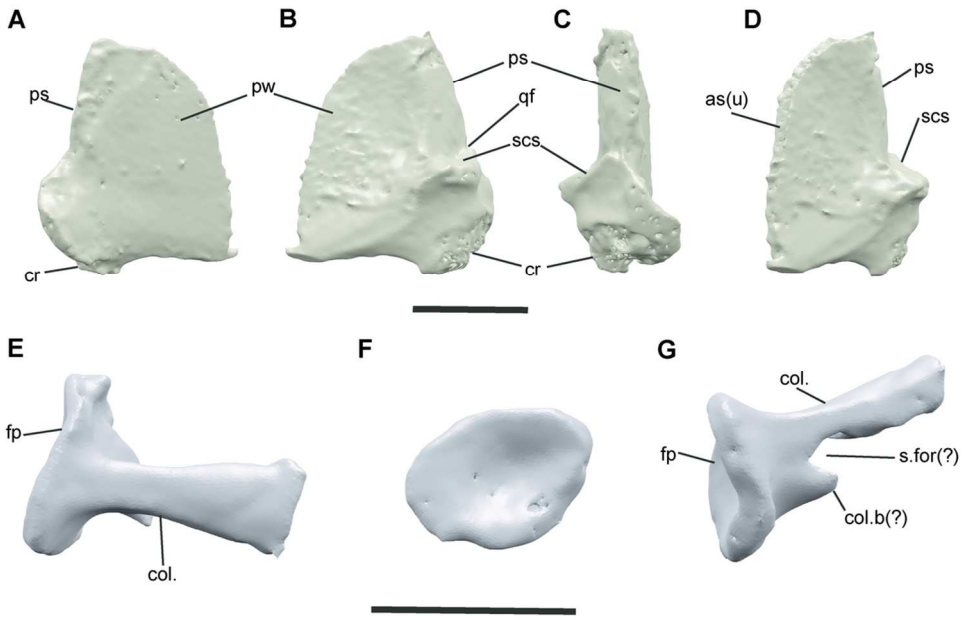

FIG. 11. OMNH 74606, right quadrate (A-D) and stapes (E-G). A, quadrate in lateral view; B, quadrate in medial view; C, quadrate in posterior view; D, quadrate in anteromedial view; E, stapes in posterior view; F, footplate of stapes in proximal view; E, stapes in ventral view. Abbreviations; (A-D) as(u), anterior surface (unfinished); cr, condylar region; ps, posterior shaft; pw, pterygoid wing; qf, quadrate foramen; scs, shelf for columella of stapes; (E-G) col., columella; col.b(?), possible base of bridge of stapedial foramen; fp, footplate; s.for(?), possible stapedial foramen. Scale bars represent 2mm.

112x76mm (300 x 300 DPI)

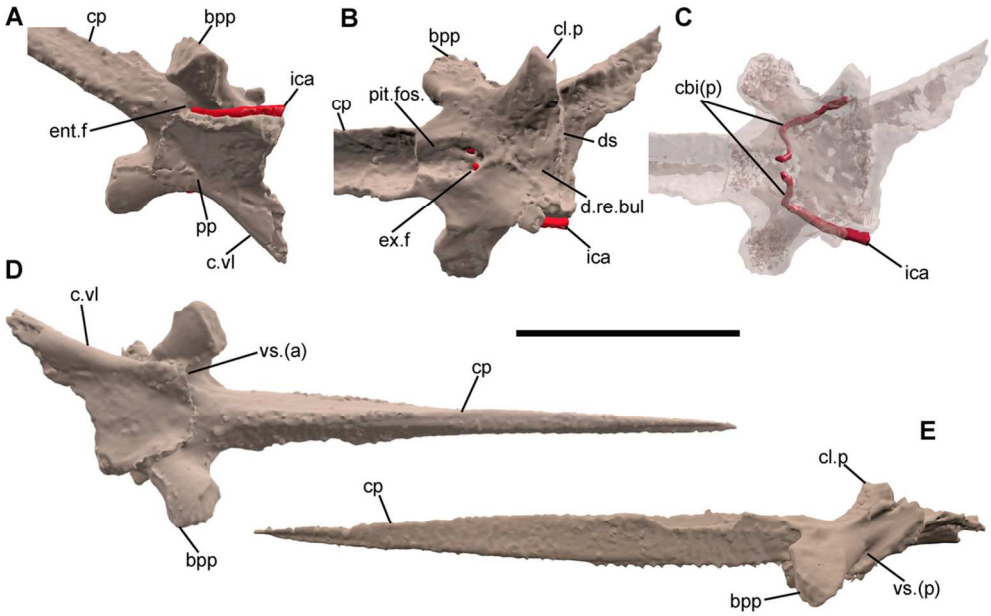

FIG. 12. OMNH 74606, parabasisphenoid, with pathway of internal carotid and cerebral arteries. A, ventrolateral view; B, dorsal view; C, dorsal view with partial transparency of parabasisphenoid; D, ventral view with cultriform process; E, left lateral view with cultriform process. Abbreviations; bpp, basipterygoid process; cbi(p), pathway of cerebral branch of internal carotid artery through parabasisphenoid; cl.p, clinoid process; cp, cultriform process; c.vl, crista ventrolaterales; d.re.bul, depression for retractor bulbi muscle; ds, dorsum sellae; ent.f, entry foramen for cerebral branch of internal carotid artery; ex.f, exit foramen for cerebral branch of internal carotid artery; ica, internal carotid artery; pit.fos, pituitary fossa; pp, parasphenoidal plate; vs.(a), anterior egress of vidian sulcus; vs.(p), posterior vidian sulcus. Scale bar represents 5mm.

104x65mm (300 x 300 DPI)

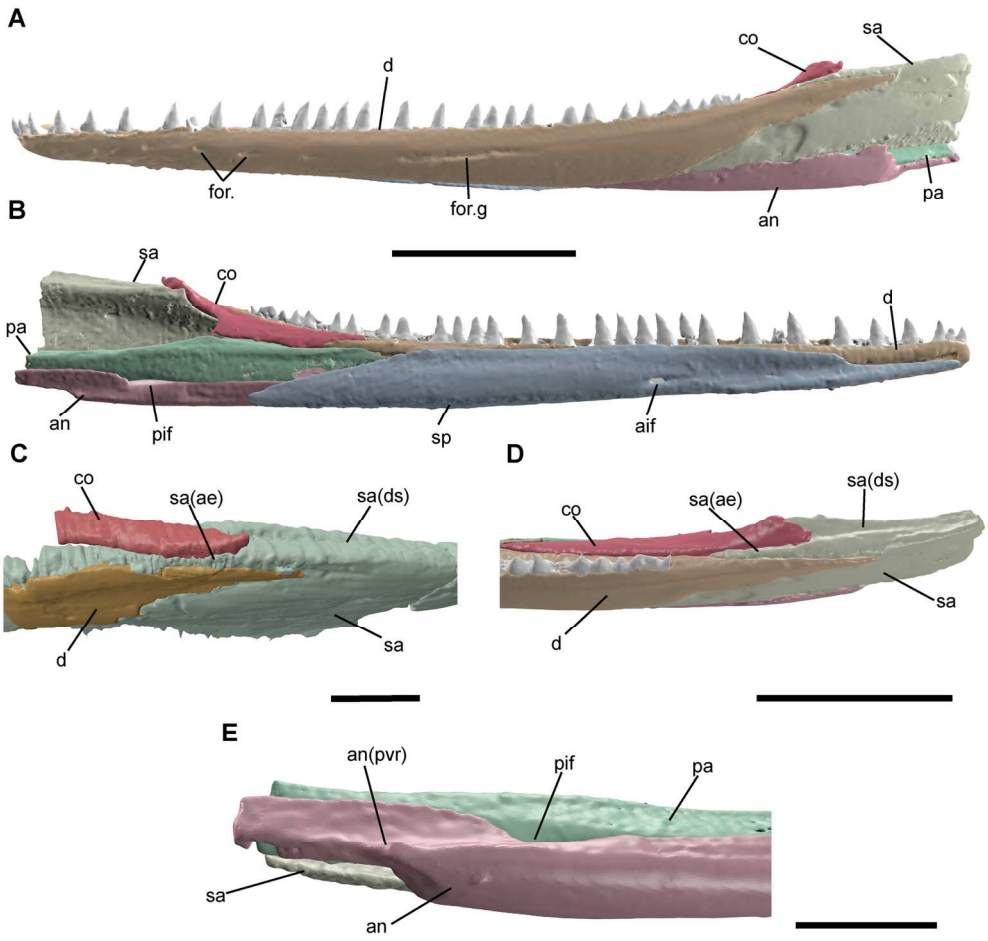

FIG. 13. Mandibles of OMNH 74606 and Mycterosaurus longiceps (FMNH UC 692 holotype). A, OMNH 74606, reconstruction of left mandible in lateral view; B, OMNH 74606, reconstruction of left mandible in medial view; C, Mycterosaurus longiceps, posterior right mandible in dorsolateral view (image reversed); D, OMNH 74606, reconstruction of posterior left mandible in dorsolateral view; E, OMNH 74606, reconstruction of posterior left mandible in ventral view. Abbreviations; aif, anterior inframeckelian foramen; an, angular; an(pvr), posteroventral ridge of angular; co, coronoid; d, dentary; for, foramina; for.g, foramen and groove; pa, prearticular; pif, posterior inframeckelian foramen; sa, surangular; sa(ae), anterodorsal extension of surangular; sa(ds), dorsomedial shelf of surangular; sp, splenial. Scale bars represent 5mm, except for fig. E which represents 2mm.

160x154mm (300 x 300 DPI)

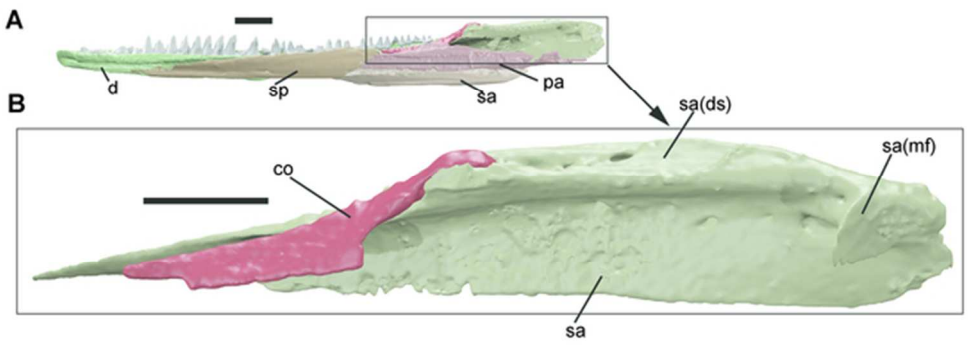

FIG. 14. OMNH 74606, right mandible. A, right mandible in medial view; B, right surangular and coronoid in medial view (inset from A). Abbreviations; an, angular; co, coronoid; d, dentary; pa, prearticular; sa, surangular; sa(ds), dorsal shelf of surangular; sa(mf), medial flange of surangular; sp, splenial. Scale bars represent 2mm.

57x19mm (300 x 300 DPI)

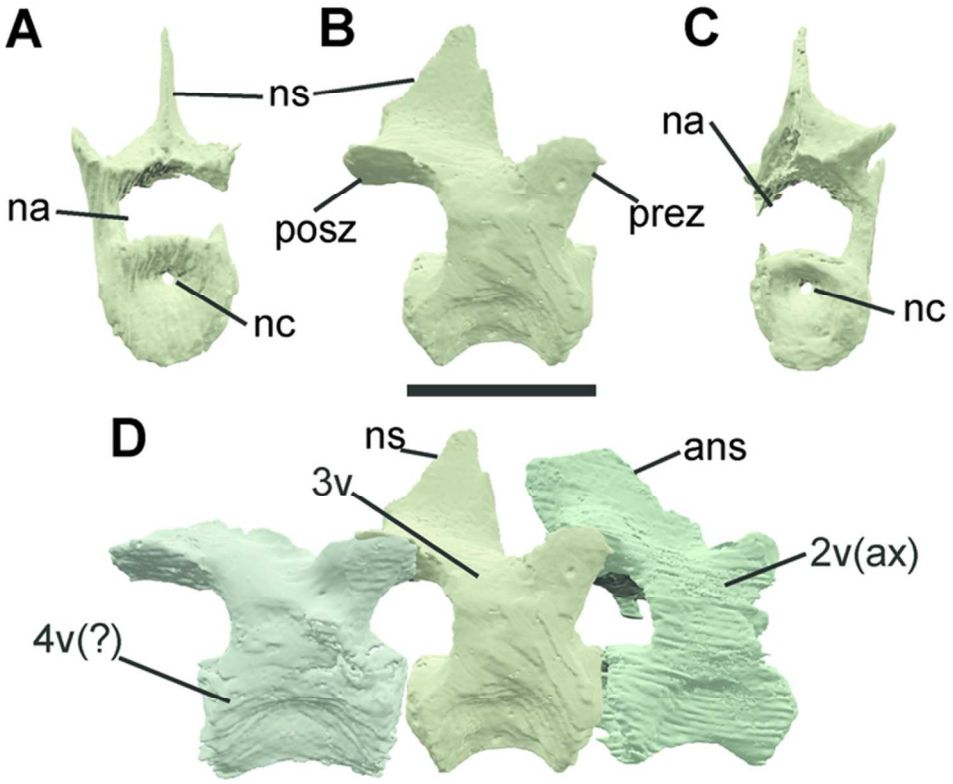

FIG. 15. OMNH 75607, cervical vertebrae. A, first post-axial vertebra (3rd cervical) in anterior view; B, 3rd cervical in right lateral view; C, 3rd cervical in posterior view; D, reconstruction of cervical vertebrae (2-4) in articulation, including possible 4th cervical (anterior to right). Abbreviations; ans, axial neural spine; na, neural arch; nc, notochordal canal; ns, neural spine; posz, postzygopophysis; prez, prezygopophysis; 2v(ax), 2nd cervical (axial) vertebra; 3v, 3rd cervical vertebra; 4v(?), possible 4th cervical vertebra. Scale bars represent 5mm.

64x51mm (300 x 300 DPI)

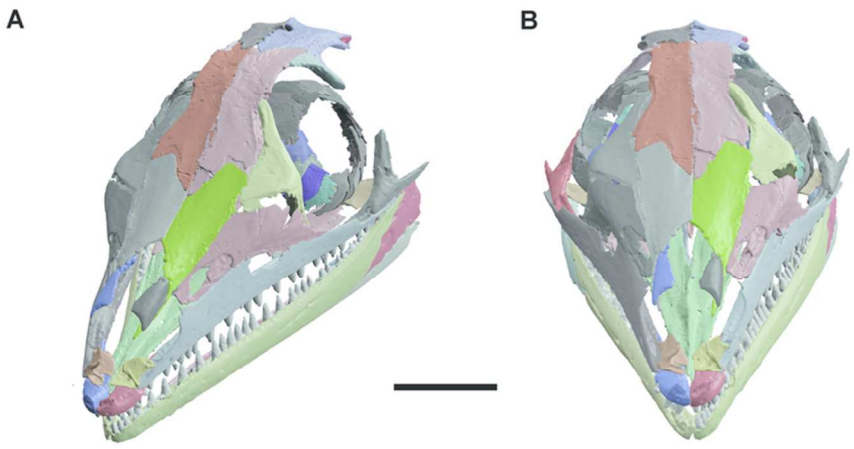

FIG. 16. Composite reconstruction of the skull of Orovenator mayorum, with mirrored or duplicated elements in grey. A, left oblique dorsolateral view; B, anterodorsal view. Scale bar represents 5mm.

76x34mm (300 x 300 DPI)

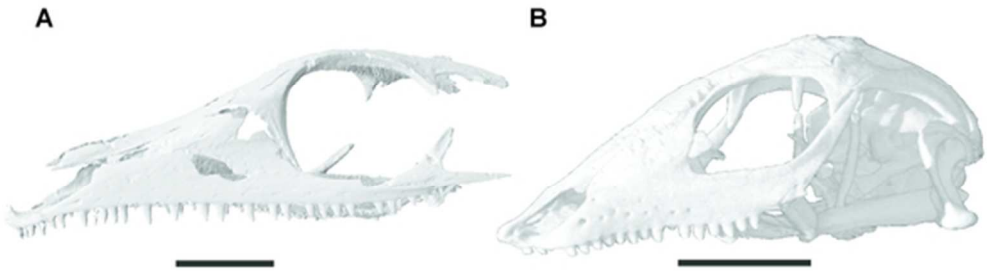

FIG. 17. Crania in anterolateral view. A, composite reconstruction of Orovenator mayorum; B, North African sandfish (Scincus scincus). Scale bars represent 5mm. CT reconstruction of Scincus scincus courtesy of DigiMorph.org.

50x15mm (300 x 300 DPI)

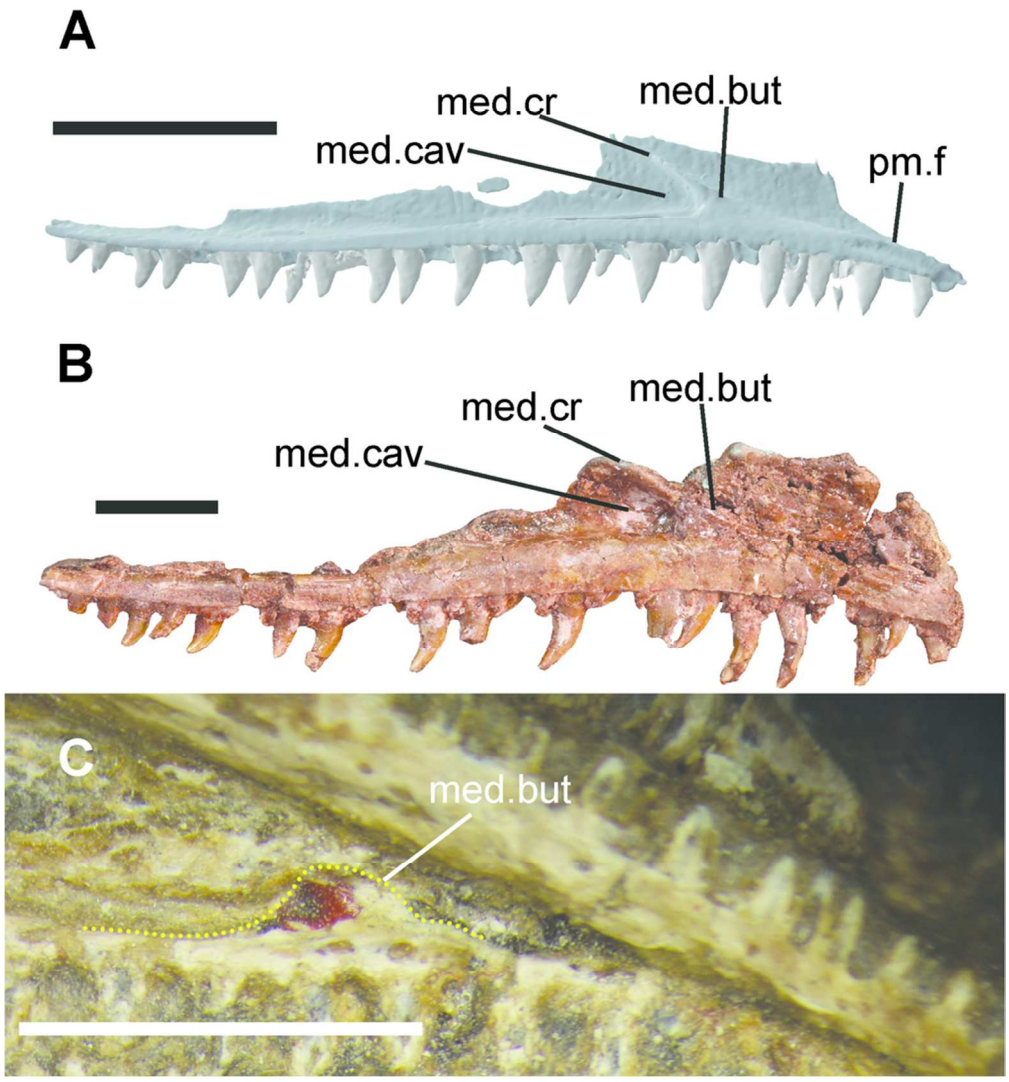

FIG. 18. Maxillae in medial view. A, OMNH 74606; B, Prolacerta broomi (BP/I/2675); C, Archaeovenator hamiltonensis (KUVP 12483) (image reversed). Abbreviations; med.cav, medial cavity of maxilla; med.cr, medial crest; med.but, medial buttress; pm.f, facet for maxillary process of premaxilla. Scale bars represent 5mm.

85x92mm (300 x 300 DPI)

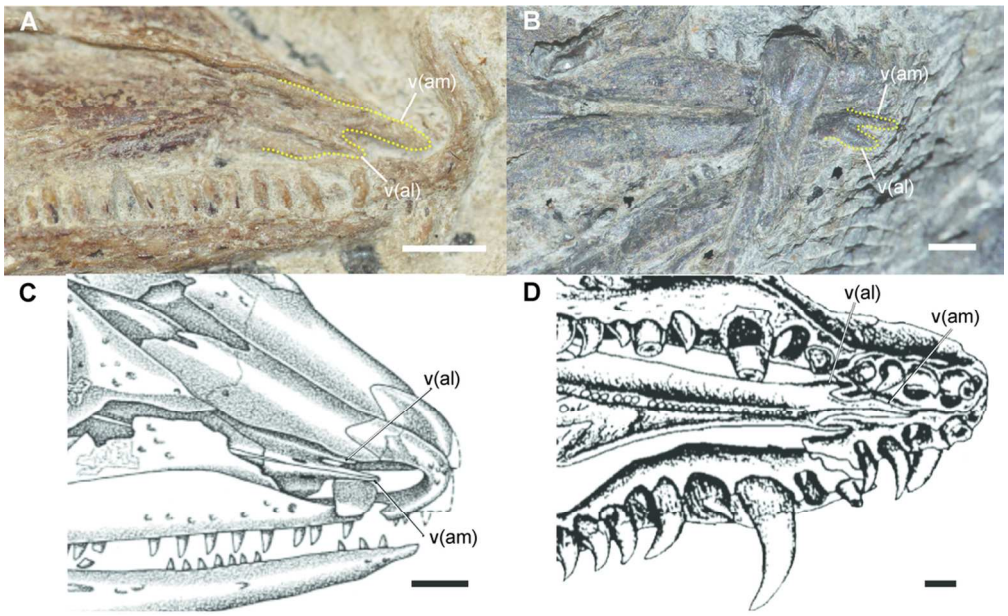

FIG. 19. Asymmetric processes of anterior vomers. A, Petrolacosaurus kansensis (KUVP 8351); B, Paleothyris acadiana (MCZ 3481); C, Archaeovenator hamiltonensis (from Reisz and Dilkes 2003); Mesenosaurus romeri (from Reisz and Berman 2001)(image reversed). Abbreviations; v(am), anteromedial process of vomer; v(al), anterolateral process of vomer. Scale bars represent 2mm.

101x61mm (300 x 300 DPI)

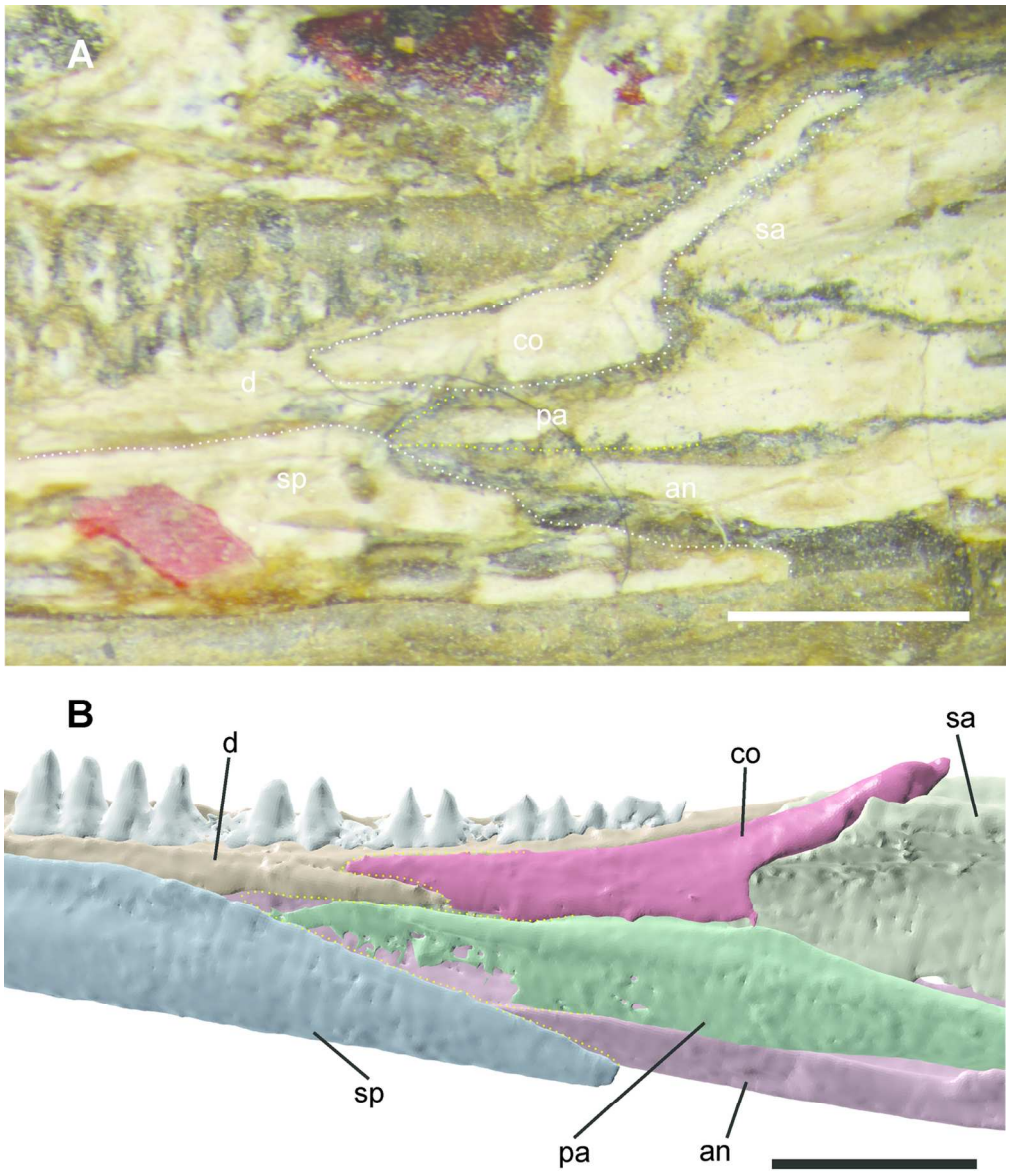

FIG.20. Coronoids in medial view. A, Archaeovenator hamiltonensis (KUVP 12483) right mandible; B, OMNH 74606 reconstruction of left mandible (image reversed). Abbreviations; an, angular; co, coronoid; d, dentary; pa, prearticular; sa, surangular; sp, splenial. Scale bars represent 2mm.

130x155mm (300 x 300 DPI)

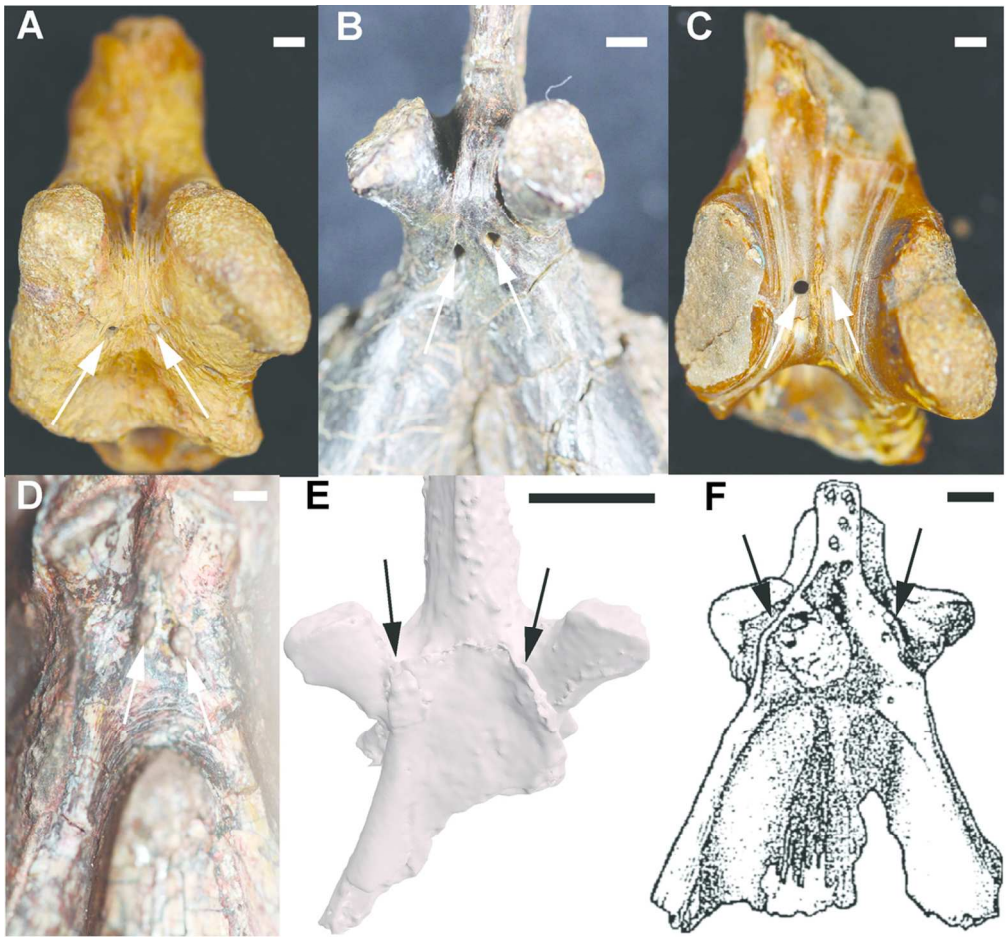

FIG.21. Parabasisphenoids in ventral view. A, Ophiacodon retroversus (MCZ 5792); B, Edaphosaurus boanerges (MCZ 1762); C, Ophiacodon retroversus (MCZ 4820); D, Secodontosaurus obtusidens (MCZ 2028); E, Orovenator mayorum (OMNH 74606); F, 'Basicranodon fortsillensis' (= Mycterosaurus longiceps) from Vaughn (1958). Arrows indicate position of entry foramina for cerebral branch of internal carotid arteries. Scale bars represent 2mm.

102x94mm (300 x 300 DPI)

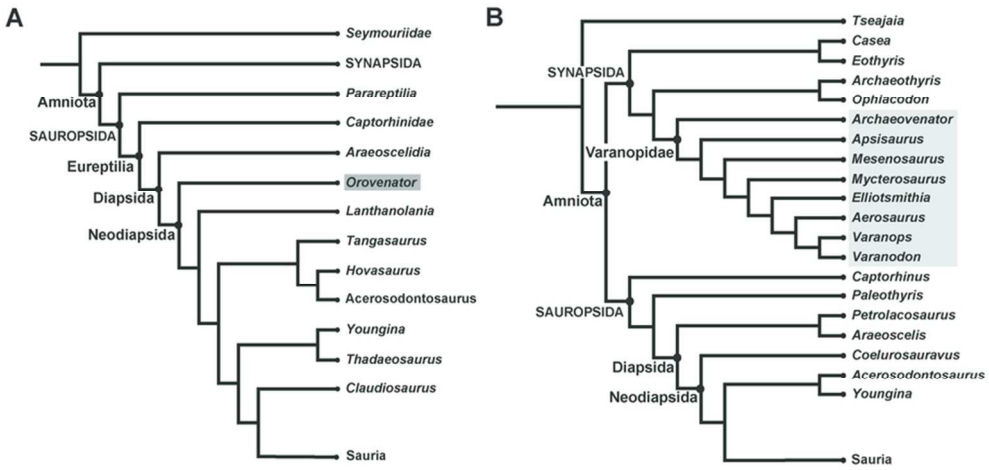

FIG. 22. Phylogenetic analyses of the character/taxon matrices of: A, Reisz et al. (2011); B, Reisz et al. (2010). Taxa recovered as Sauria in both datasets have been condensed to a single operational taxonomic unit.

78x36mm (300 x 300 DPI)

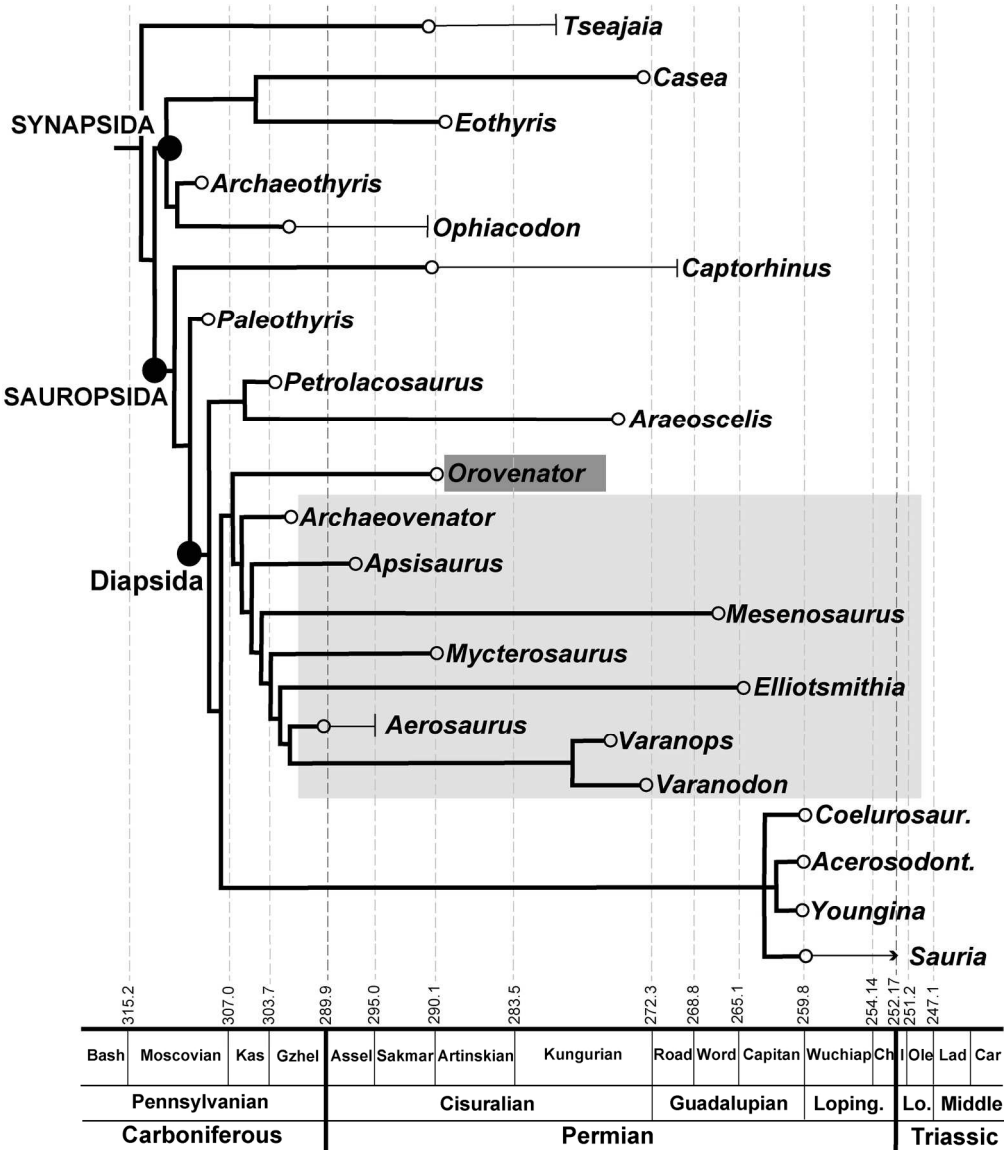

FIG. 23. Time calibrated strict consensus of the three most-parsimonious trees recovered from the dataset of Reisz et al. (2010) after the inclusion of Orovenator mayorum into the character/taxon matrix. White circles denote first appearance datum, lines ending with vertical bars denote range. Taxa recovered as Sauria in have been condensed to a single operational taxonomic unit. Abbreviations; Coelurosaur. = Coelurosauravus, Acerosodont. = Acerosodontosaurus.

189x217mm (300 x 300 DPI)

Taxa	Original description	assignment	Revision to Varanopidae
Apsisaurus witteri	Laurin 1991	diapsid	Reisz et al. 2010
Mesenosaurus romeri	Efremov 1940	synapsid	Reisz and Berman 2001
	Ivakhnenko and Kurzanov 1979	diapsid (archosaur)	
Heleosaurus scholtzi	Broom 1907	diapsid	Reisz and Modesto 2007
	Carroll 1976	diapsid	
	Benton 1985	diapsid	
Archaeovenator hamiltonensis	Reisz 1989	diapsid	Reisz and Dilkes 2003

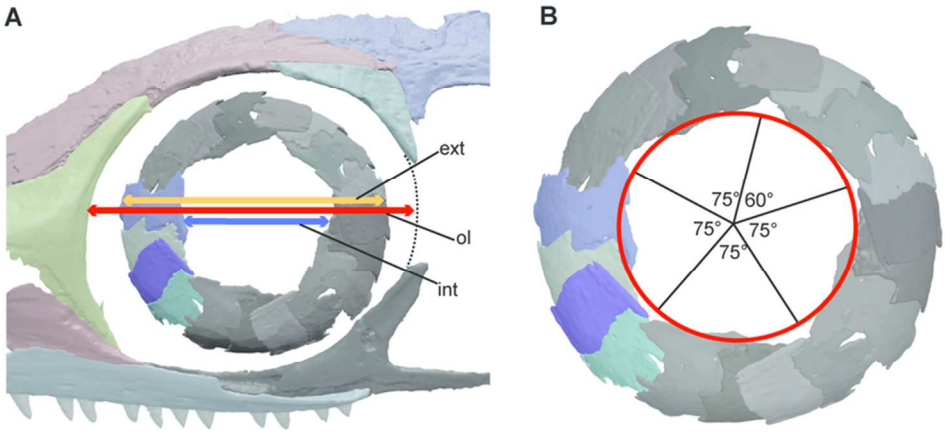

Fig. 1 (Supp.1). Reconstruction of the circumorbital elements and scleral ring of Orovenator mayorum. A, orbit and scleral ring, with dotted line denoting estimated position of the orbital margin of postorbital. B, ring of 19 scleral plates, articulated in situ plates in blue, duplicated plates in grey. Abbreviations; ext (yellow bar), maximum external diameter of scleral ring; ol (red bar), maximum orbital length; int (blue bar), maximum internal diameter of scleral ring.

76x34mm (300 x 300 DPI)